Hashemite Kingdom of Jordan

صندوق دعم البحث العلمي
Scientific Research Support Fund

Scientific Research Support Fund

AL-BALQA APPLIED UNIVERSITY

Jordanian Journal of Engineering And Chemical Industries

June 2018	VOLUME 01	NUMBER 01	ISSN 2616 - 9584 (Online) ISSN 2616 - 9584 (Print)

JJECI

www.jjeci.com

info@jjeci.com

An International Peer-Reviewed Scientific Journal Financed by the Scientific Research Support Fund

JORDANIAN JOURNAL OF ENGINEERING AND CHEMICAL INDUSTRIES (JJECI)

Jordanian Journal of Engineering and Chemical Industries (JJECI) is an international quarterly peer-reviewed research journal issued by the Scientific Research Fund, Ministry of Higher Education and Scientific Research, Amman, Jordan. JJECI is published by the Deanship of Research, Al-Balqa Applied University, Al-Salt, Jordan. The Journal publishes new and original Research Articles, Short Communications, Technical Notes, Feature Articles and Review Articles encompassing all fields of industrial and chemical engineering fields.

AIMS AND SCOPE

The Journal focuses on broad field of chemical engineering and industrial applications in which original contributions in the following areas appear
Physical Properties and Physical Chemistry
Transport Phenomena and Fluid Engineering
Separation Engineering
Thermal Engineering
Chemical Reaction Engineering
Process Systems Engineering and Safety
Biochemical, Food and Medical Engineering
Nanotechnology
Mathematical Modeling and Computer Simulation
Materials Sciences and Engineering
Energy, Water, Environment and Engineering
Industrial Management and Economics
Oil and Gas Processing
Chemical Engineering Education
Quality control and Standardization
Extractive Metallurgy
Industrial Chemistry

Other related Topics in Chemical Engineering are also welcomed

JJECI ADDRESS

Website: www.jjeci.com
E-mail: info@jjeci.com
Address: Al-Salt, Prince Ghazi Street
P.O.Box: Al-Salt, 19117 Jordan
Telephone: +962-5-3491111
Fax: +962-5-3532312

EDITOR'S NOTE

It is a great honor for me to head the Editorial Board of the Jordanian Journal of Engineering and Chemical Industries (JJECI). The Editorial Board consists of a group distinguished colleagues who have a well-recognized research record.

This issue is the first published by JJECI, We have started our first call for papers in January 2018. The submitted manuscripts have undergone a strict review process in which, at least, three specialized reviewers with well-recognized research track in the subject area reviewed each manuscript. While we received 9 manuscripts, just five papers were accepted and are published in this issue .

I would like to sincerely thank all authors who submitted their latest research work to JJECI. I also would like to thank all the reviewers of the Journal for their efforts to ensure a very high quality review process while keeping a reasonable timelines for submitting their reviews and recommendations.

I hope to receive from all potential authors, readers and researchers their opinions, suggestions and comments at (info@jjeci.com). My colleagues in the Editorial Board and I are very willing to adopt new ideas and thoughts that may be sent to us to improve the content quality and journal presentation.

Editor-in-Chief

Prof. Mohammed Matouq

JORDANIAN JOURNAL OF ENGINEERING AND CHEMICAL INDUSTRIES (JJECI)

TYPES OF CONTRIBUTION

Research Paper: Manuscripts are not to exceed ٥٠٠٠ words excluding references as maximum limit to the length of the research paper including all text, figures, Table and references. It should include a set **of keywords and an abstract followed by Introduction, Materials and Methods, Results and Discussion, Acknowledgments, and References**.

Short Communication: deals with a concise study or preliminary findings that indicate an innovative piece of research that could be less substantial than a full research paper. Short Communication is limited to 2000 words. It should include a set of keywords, an Abstract and a 'Results and Discussion' Section (should be combined) and followed by Conclusion. The number of references is limited to 20 and the number of figures and/or tables is limited to 3.

Letter: Description of novel finding that might not be suitable for a regular research paper or short communication. Letter is limited to 1000 words. The number of references is 10 and the number of figures and/or tables is 2, and 10 references.

Review or mini-review: invited reviews should be of high interest to the readers of the scientific community.

JORDANIAN JOURNAL OF ENGINEERING AND CHEMICAL INDUSTRIES (JJECI)

PUBLICATION ETHICS

1. **Ethical Standards: JJICE** adheres to the principles of transparency and best ethical practices in scholarly publishing as recommended by the international committees like COPE, DOAJ, OASPA, and WAME.

2. **Plagiarism: JJECI** has strict policies against plagiarism. During the submission, authors require to state that their work is not a copy of another published work and their article is not submitted elsewhere (in full or in part). **JJECI** cross checks every submission for the plagiarism misconduct. Any submission containing partially/completely plagiarized content is rejected immediately.

3. **Attribution Practice:** Citations must be attributed for previously published content. If the authors have used content from any previouslypublished work and fail to provide credit to original source then it will be considered as technical plagiarism and the manuscript might be rejected or retracted.

4. **Conflicts of Interest: JJECI** conduct double blind peer review process to avoid conflicts. The authors should hold responsibility in disclosing any conflicts of interest during article submission to avoid any potential conflicts of interest.

5. **Confidentiality Protection: JJECI** undertakes multiple measures to safeguard the confidentiality and integrity of the authors' work. Editors, peer reviewers and journal staff require maintaining the confidentiality of authors' work. It is ethically not acceptable to use or disseminate the unpublished work.

6. **Human and Animal Rights:** All articles published with **JJECI** must adhere to high ethical standards concerning human volunteers and animal welfare. For animal models and human volunteers ethical clearance letter and documents are required, if applicable.

7. **Consents/Instances:** Authors require obtaining consent for publication from all contributors and participants of the work. Authors must submit the clear statements regarding consents with original signature while submitting their work.

8. **Professional Conduct:** Editors, Reviewers, Authors and the journal staff are expected to adhere to the basic professional courtesy.

JORDANIAN JOURNAL OF ENGINEERING AND CHEMICAL INDUSTRIES (JJECI)

AIM AND SCOPE:

Jordanian Journal of Engineering and Chemical Industries (JJECI) is an international quarterly peer-reviewed research journal issued by the Scientific Research Fund, Ministry of Higher Education and Scientific Research, Amman, Jordan. JJECI is published by the Deanship of Research, Al-Balqa Applied University, Al-Salt, Jordan. The Journal publishes new and original Research Articles, Short Communications, Technical Notes, Feature Articles and Review Articles encompassing all fields of industrial and chemical engineering fields.

The Journal focuses on broad field of chemical engineering and industrial applications in which original contributions in the following areas appear:

Physical Properties and Physical Chemistry
Transport Phenomena and Fluid Engineering
Separation Engineering
Thermal Engineering
Chemical Reaction Engineering
Process Systems Engineering and Safety
Biochemical, Food and Medical Engineering
Nanotechnology
Mathematical Modeling and Computer Simulation
Materials Sciences and Engineering
Energy, Water , Environment and Engineering
Industrial Management and Economics
Oil and Gas Processing
Chemical Engineering Education
Quality control and Standardization
Extractive Metallurgy
Industrial Chemistry

Other related Topics in Chemical Engineering are also welcomed

INSTRUCTION FOR CONTRIBUTORS
TYPES OF CONTRIBUTION

Research Paper: Manuscripts are not to exceed eight t (8) pages as maximum limit to the length of the research paper including all text, figures, Table and references. It should include a set **of keywords and an abstract followed by Introduction, Materials and Methods, Results and Discussion, Acknowledgments, and References**.

Short Communication: deals with a concise study or preliminary findings that indicate an innovative piece of research that could be less substantial than a full research paper. Short Communication is limited to 2000 words. It should include a set of keywords, an Abstract and a 'Results and Discussion' Section (should be combined) and followed by Conclusion. The number of references is limited to 20 and the number of figures and/or tables is limited to 3.

Letter: Description of novel finding that might not be suitable for a regular research paper or short communication. Letter is limited to 1000 words. The number of references is 10 and the number of figures and/or tables is 2, and 10 references.

Review or mini-review: invited reviews should be of high interest to the readers of the scientific community.

MANUSCRIPT PREPARATION AND SUBMISSION

Manuscripts must be written in English and formatted to A4 or US letter size. Authors are recommended to refer to recent issues for guidance on style.

Preparation of Manuscripts

Manuscripts must be written in English typed in two columns fifty-seven lines per column on numbered pages of A4 or US letter size. All figures and tables should be included in the most appropriate locations within the main text, and not placed on separate pages.
A corresponding author will be requested to consent to an agreement transferring copyright on behalf of all authors. All authors will be requested to consent to agreements of submission and authorship.

All authors are encouraged to register or add their ORCID ID when submitting their manuscript or creating their account. The ORCID ID will appear in the

published manuscript if an author registers or adds their ORCID ID. Please visit http://www.orcid.org to learn more.

1)Title and authors: This should contain the following items in the given order.

i) Title: The title is to be written in 20 pt. Garamond font, centered and using the bold and "Capital Caps" formats. There should be 24 pt. (paragraph) spacing after the last line

ii) Author's names (given name, and surname), affiliations and addresses. If authors' affiliations differ, these should be identified by use of superscripts 1, 2, etc. Identify the corresponding author and give the telephone number, fax number and e-mail address.

iii) If the research has been presented in part at a meeting, give the name, place and date of the meeting.

2) Abstract:

A brief summary (less than 300 words for research papers and journal reviews and 150 words for other types of papers, significant results and conclusions, followed by five keywords. Each keyword should consist of no more than three words.

1) Main Text: main headings will be followed after abstract by Introduction, Materials and Methods, Results and Discussion, Acknowledgments, and References. Leave a blank line above and below each main heading.
Equations: Number of equations in order with parentheses. Cite as Eq. (1), Eqs. (3) and (5). Spell out "Equation" if at the beginning of a sentence.
Figures and Tables: Each figure and table must have a caption. Cite as Figure 1, Figures 2 and 3, and Table 1. Color reproduction will be provided at no cost, if it is essential to clarify the description.
Literature: Cite in the text as follows: Matouq and Tagawa (1960), Matouq and Goto (1989a, 1989b), (Carslaw and Jaeger, 1960), and (Tan and Liou, 1989a, 1989b)
Units: The use of SI units is recommended.
Examples: k[W/(m K)] or k[$Wm^{-1}K^{-1}$], k= 0.58 W/(m K) or k= 0.58 $Wm^{-1}K^{-1}$
Chemical Nomenclature: Use IUPAC or Chemical Abstract conventions.

4) Nomenclature: List symbols in alphabetical order with their definition and SI units. Greek letters, subscripts and superscripts should follow Roman symbols.
5) Literature Cited: Arrange in alphabetical order according to last name of first author, patentee or editor.

1. **Journal Article:** Matouq, M., T. Tagawa and S. Goto: Micro-channel reactor with guideline structure for organic–aqueous binary system, *J. Chem. Eng. Japan*, **26**, 254–258 (1993)
2. **Book Reference:** Carslaw, H. C. and J. C. Jaeger; Conduction of Heat in Solids, 2nd ed., pp. 198-201, Clarendon Press, Oxford, U.K. (1960).
3. **Chapter in a Book Reference:** Misra NC, Misra S, Chaturvedi A. Carcinoma gallbladder. In: Johnson CD, Taylor I, editors. Recent advances in surgery. London: Churchill Livingstone. 1997; 69-87.
4. **Conference proceedings:** Harnden P, Joffe JK, Jones WG, editors. Germ cell tumours V. Proceedings of the 5th Germ Cell Tumour Conference, 2001 Sep 13-15. Leeds, UK. New York: Springer, 2002.
5. **Dissertation:** Borkowski MM. Infant sleep and feeding: a telephone survey of Hispanic Americans [dissertation]. Mount Pleasant (MI): Central Michigan University. 2002.
6. **Patent:** Primack, H. S.; "Method of Stabilizing Polyvalent Metal Solution," U.S Patent 4, 374,104 (1983),

Submission of Manuscripts

The author must provide a detailed cover letter including a declaration that the work has not been published elsewhere. It is author's sole responsibility that articles publishing from institutions have necessary approvals if needed.

All the articles must be submitted to the email: submission.info@jjeci.com All the manuscripts submitted should be in the Word (docx, doc format) or PDF format.

Submission of a manuscript implies that it has not previously been published, and is not under consideration for publication elsewhere (except patent disclosure(s) of the author(s)). The Editorial Committee will withdraw a submitted manuscript and retract acceptance and the published article, if any misconduct of publication ethics, which are specified in Guidelines on Publication Ethics for the Journal.

Peer Review Processing:

All articles submitted will undergo double blind peer review processing to meet the international standards. The editor handles the complete editorial process of the articles and peer reviewers remain anonymous to the authors. Editor decisions are strictly followed for quality publications.

AFTER ACCEPTANCE

After acceptance, the author(s) cannot modify the submitted manuscript. Any changes must be addressed through the Editorial office. For the typesetting of the publication, authors will be requested to submit original text and figures online in separate files. All the figures should be of professional quality.

COPYRIGHT

Authors must agree to transferring copyright to the Jordan Journal of Industrial and Chemical Engineering. No article can be published without this agreement.

PROOFS AND REPRINTS

Electronic proofs will be sent as an E-mail attachment to the corresponding author as a PDF file. Page proofs are considered to be the final version of the paper. With the exception of typographical or minor clerical errors, no changes will be made in the paper at the proof stage. Authors will have free electronic access to the full text of the paper. Authors can freely download the PDF file from which they can print unlimited copies of their chapters. Hard copy of three journal issues of which the article appears in will be supplied free of charge to the corresponding author.

PUBLICATION ETHICS

1. **Ethical Standards: JJICE** adheres to the principles of transparency and best ethical practices in scholarly publishing as recommended by the international committees like COPE, DOAJ, OASPA, and WAME.

2. **Plagiarism: JJECI** has strict policies against plagiarism. During the submission, authors require to state that their work is not a copy of another published work and their article is not submitted elsewhere (in full or in part). **JJECI** cross checks every submission for the plagiarism misconduct. Any submission containing partially/completely plagiarized content is rejected immediately.

3. **Attribution Practice:** Citations must be attributed for previously published content. If the authors have used content from any previouslypublished work and fail to provide credit to original source then it will be considered as technical plagiarism and the manuscript might be rejected or retracted.

4. **Conflicts of Interest: JJECI** conduct double blind peer review process to avoid conflicts. The authors should hold responsibility in disclosing any conflicts of interest during article submission to avoid any potential conflicts of interest.

5. **Confidentiality Protection: JJECI** undertakes multiple measures to safeguard the confidentiality and integrity of the authors' work. Editors, peer reviewers and journal staff require maintaining the confidentiality of authors' work. It is ethically not acceptable to use or disseminate the unpublished work.

6. **Human and Animal Rights:** All articles published with **JJECI** must adhere to high ethical standards concerning human volunteers and animal welfare. For animal models and human volunteers ethical clearance letter and documents are required, if applicable.

7. **Consents/Instances:** Authors require obtaining consent for publication from all contributors and participants of the work. Authors must submit the clear statements regarding consents with original signature while submitting their work.

8. **Professional Conduct:** Editors, Reviewers, Authors and the journal staff are expected to adhere to the basic professional courtesy.

Reviewer **Guidelines**

Peer review (see form) is the system for evaluating the quality, validity, and relevance of scholarly research. The process aims to provide authors with constructive feedback from relevant experts which they can use to make improvements to their work, thus ensuring it is of the highest standard possible.

The Review Process

The steps below are the high-level steps in the review process.

Receive Invitation to review

- Accept Invitation
- Review Manuscript
- Submit Review

As a reviewer, you will be notified by e-mail of an invitation to review a manuscript.

- Only agree to review manuscripts for which they have the subject expertise required to carry out a proper assessment and which they can assess in a timely manner.
- Respect the confidentiality of peer review and not reveal any details of a manuscript or its review, during or after the peer-review process, beyond those that are released by the journal.

Double-check the manuscript title page and the Acknowledgments section to determine whether there is any conflict of interest for you (with the authors, their institution, or their funding sources) and whether you can judge the article impartially.

Abstract -Has this been provided (if required)? Does it adequately summarize the key findings/approach of the paper?

Length - Reviewers are asked to consider whether the content of a paper is of sufficient interest to justify its length. Each paper should be of the shortest length required to contain all useful and relevant information, and no longer.

Originality - Is the work relevant and novel? Does it contain significant additional material to that already published?

Presentation –Is the writing style clear and appropriate to the readership? Are any tables or graphics clear to read and labeled appropriately?

References -Does the paper contain the appropriate referencing to provide adequate context for the present work?

Once you've read the paper and have assessed its quality, you need to make a recommendation to the editor regarding publication. The specific decision types used by a journal may vary but the key decisions are:

Accept -if the paper is suitable for publication in its current form.
Minor revision - if the paper will be ready for publication after light revisions. Please list the revisions you would recommend the author makes.
Major revision - if the paper would benefit from substantial changes such as expanded data analysis, widening of the literature review, or rewriting sections of the text.
Reject - if the paper is not suitable for publication with this journal or if the revisions that would need to be undertaken are too fundamental for the submission to continue being considered in its current form.

In your comments intended for the author, do not make statements about the acceptability of a paper (see the next paragraph); suggested revisions should be stated as such and not expressed as conditions of acceptance. Organize your review so that an introductory paragraph summarizes the major findings of the article, gives your overall impression of the paper, and highlights the major shortcomings. This paragraph should be followed by specific, numbered comments, which, if appropriate, may be subdivided into major and minor points. (The numbering facilitates both the editor's letter to the author and evaluation of the author's rebuttal.) Criticism should be presented dispassionately; offensive remarks are not acceptable.

Sometimes you will be asked to review a paper when you do not have sufficient time available. In this situation, you should make the editorial office aware that you are unavailable as soon as possible. It is very helpful if you are able to recommend an alternative expert or someone whose opinion you trust.

If you are unable to complete your report on a paper in the agreed time-frame required by the journal, please inform the editorial office as soon as possible so that the refereeing procedure is not delayed.

Make the editors aware of any potential conflicts of interest that may affect the paper under review. Decision of the Editorial Board is final regarding publication of any manuscript.

COPYRIGHT AGREEMENT

JORDANIAN JOURNAL OF ENGINEERING AND CHEMICAL INDUSTRIES (JJECI)

Please complete and sign the form and send it with the final version of your manuscript. It is required to obtain written confirmation from the authors in order to acquire copyrights for papers published in the Journal so as to index them to various repositories.

Title of paper:

_____
_____
_____

Author(s):

_____
_____
_____

The undersigned hereby transfers any and all rights in and to the paper, including, without limitation, all copyrights to the JJECI. The undersigned hereby represents and warrants that the paper is original, is not considered for possible publication elsewhere and that he/she is the author of the paper, except for material that is clearly identified as to its original source, with permission notices from the copyright owners where required. The undersigned represents that he/she has the power and authority to make and execute this assignment.
This agreement is to be signed by corresponding authors and on behalf of co-authors who have obtained the assent of the co-author(s) where applicable.

_____

Author's Signature and Date

_____

Typed or Printed Name

_____

Institution or Company

.

Manuscript Formatting Guidelines

Title: Title must be precise, self-explanatory and short. Abbreviations need to be avoided to the most possible. Except the conjunctions, prepositions and articles rest of the title must be presented in title case. The Font Size of the Title should be Times New Roman 15, bold and centered.

Abstract: Each manuscript must contain an abstract to be concise, informative, self explanatory of the work and must be free from citations.

Keywords: For review and research articles keywords remain mandatory. Keywords should be precisely picked from the manuscript which is most commonly used in the article.

Introduction: This section should lay a strong background for the study leaving the readers to understand the purpose and need for the study. This sector should contain citations for mentioned statements from the supporting papers.

Materials and Methods: This section should provide detailed procedures if the techniques are new and if they are applied from well established procedures, they should be cited. This sector can have multiple sub sections as per the number of methods and methodologies used. Anyhow none of the techniques should be exactly copied with same data mentioned.

Results and Discussion: This sector should be describing the results and interpretations of the above experiments. There could be multiple subheadings or described in a single paragraph. None of the content/data should be copied.

Conclusions: This should be clearly explaining the author thoughts, highlights and limitations of the study.

Acknowledgements: Author could provide the grant details if any or express his gratitude towards his interest.

Funding Acknowledgement: Author could provide the grant details if any or express his gratitude towards his interest.

JORDANIAN JOURNAL OF ENGINEERING AND CHEMICAL INDUSTRIES (JJECI)

Submission of Manuscripts

The author must provide a detailed cover letter including a declaration that the work has not been published elsewhere. It is author's sole responsibility that articles publishing from institutions have necessary approvals if needed.

All the articles must be submitted to the email info@jjeci.com All the manuscripts submitted should be in the Word (docx, doc format) or PDF format.

Submission of a manuscript implies that it has not previously been published and is not under consideration for publication elsewhere (except patent disclosure(s) of the author(s)). The Editorial Committee will withdraw a submitted manuscript and retract acceptance and the published article, if any misconduct of publication ethics, which are specified in Guidelines on Publication Ethics for the Journal

Peer Review Processing:

All articles submitted will undergo double blind peer review processing to meet the international standards. The editor handles the complete editorial process of the articles and peer reviewers remain anonymous to the authors. Editor decisions are strictly followed for quality publications.

AFTER ACCEPTANCE

After acceptance, the author(s) cannot modify the submitted manuscript. Any changes must be addressed through the Editorial office. For the typesetting of the publication, authors will be requested to submit original text and figures online in separate files. All the figures should be of professional quality.

COPYRIGHT

Authors must agree to transferring copyright to the Jordan Journal of Industrial and Chemical Engineering. No article can be published without this agreement.

PROOFS AND REPRINTS

Electronic proofs will be sent as an E-mail attachment to the corresponding author as a PDF file. Page proofs are considered to be the final version of the paper. With the exception of typographical or minor clerical errors, no changes will be made in the paper at the proof stage. Authors will have free electronic access to the full text of the paper. Authors can freely download the PDF file from which they can print unlimited copies of their chapters. Hard copy of three journal issues of which the article appears in will be supplied free of charge to the corresponding author.

JORDANIAN JOURNAL OF ENGINEERING AND CHEMICAL INDUSTRIES (JJECI)

Preparation of Manuscripts

Manuscripts must be written in English typed in two columns fifty-seven lines on numbered pages of A4 or US letter size. All figures and tables should be included in the most appropriate locations within the main text, and not placed on separate pages.
A corresponding author will be requested to consent to an agreement transferring copyright on behalf of all authors. All authors will be requested to consent to agreements of submission and authorship.

All authors are encouraged to register or add their ORCID ID when submitting their manuscript or creating their account. The ORCID ID will appear in the published manuscript if an author registers or adds their ORCID ID. Please visit http://www.orcid.org to learn more.

1)Title and authors: This should contain the following items in the given order.

i) Title: The title is to be written in 20 pt. Garamond font, centered and using the bold and "Capital Caps" formats. There should be 24 pt. (paragraph) spacing after the last line
ii) Author's names (given name, and surname), affiliations and addresses. If authors' affiliations differ, these should be identified by use of superscripts 1, 2, etc. Identify the corresponding author and give the telephone number, fax number and e-mail address.
iii) If the research has been presented in part at a meeting, give the name, place and date of the meeting.

2) Abstract:

A brief summary (less than 300 words for research papers and journal reviews and 150 words for other types of papers, significant results and conclusions, followed by five keywords. Each keyword should consist of no more than three words.

1) Main Text: main headings will be followed after abstract by Introduction, Materials and Methods, Results and Discussion, Acknowledgments, and References. Leave a blank line above and below each main heading.
Equations: Number of equations in order with parentheses. Cite as Eq. (1), Eqs. (3) and (5). Spell out "Equation" if at the beginning of a sentence.
Figures and Tables: Each figure and table must have a caption. Cite as Figure 1, Figures 2 and 3, and Table 1. Color reproduction will be provided at no cost, if it is essential to clarify the description.

Literature: Cite in the text as follows: Matouq and Tagawa (1960), Matouq and Goto (1989a, 1989b), (Carslaw and Jaeger, 1960), and (Tan and Liou, 1989a, 1989b)
Units: The use of SI units is recommended.
Examples: k[W/(m K)] or k[$Wm^{-1}K^{-1}$], k= 0.58 W/(m K) or k= 0.58 $Wm^{-1}K^{-1}$
Chemical Nomenclature: Use IUPAC or Chemical Abstract conventions.

4) Nomenclature: List symbols in alphabetical order with their definition and SI units. Greek letters, subscripts and superscripts should follow Roman symbols.
5) Literature Cited: Arrange in alphabetical order according to last name of first author, patentee or editor.

1. **Journal Article:** Matouq, M., T. Tagawa and S. Goto: Micro-channel reactor with guideline structure for organic–aqueous binary system, *J. Chem. Eng. Japan*, **26**, 254–258 (1993)
2. **Book Reference:** Carslaw, H. C. and J. C. Jaeger; Conduction of Heat in Solids, 2nd ed., pp. 198-201, Clarendon Press, Oxford, U.K. (1960).
3. **Chapter in a Book Reference:** Misra NC, Misra S, Chaturvedi A. Carcinoma gallbladder. In: Johnson CD, Taylor I, editors. Recent advances in surgery. London: Churchill Livingstone. 1997; 69-87.
4. **Conference proceedings:** Harnden P, Joffe JK, Jones WG, editors. Germ cell tumours V. Proceedings of the 5th Germ Cell Tumour Conference, 2001 Sep 13-15. Leeds, UK. New York: Springer, 2002.
5. **Dissertation:** Borkowski MM. Infant sleep and feeding: a telephone survey of Hispanic Americans [dissertation]. Mount Pleasant (MI): Central Michigan University. 2002.
6. **Patent:** Primack, H. S.; "Method of Stabilizing Polyvalent Metal Solution," U.S Patent 4, 374,104 (1983),

JORDANIAN JOURNAL OF ENGINEERING AND CHEMICAL INDUSTRIES (JJECI)

Manuscript Formatting Guidelines

Title: Title must be precise, self-explanatory and short. Abbreviations need to be avoided to the most possible. Except the conjunctions, prepositions and articles rest of the title must be presented in title case. The Font Size of the Title should be Times New Roman 15, bold and centered.

Abstract: Each manuscript must contain an abstract to be concise, informative, self-explanatory of the work and must be free from citations.

Keywords: For review and research articles keywords remain mandatory. Keywords should be precisely picked from the manuscript which is most commonly used in the article.

Introduction: This section should lay a strong background for the study leaving the readers to understand the purpose and need for the study. This sector should contain citations for mentioned statements from the supporting papers.

Materials and Methods: This section should provide detailed procedures if the techniques are new and if they are applied from well established procedures, they should be cited. This sector can have multiple sub sections as per the number of methods and methodologies used. Anyhow none of the techniques should be exactly copied with same data mentioned.

Results and Discussion: This sector should be describing the results and interpretations of the above experiments. There could be multiple subheadings or described in a single paragraph. None of the content/data should be copied.

Conclusions: This should be clearly explaining the author thoughts, highlights and limitations of the study.

Acknowledgements: Author could provide the grant details if any or express his gratitude towards his interest.

Funding Acknowledgement: Author could provide the grant details if any or express his gratitude towards his interest.

JORDANIAN JOURNAL OF ENGINEERING AND CHEMICAL INDUSTRIES (JJECI)

Table of contents

Adsorption of Diazo Dye C.I. Acid Red 97 from Aqueous Solution onto Yemen Natural Clay: Equilibrium and Thermodynamic Studies

Abdulrakib A. Al-Wahbi*

Chemical Engineering Department, Faculty of Petroleum and Engineering, Hadramout University, Al-Mukalla, Hadramout, Republic of Yemen

Keywords: Ultrasound, High frequency, Pesticide, Diazon, Pesticide, Environmental pollution, kinetics

The equilibrium adsorption of diazo dye C.I. Acid Red 97 (AR97) from aqueous solutions onto Yemen natural clay has been studied as a function of temperature and particle size range. The equilibrium data were correlated using Langmuir, Fruendlich, Temkin, Redlich-Peterson, and Sips isotherm models. Thermodynamic parameters such as standard enthalpy (ΔHº), standard entropy (ΔSº) and standard Gibbs free energy (ΔGº) were calculated.

It was found that the adsorption capacity of clay for AR97 decreases with increasing temperature and particle size range. The results show that Fruendlich and Sips isotherm models best fit the experimental data over the whole concentration range. The maximum adsorption capacity for Yemen natural clay was 196.7 (mg.g-1). The value of ΔHº was -20.5 (kJ.g-mol−1) indicating that the adsorption of AR79 onto Yemen natural clay is characterized by physical adsorption. ΔGº values obtained were all negatives indicating a spontaneous adsorption process.

Introduction

Many industries, such as textiles, pulp mills, leather, printing, food, and plastics, use dyes in order to color their products and consume substantial volumes of water. The presence of very small amounts of dyes in water (less than 1 ppm for some dyes) is highly visible and undesirable (Robinson *et al*. 2001, Banat *et al*. 1996). As a result; they generate a considerable amount of colored wastewater. It is recognized that public perception of water quality is greatly influenced by the color. Over 100,000 commercially available synthesis dyes exist and more than 7*105 tons per year are produced annually (Yener *et al*. 2008). Azo dyes are an important class of synthetic dyes and used as coloring agents in the textile, paint, ink and plastic industries, accounting for 50 % of all commercial dyes (Zollinger, H., 1991). Azo dyes, containing one or more azo bond (–N=N–), account for 60-70% of all textile dyestuffs used (Carliell *et al.* 1995). Large amounts of these dyes remain in the effluent after the completion of dyeing process. Due to their stable and complex composition, high toxicity, poor degradability, great solubility in water, difficulty of treatment in the biological treating station, and because of their association with various human health problems, Azo dyes have been considered as an extremely important pollutants in the environment and received considerable attention (Ramakrishna et al. 1997, Vandevivere et al. 1998, Robinson *et al*. 2002, and Baughman and Weber 1994). Hence, it becomes imperative that azo dyes are to be removed from the effluents before it is disposed. Among various treatment technologies, adsorption onto activated carbon proved to be one of the most effective and reliable physicochemical treatment methods (El Qada *et al*. 2007, Chan *et al*. 2009, El Nemr *et al*. 2009 and Gad and El-Sayed 2009). However, the overlying cost of activated carbon and its regeneration problems led researchers to produce and use low-cost, abundance, and not need to regeneration adsorbents.

Clay materials have been increasingly paid attention because of their low cost, abundance in most continents of the world, high specific surface area, and chemical and mechanical stabilities. In addition, Clay materials have shown good results as an adsorbent for the removal of various metals (Bhattacharyya and Gupta, 2008) surfactants (Rao and He, 2006), and basic and acid dyes (Bulut *et al*. 2008, Dögan, 2009 and Branuer *et al*. 1938).

Up to our knowledge, no research has been conducted using Yemen natural clay for adsorption Diazo Dye C.I. Acid Red 97. Therefore, the main aim of this study is to investigate the suitability of Yemen natural clay as low-cost adsorbent for the removal of diazo dye C.I. Acid Red 97.

Received on July 14, 2018; accepted on August 20, 2018

Correspondence concerning this article should be addressed to Abdulrakib A. Al-Wahbi, Abdalwahby_73@yahoo.com).

1. Material and Methods

1.1. Materials

The natural clay used in this work was collected from Al-Rayan zone, Al-Mukalla City, Hadramout Governorate, Republic of Yemen. The adsorbent was washed, crushed and sieved through different standard sieves into the desired particle size and used without any pre-treatment. The resulting sample was dried at 105 ºC and stored in sealed containers prior to use. Diazo dye [C.I. Acid Red 97(AR97), λmax: 498 nm] supplied by Techno Color Corporation (Bombay, India) was used as principal adsorbate. Chemical structure of dye is shown in **Figure 1**.

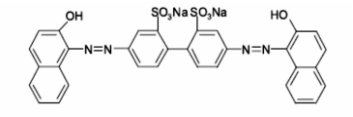

Fig. 1 Chemical Structure of Acid Red 97.

1.2. Characterization of Natural Clay

Chemical composition of natural clay was obtained using XRF Spectrometer, ARL 9800, Switzerland. Solid density, particle density and porosity for natural clay were obtained using mercury Poresizer 9320, Micromertics, USA. The surface physical properties such as specific surface area, pore size distribution and total pore volume were measured by nitrogen adsorption–desorption isotherms using a multipurpose apparatus Nova 2000 analyzer, Quantachrome Instruments, Japan. A BET analysis from the amount of N_2 gas adsorbed at various partial pressures (five points $0.05 < p/p_0 < 0.3$, nitrogen molecular cross-sectional area = 0.162 nm^2) was used to determine the surface area (SBET), and a single condensation point ($p/p_0 = 0.95$) was used to find the total pore volume (VT). The average pore radius (rav) was calculated using total surface area and total pore volume (rav = 2VT/SBET). The volumes of micropores, mesopores, and macropores were calculated from N_2 adsorption isotherm by applying the Barrett Joyner-Hallenda (BJH) method (Barrett 1951). Mineralogical analysis (XRD analysis) was obtained using Panalytical X'Pert PRO X-ray diffractometer.

1.3. Experimental

Batch adsorption experiments were carried out using bottle-point method (El-Geundi, M. S. 1990). A stock solution of AR97 (1000 $mg.dm^{-3}$) was prepared and was subsequently diluted to the required initial concentrations. Adsorption capacity of the clay towards AR97 was determined by contacting a constant mass (0.1 g) of clay with a fixed volume (50 ml) in sealed glass bottles of different initial concentrations (25-600 mg.dm-3) of dye solution at pH 5±0.2. The bottles were agitated in an isothermal water-bath shaker for 5 h until equilibrium was reached. At the end of the adsorption time, a known volume of the solution was removed and centrifuged for analysis of the supernatant. Calibration curve for AR97 was prepared by recording the absorbance values for a range of known concentrations of dye solution and the maximum absorbance was determined (λmax = 498 nm). The value of λmax was used in all subsequent investigations using this dye. The concentration of AR97 in aqueous solution was then determined at λmax = 498 nm using double beam UV-visible spectrophotometer (Shimadzu, Model UV 1601, Japan). The amount of AR97 adsorbed onto clay, qe (mg.g-1), was calculated by the following equation

$$q_e = \frac{(C_o - C_e)}{m} * V \qquad (1)$$

2. Results and Discussion

2.1. Characterization of Natural Clay

Chemical analysis indicates the following composition: SiO2, 62.38%; Al_2O_3, 13.60%; Fe_2O_3, 7.05%; CaO, 3.75%; MgO, 3.11%; K_2O, 2.63%. The ratio SiO_2: Al_2O_3 is 4.598, which is higher than that of pure montmorillonite (2.81:1), (El-Geundi, M. S. 1990).

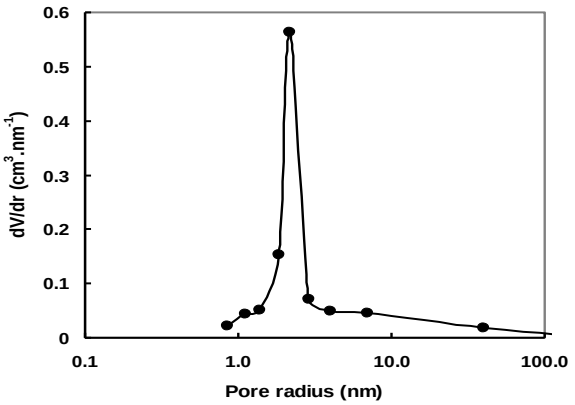

Fig. 2 Adsorption isotherms of clay tested with N2 at 77.35 K.

The N2 adsorption-desorption isotherm obtained for porous natural clay is shown in **Figure 2**. As shown in Figure 2, the desorption branch of this isotherm exhibited hysteresis and correspond to the Type IV isotherm. The existence of the hysteresis loop in the isotherm is due to the capillary condensation of N_2 gas occurring in the mesopores and therefore, the Type IV

isotherm is considered as the characteristic feature of the mesoporous materials (Gregg, S. J.; Sing, K. S. W., 1982). The sharp rise near P/Po = 0.4 corresponds to condensation in the primary mesopores. The well-defined hysteresis loop between the adsorption and desorption branches can be classified as type H4 according to the IUPAC classification (Gregg, S. J.; Sing, K. S. W, 1982). The shape of hysteresis loop indicates that the pores have ink-bottle type pores. Physical characteristics of the Yemen natural clay such as the values of BET surface area (SBET), total pore volume (VT), micropores volume (Vmic), mesopores volume (Vmes), macropores volume (Vmac), and average pore radius (rav) are listed in **Table 1**.

It is obvious from Table 1 that natural clay has high specific surface area (82.3 cm2. g-1) and total pore volume (0.109 $cm^3. g^{-1}$). The high surface area and total pore volume of the natural clay gained high adsorption capacity towards AR97.

Table 1. Surface characteristics of natural clay

Total surface area (S_{BET}) (m^2/g)	82.34
Total pore volume (V_T) (cm^3/g)	0.109
Average pore radius (r_{av}) (Å)	26.40
Micropores volume (V_{mic}) (cm^3/g)	0.012
Mesopores volume (V_{mes}) (cm^3/g)	0.096
Macropores volume (V_{mac}) (cm^3/g)	0.001
Solid-phase density (ρ_s) (g/cm^3)	2.526
Particle density (ρ_p) (g/cm^3)	1.859
Particle porosity (ε_p)	0.264

Table 2. Value of separation factor RL

Value of	Types of isotherm
$R_L>1$	Unfavorable
$R_L = 1$	Linear
$0<R_L<1$	Favorable
$R_L = 0$	Irreversible

Pore size distribution is one of the most important parameters for any porous adsorbent because the size of pores must be larger than the adsorbate molecule volume to allow it to enter inside the adsorbent particle pores. Figure 3 shows pore size distribution (PSD) of natural clay calculated from N_2 adsorption isotherm by applying the Barrett-Joyner-Hallenda (BJH) method using desorption branch of the isotherms (Barrett *et al*. 1951).

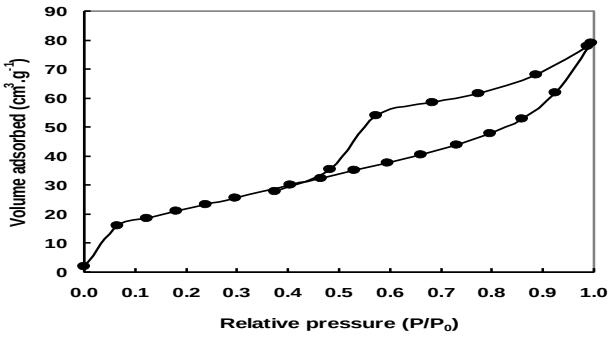

Fig. 3 Pore size distributions of clay determined by using BJH technique.

Their average pore size is 2.997 nm determined by (BJH) method, which was in the mesopores range (pore size, 2–50 As illustrated in Figure 3, pores between 1.4 and 2.9 nm were dominant. nm). Mineralogical analysis (XRD analysis) proved that clay is composed of montomorillonite and illite as clay minerals and quartz and gypsum as non-clay minerals.

2.2. Adsorption Isotherms

The adsorption isotherm indicates that the adsorption molecules distribute between the liquid phase and the solid phase when the adsorption process reaches an equilibrium state. Determining the distribution of AR97 between natural clay and the liquid phase when the system is a state of equilibrium is important in establishing the capacity of the clay for AR97. Preliminary experiments showed that such equilibrium was established within 180 min; however, all equilibrium experiments were allowed to run for 300 min.

Plotting the amount of AR97 adsorbed at equilibrium, qe, against final concentration in the aqueous phase, Ce, at different temperatures and different particle size ranges gave a characteristic S-shaped curve as shown in Figures 4 and 5. From the shapes of the initial portions of the curves, the isotherms corresponding to the AR97 may be classified as S-shape (Giles classification) suggesting a low affinity of natural clay toward AR97 with strong competition from the solvent molecules for the available adsorption sites (Gilles *et al*. 1960). The S-shape isotherm suggests a cooperative adsorption that operates if adsorbate–adsorbate interaction is stronger than adsorbate–adsorbent interaction. In addition to these, the S-type isotherm is more indicative of physical adsorption (Yurdakoc *et al*. 2005). The same type of isotherm (S-shape) was obtained for the adsorption of AR97 onto activated carbon by (Gömez *et al.*1998). Similar results were reported by (Grant *et al.* 1998, El-Nahal and Safi, 2004 and El-Guendi *et al.* 2005).

Figure 4 shows that the experimental equilibrium adsorption capacity of AR97 onto clay decreases with increasing temperature, decreasing from 196.7 (mg.g^{-1}) at 15 ºC to 145.7 (mg.g^{-1}) at 65 ºC indicating that physical adsorption takes place. This decrease in adsorption capacity with the increase in temperature may be due to the enhancement of dye solubility and desorption step in the adsorption mechanism. It is also due to the weakening of adsorptive forces between the active sites on the clay and the dye species, and also between adjacent dye molecules on the solid phase (Tan, I. A. W., 2008).

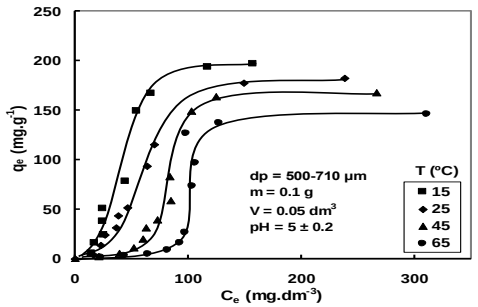

Fig. 4 Adsorption isotherms of AR97 onto clay at different Temperatures

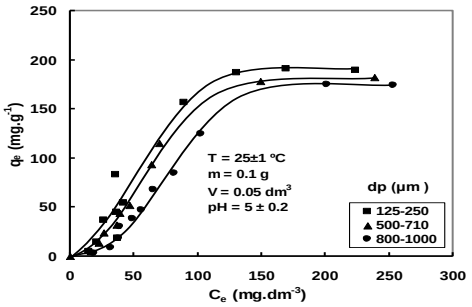

Fig. 5 Adsorption isotherms of AR97 onto clay at different particle size ranges

Figure 5 shows that a decrease in clay particle size led to an increase in equilibrium adsorption capacity. The experimental equilibrium adsorption capacity of clay for AR97 increased from 174.3 (mg.g^{-1}) to 189.1 (mg.g-^{1}) with decreasing particle size range from 800-1000 µm to 125-250 µm. This behavior can be attributed to the inability of the large dye molecules to penetrate into the internal pore structure of clay. Apparently, breaking up large particle diameter to form smaller ones probably serves to open some tiny, sealed pores in the clay which become available for adsorption, thus slightly increasing the total specific surface area of a given mass of clay (Al-Degs *et al*. 2000). The higher efficiency in removing AR97 observed in the case of smaller-sized fraction of clay can be attributed to the increase in the available surface area with the decrease in particle size, in which smaller diffusion distance expected over smaller particles and the ability of the large dye molecules to access most of the active sites in the internal pore structure of clay will increase. Several investigations have been shown similar observation for clay minerals and other adsorbents (Wong, *et al.* 2008, Ponnusami *et al.* 2008).

2.3. Analysis of adsorption isotherms

The adsorption equilibrium data obtained for the AR97 onto natural clay were fitted into five different isotherm models to determine the most suitable model to represent the adsorption process. The isotherms used are the Langmuir isotherm, the Freundlich, the Temkin, the Redlich-Peterson and the Sips isotherms. In order to quantitatively compare the applicability of different models, the average relative error (ARE) was calculated using equations (2):

$$ARE = \frac{1}{N}\left[\sum_{i=1}^{N}\left|\frac{q_{e,cal}-q_{e,exp}}{q_{e,exp}}\right|\right] \qquad (2)$$

where N is the number of data points, qexp and qcal (mg.g^{-1}) are the experimental and the calculated values of the equilibrium adsorbate solid concentration in the solid phase, respectively. The values of ARE is used as measures of the fitting of the data to an isotherm equation, small values of ARE would indicate a perfect fit.

2.3.1. Langmuir isotherm

The Langmuir isotherm (Langmuir, I. 1918) is valid for monolayer adsorption on a homogenous adsorbent surface containing a finite number of identical site and no interaction between adsorbate molecules. The Langmuir expression is represented by the following equation.

$$q_e = \frac{1+ K_L C_e}{1+ a_L C_e} \qquad (3)$$

Where qe is the solid phase equilibrium concentration (mgg^{-1}), Ce is the liquid phase equilibrium concentration (mg.dm-3), K_L (dm^{3}g^{-1}) and aL (dm^3.mg^{-1}) are the Langmuir constants. This may be converted into a linear form which is convenient for plotting and determining the constants KL and a_L:

$$\frac{C_e}{q_e} = \frac{a_L}{K_L} C_e + \frac{1}{K_L} \quad (4)$$

Linear plots of ($C_e q_e^{-1}$) versus (C_e) suggest the applicability of the Langmuir isotherm and demonstrate monolayer coverage of the adsorbate on the outer surface of the adsorbent (Panday *et al*. 1984). The essential characteristics of the Langmuir isotherm can be expressed in terms of a dimensionless equilibrium parameter (R_L) which is defined by:

$$R_L = \frac{1}{(1+ K_L C_o)} \quad (5)$$

Where R_L is a dimensionless constant separation factor, C_o is the initial concentration of dye ($mgdm^{-3}$) and K_L is the Langmuir adsorption constant ($dm^3.g^{-1}$) (Weber *et al*. 1974). The equilibrium parameter indicates the shape of the isotherm and whether the adsorption is favorable or not, as listed in Table 2. The values of K_L and a_L have been calculated for the different variables studied using Eqn. (4) and listed in **Table 3**. The values of the constant (K_L/a_L) correspond to the maximum adsorption capacity (q_{max}) of the clay for AR97 were determined.

Table 3 Estimated Langmuir parameters and Freundlich parameters for the adsorption of AR97 onto natural clay at different variables.

	Langmuir					**Freundlich**									
Adsorption conditions						**First section of plot**			**Second section of plot**			**Third section of plot**			**ARE**
T (ºC)	**K_L**	**a_L**	**q_m**	**R_L**	**ARE**	**K_F**	**n**	**C.R.**	**K_F**	**n**	**C.R.**	**K_F**	**n**	**C.R[1].**	
15	٢٧,٧٨	٠,١٣٦	٢٠٤,١	٠,١٥٨	3.532	0.029	0.465	0-47.4	54.51	3.856	47.4 - 157.6	---	---	---	0.275
25	19.84	0.106	188.7	0.234	6.877	0.017	0.474	0-66.0	13.64	2.531	66.0-238.5	---	---	---	0.144
45	11.27	0.063	178.6	0.056	8.891	0.007	0.540	0-52.3	$2.9x10^{-05}$	0.302	52.3-108.5	98.13	10.21	108.5-266.0	0.110
65	7.930	0.052	153.9	0.015	1.358	0.029	0.820	0-78.2	$2.2x10^{-18}$	0.103	78.2-110.0	79.03	9.32	110.0-311.0	0.146
dp (µm)															
125-250	٩٣,٥٠	٠,٤٨٦	١٩٢,٣	0.110	5.778	0.001	0.287	0-26.2	0.605	0.817	26.2-98.0	64.46	4.84	98.0-224.0	0.261
500-710	19.84	0.106	188.7	0.234	6.877	0.017	0.474	0-66.0	13.64	2.531	66.0-238.5	---	---	---	0.144
800-1000	51.80	0.300	172.4	0.567	7.377	0.001	0.369	0-45.5	0.118	0.666	45.5-104.1	20.07	2.51	104.0-253.7	0.102

[1]C.R.: Concentration Range

It is clear from Table 3 that temperature plays an interesting role in the adsorption of AR97. Increasing temperature from 15ºC to 65ºC led to a decrease in the maximum adsorption capacity from 204.1 ($mg.g^{-1}$) to 153.9 ($mg.g^{-1}$) as shown in Table 3. This demonstrates the exothermic nature of the process. Similar observation was reported for the adsorption of Acid Blue 193 onto modified sepiolite (Özcan *et al.* 2006). The data listed in Table 3 indicate also a decrease in the maximum adsorption capacity (q_m) with the increase in particle size range. Increasing particle size ranges from 125-250 µm to 800-1000 µm led to a decrease in the maximum adsorption capacity from 192.3 ($mg.g^{-1}$) to 172.4 ($mg.g^{-1}$). Comparing the results obtained in this study to that in literature, it was found that Yemen natural clay and activated carbon have the same shape of isotherm (S-shape), however the maximum adsorption capacity for Yemen natural clay was 204.1 ($mg.g^{-1}$) compared to that 52.1 ($mg.g^{-1}$) for activated carbon (Gömez *et al*. 2007). Values of R_L for natural clay/AR97 system have been calculated and listed in Table 3. According to R_L values in Table 3, the adsorption behavior of AR97 was favorable ($0< R_L< 1$).

2.3.2. Freundlich Isotherm

The Freundlich isotherm (Freundlich, H. M. F. 1906) is the first known relationship describing the adsorption equilibrium. This isotherm can be used for non-ideal adsorption on heterogeneous surfaces and derived by assuming an exponentially decaying adsorption site energy distribution. The heterogeneity arises from the presence of different functional groups on the surface, and the various adsorbent–adsorbate interactions. The experimental equilibrium data for the adsorption of AR97 onto clay at different temperatures and particle size ranges have been analyzed using the Freundlich isotherm as given by equation (6).

$$q_e = K_F C_e^{\,1/n} \quad (6)$$

Where q_e is the equilibrium solid-phase concentration (mgg^{-1}), C_e is the equilibrium liquid-phase concentration ($mgdm^{-3}$), K_F is Freundlich constant $(mg.g^{-1})/(dm^f.mg^{-1})^n$ and n is the heterogeneity factor. The K_F value is related to the adsorption capacity; while 1/n value is related to the adsorption intensity**.** The magnitude of exponent (n) gives an indication of the favorability and

capacity of the adsorbent/adsorbate system. Values of (n) greater than 1 represent favorable adsorption according to Treybal (Treybal, R. E, 1985).Equation 6 may be linearized via a logarithmic plot which enables the exponent (n) and the constant (K_F) to be determined:

$$log(q_e) = log(K_F) + (1/n)log(C_e) \quad (7)$$

However, a Log-Log plot of the equilibrium data for the adsorption of AR97 onto clay did not quite give straight lines, as required by the Freundlich equation, when only one line was used to represent the whole concentration range of experimental data but showed some curvature. However, if the whole concentration range is divided into sections of plot, i.e. first section of plot, second section of plot third section of plot, good fits to the experimental data can be observed. This method was used by different researchers as reported in the literature whereby it has been divided up into sections (El-Geundi *et al*. 2005, Wong *et al*. 2003, Nassar *et al*. 2002). For this reason the Freundlich constants had to be changed, in terms of equation (8), to obtain a good representation of the data over the entire concentration range. A general equation for the entire concentration range may be expressed as:

$$q_e = K_{F,i}\, C_e^{1/ni} \quad (8)$$

Figures 6 show the fit of the Freundlich isotherm model to the experimental data obtained at different temperatures. Similar behavior was obtained at different particle size ranges as shown in **Figure 7**. The Freundlich parameters (K_F and n) have been calculated using the least-squares method applied to the straight lines shown in Figures 6 and 7 and are listed in Table 3 together with the appropriate concentration ranges and the error functions values obtained. According to the results, the values of n are greater than unity indicating that the adsorption of dye onto clay is favorable. This is in great agreement with the findings regarding to R_L values.

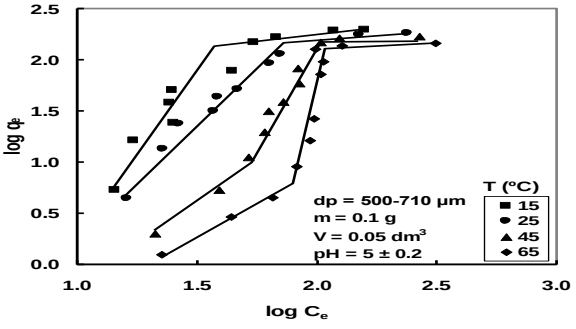

Fig. 6 Freundlich plots for the adsorption of AR97 onto clay different particle size ranges.

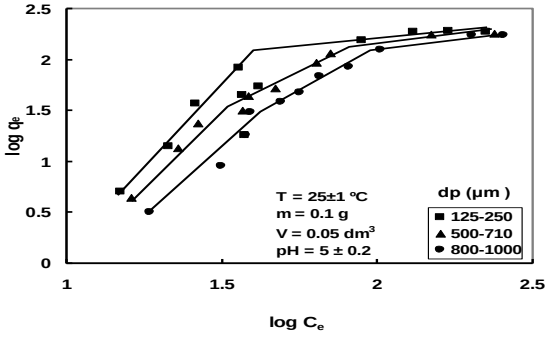

Fig. 7 Freundlich plots for the adsorption of AR97 onto clay at at different temperatures

2.3.3. Temkin Isotherm

The Temkin isotherm (Temkin M. I., 1941) has been used in the following form:

$$q_e = \frac{RT}{b_T}\left(ln(A_T C_e)\right) \quad (9)$$

Equation (9) can be expressed in its linear form as:

$$q_e = B_T ln(A_T) + B_T ln(C_e) \quad (10)$$

Where , $B_T = \frac{RT}{b_T}$ (11)

And T is the absolute temperature (K), R is the universal gas constant (J.g-mol^{-1}.K^{-1}), A_T is the equilibrium binding constant corresponding to the maximum binding energy (dm^3.mg^{-1}), b_T is Temkin isotherm constant (J.g-mol^{-1}) and the constant B_T is related to the heat of adsorption (dimensionless) (Bulut, *et al*. 2008). According to equation (10), a plot of (q_e) against ln (C_e) enables the determination of the isotherm constants (A_T and B_T). The linearized Temkin adsorption isotherms for AR97 onto clay at different temperatures and particle size ranges are presented in Figures 8 and 9. The estimated Temkin isotherm constants values (A_T and B_T) calculated from the slopes and the intercepts of the straight lines of **Figures 8** and **9** are listed in **Table 4**. Table 4 estimated Langmuir parameters and Freundlich parameters for the adsorption of AR97 onto natural clay at different variables. As shown in the figures, high deviation from the linearity occurred for the temperatures and pracle size ranges studied. This indicates that the equilibrium adsorption behavior of the AR97 onto clay does not follow Temkin isotherm model. Fig. 8 also show that deviation from linearity increased by increasing temperature which indicates a nonliner

decrease in the heat of adsortopn with coverag at high temperature for the adsorption of AR97 onto clay. Similar results have been reported (Mane, *et al*. 2007.

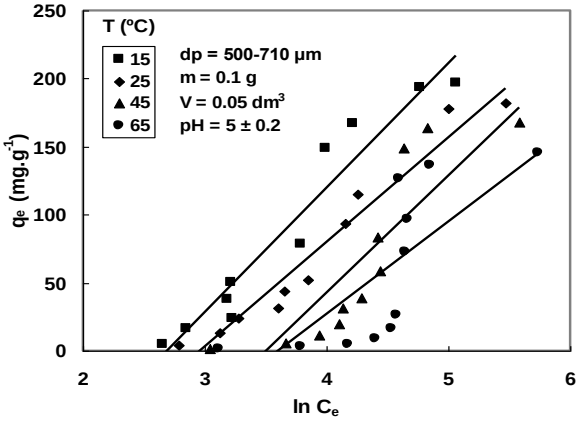

Fig.8 Temkin plots for the adsorption of AR97 onto clay at different temperatures.

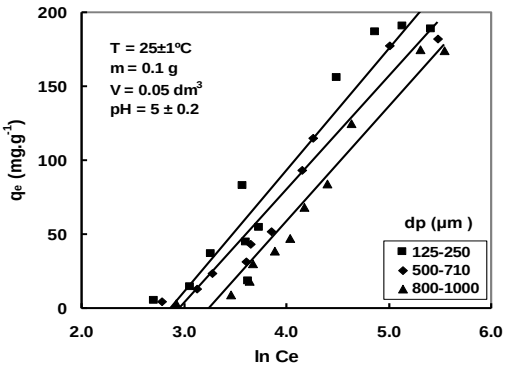

Figure 9. Temkin plots for the adsorption of AR97 onto clay at different particle size ranges

2.3.4. Redlich-Peterson Isotherm

The Redlich–Peterson isotherm contains three parameters and involves the features of both the Langmuir and the Freundlich isotherms (Redlich, O.; Peterson, D. L, 1959). It can be described as follows:

$$q_e = \frac{(K_{RP} \cdot C_e)}{\left(1 + a_{RP} \cdot C_e^{\beta}\right)} \qquad (12)$$

Where K_{RP} is the modified Langmuir constant (dm^3/g), a_{RP} (dm^3/mg) and β are constant. $\beta \leq 1$.

The isotherm parameters in equation (12) was calculated by optimization routine to minimize the ARE between experimental data and Redlich- Peterson model across the concentration range studied using the solver add-in with Microsoft's excel spreadsheet, (Ho *et al*. 2002, Ho, Y,S. 2006), and listed with the values of ARE in Table 4.

2.3.5. Sips Isotherm

Sips isotherm (Sips, R. 1948) is a combination of the Langmuir and Freundlich isotherm type models and expected to describe heterogeneous surfaces much better. At low adsorbate concentrations it effectively reduces to a Freundlich isotherm and thus does not obey Henry's law, while at high adsorbate concentrations it predicts a monolayer adsorption capacity characteristic of the Langmuir isotherm (Günay *et al*. 2007). The model can be written as:

$$q_e = \frac{q_m a_s C_e^{n_s}}{\left(1 + a_s C_e^{n_s}\right)} \qquad (13)$$

Where q_{ms} is the Sips maximum adsorption capacity (mgg^{-1}), a_s is Sips constant $(dm^3.mg^{-1})^{ns}$ and (n_S) is the heterogeneity factor. Sips constants were evaluated by the same method used for Redlich-Peterson isotherm. Table 4 shows the values of maximum adsorption capacity (q_{ms}) and Sips constants for the adsorption of AR97 onto clay at different temperatures and particle size ranges. As shown in Table 4, maximum adsorption capacity decreases with increasing temperature and particle size ranges.

2.4 Simulation Results and Correlations

To optimize the design of an adsorption system for the adsorption of adsorbate, it is important to establish the most appropriate correlation for the equilibrium curves. Various isotherm equations like those of Langmuir, Freundlich, Temkin, Redlich-Peterson and Sips have been used to describe the equilibrium characteristics of adsorption of AR97 onto clay. Using the appropriate constants of the Langmuir, the Freundlich, the Temkin, the Redlich-Peterson, and the Sips equations, the theoretical isotherm curves were predicted for the adsorption of AR97 and clay using known values of (C_e).

Table4 Estimated Temkin parameters, Redlich-Peterson model parameters and Sips model parameters for the adsorption of AR97 onto natural clay at different variables.

Adsorption Conditions	Temkin			Redlich-Peterson				Sips			
T (ºC)	**B_T**	**A_T**	**ARE**	**K_{RP}**	**a_{RP}**	**β**	**ARE**	**q_m**	**a_s**	**n_S**	**ARE**
15	91.67	0.068	0.317	2.577	0.005	0.999	0.871	204.97	1.76E-5	0.345	0.206
25	76.68	0.052	0.549	1.585	0.004	0.999	0.819	188.93	9.64E-6	0.358	0.106
45	86.08	0.030	2.577	0.973	0.001	0.999	1.896	174.93	5.36E-14	0.146	0.342
65	67.61	0.027	4.383	0.708	0.001	0.999	3.511	146.61	6.90E-23	0.090	0.593
dp (µm)											
125-250	82.01	0.057	0.685	1.875	0.004	0.999	0.869	200.86	2.59E-5	0.383	0.276
500-710	76.68	0.052	0.549	1.585	0.004	0.999	0.819	188.93	9.64E-6	0.358	0.106
800-1000	77.89	0.039	0.1027	1.069	0.002	0.999	0.894	185.77	6.74E-6	0.370	0.105

In order to confirm the fit model for the adsorption system, it is necessary to analyze the data using error function ARE. The traditional approach of determining isotherm parameters is based on the linearized form of isotherm equation by best fitting the linearized isotherm equation to the experimental data. However, the correlation coefficient (R^2) generated from this method has the drawback that it may not provide the best isotherm constants for correlating the original (non-linearized) isotherm equation with experimental data points (Cheung *et al*. 2009). Because the use of (R^2) is limited to solving linear forms of isotherm equations which measure the difference between experimental and theoretical data in linear plots only, but not the errors in isotherm curves (Crini *et al*. 2008). For that reason, the error functions were used to confirm the best model that gave the best fit to the experimental data. These values are a measure of the fitting of the data to an isotherm equation, a small of error function would indicate a perfect fit. **Figures 10** and **11** shows the fit of the isotherm models to the experimental data for the adsorption of RA97 onto Yemen natural clay at T = 45ºC and dp =800-1000 µm, respectively. It is clear from the Figures that the Freundlich and Sips isotherms gave the best fit for the experimental data among the five isotherms were used. The in ability of Langmuir model to simulate the experimental data can be attributed to the fact that Langmuir model does not take into account adsorbate-adsorbate interactions which were active in this adsorption process (Gómez *et al*. 2007). According to the data in Tables 2 and 3 it is clear that the values of the error functions for the Freundlich isotherm was found to be smallest at different temperatures and particle size ranges, whereas at temperatures 15, 25ºC with particle size ranges 500-710 µm the Sips isotherm was found to be the best isotherm to fit the experimental data according to the smallest values of the ARE and the graphical representation.

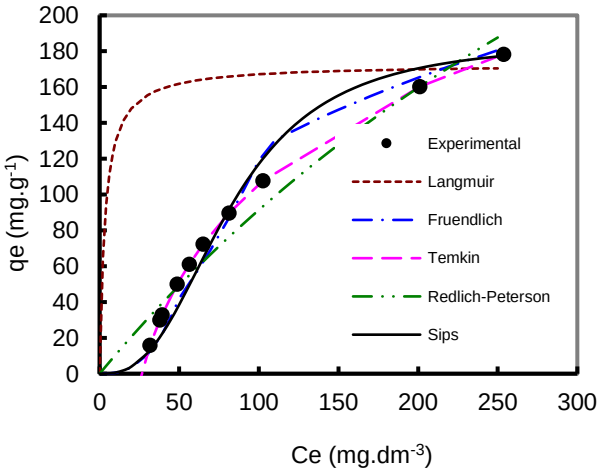

Fig. 10 Comparison between experimental and theoretical isotherms for the adsorption of AR97 onto clay at T = 45°C.

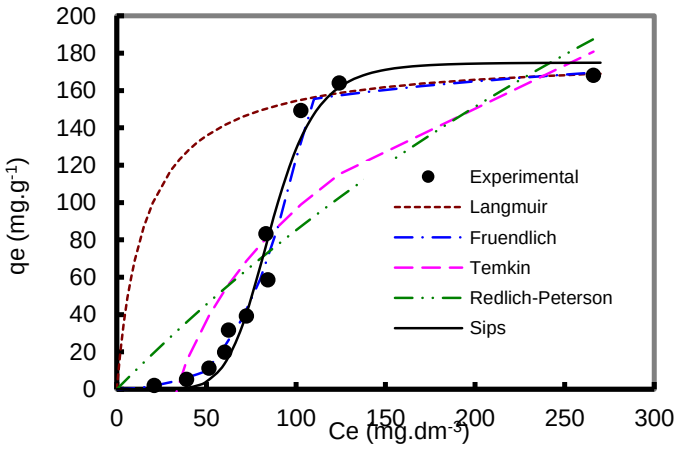

Fig. 11 Comparison between experimental and theoretical for adsorption of AR97 on clay, 800-1000 µm

2.5 Thermodynamic study

The thermodynamic parameters that must be considered to determine the process are changes in standard enthalpy (ΔHº), standard entropy (ΔSº) and standard Gibbs free energy (ΔGº) due to transfer of unit mole of solute from solution onto the solid–liquid interface.
The Gibbs free energy change of adsorption is defined as:

$$\Delta G^o = RTln(K_L) \quad (14)$$

Where K_L is Langmuir equilibrium constant (dm^3g^{-1}), (R) is the universal gas constant (8.314 J.g-mol^{-1}.K^{-1}) and (T) is the absolute temperature (K).
The values of (ΔHº) and (ΔSº) was computed using Van't Hoff equation:

$$\log(K_L) = \frac{1}{2.303R}\left(\Delta S^o - \frac{\Delta H^o}{T}\right) \quad (15)$$

A plot of (log K_L) versus (1/T) should produce straight line with slope equals to -ΔHº/RT and intercept equals to ΔSº/R (Cheung *et al*. 2001). **Figure 12** shows linear relation between (log K_L) and (1/T) with very high correlation coefficient ($R^2 > 0.99$). The values of (ΔHº) and (ΔSº) are calculated from the slope and the intercepts of straight line in Figure 12 and listed in Table 5. The values of standard Gibbs free energy (ΔGº) are calculated using equation 14 and also listed in **Table 5**. The standard enthalpy (ΔHº) and entropy (ΔSº) changes of adsorption of AR97 onto clay determined from equation (15) were found to be -20.5 (kJ.g-mol^{-1}) and -43.6 (J.g-mol^{-1}.K^{-1}). Typically the magnitude of (ΔHº) for physical adsorption ranges from 4 to 40 (kJ.g-mol^{-1}), compared to that of chemical adsorption ranging from 40 to 800 (kJ.g-mol^{-1}) (Cheung *et al*. 2001). The negative value of (ΔHº) for AR97/clay system indicates the exothermic nature of the process. As the temperature increases, the mobility of dye molecules increases causing the molecules to escape from the solid phase to the liquid phase. Therefore, the amount of dye that can be adsorbed will decrease. The values of standard Gibbs energy change (ΔGº) in all the cases are indicative of the spontaneous nature of the interaction without requiring large activation energies of adsorption and no energy input from outside of the system is required. The results in Table (5) show that the value of (ΔGº) increase with an increase in temperature, indicating lower temperature favored the adsorption. Generally, the change in free energy for physisorption is between −20 and 0 (kJ.g-mol^{-1}), but chemisorption (Crini, G.; Badot, P., 2008) is in a range of −400 to−80 (kJ.g-mol^{-1}).

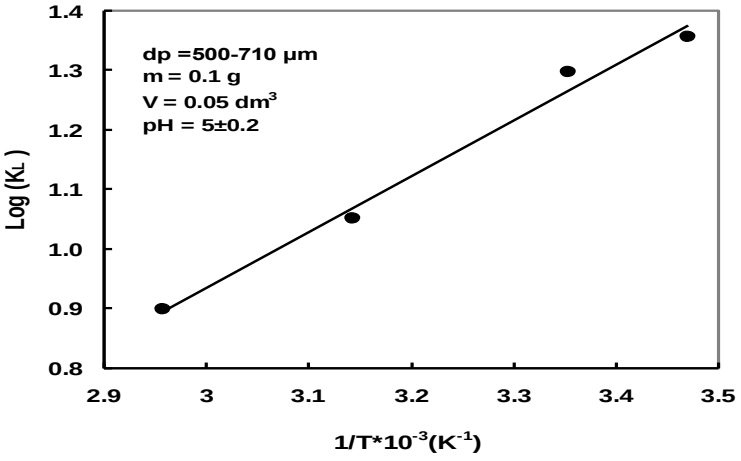

Fig. 12. Plot of Log K_L against 1/T for the Adsorption of AR97 onto Clay.

Table 5 Thermodynamic Parameters for the dsorption of

T (K)	ΔGº (kJ. g-mol^{-1})	ΔHº (kJ. g-mol^{-1})	ΔSº (J. $gmol^{-1}.K^{-1}$)	R^2
288.15	-7.8			
298.15	-7.4			
318.15	-6.4			
338.15	-5.8	-20.5	-43.6	0.99

Conclusions

The equilibrium adsorption of AR97 onto Yemen natural clay at different temperatures and particle size ranges has been studied. Experimental data were mathematically modeled using Langmuir, Freundlich, Temkin, Redlich-Peterson, and Sips isotherm models. Thermodynamic parameters such as standard enthalpy (ΔHº), standard entropy (ΔSº) and standard Gibbs free energy (ΔGº) have been evaluated. Adsorption capacity increases with decreasing particle size range indicating that the dye molecules may not completely penetrate the particle or partly that the dye molecules preferentially adsorb near the external surface of the

particle. Thus it can be concluded that smaller clay particles are needed for such adsorption processes. As the temperature increases, the adsorption capacity of AR97 onto clay decreases. The decrease in adsorption capacity with the increase in temperature exhibits the role of temperature in enhancing the dye solubility and desorption step during the adsorption processes. Therefore, one conclusion which can be drawn is that the adsorption process of AR97 onto clay is exothermic process, a fact proved by the negative value of (ΔH^o). Among the five isotherm models applied, Freundlich and Sips models was found to best fit the experimental data as indicated from the low value of the average percent deviation (ARE). This would indicate the heterogeneity of the adsorbent surface and the significant role of the adsorbate-adsorbate interactions. The values of thermodynamic parameters indicated that the process is spontaneous and exothermic. In laboratory-scale studies, Yemen natural clay proved potentially good adsorbent and low-cost adsorbent for removing azo dye from aqueous solutions and can be used as an alternative of the high cost commercial activated carbon.

Nomenclature

A_T = Equilibrium binding constant, $dm^3.g^{-1}$.
a_L = Langmuir constant $dm^3.g^{-1}$, eqn. (3).
a_{RP} = Constant eqn. (12).
a_s = Sips constant, $(dm^3.mg^{-1})^{ns}$.
B_T = Dimensionless, heat adsorption parameter.
b_T = Temkin isotherm constant, $J.g\text{-}mol^{-}1.K^{-1}$.
C_o = Initial concentration of dye solution, $mg.dm^{-3}$.
C_e = Equilibrium concentration of dye solution, $mg.dm^{-3}$.
K_F = Freundlich constant, $(mg.g^{-1}/dm^3.mg^{-1})^n$, eqn. (6).
K_L = Langmuir constant, $dm^3.g^{-1}$, eqn. (3)
K_{pp} = Modified Langmuir constant, $dm^3.g^{-1}$.
N = Number of data points.
n, ns = Homogeneity factor.
m = Mass of clay, g.
q_e = Amount absorbed, $mg.g^{-1}$.
q_{cal} = Calculated data point, mgg^{-1}.
q_{exp} = Calculated data point, $mg.g^{-1}$.
q_{max} = Maximum adsorption capacity, $mg.g^{-1}$.
q_{ms} = Sips maximum adsorption capacity, $mg.g^{-1}$.
R = Universal gas constant, $J.g\text{-}mol^{-1}.K^{-1}$.
R_L = Dimensionless equilibrium parameter.
V = Total volume of dye solution, dm^3.
β = Constant parameter, eqn. (12).
ΔH^o = Standard enthalpy, $kJ.g\text{-}mol^{-1}$.
ΔG^o = Standard Gibbs free energy, $kJ.gmol^{-1}$.
ΔS^o = Standard entropy, $J.gmol^{-1}.K^{-1}$.

References

Ahmad, A. L. and Hameed, B. H. "Adsorption of Basic Dye Using Activated Carbon Prepared from Oil Palm Shell: Batch and Fixed Bed Studies": *Desalination*, **255**, 13-28**, (**2008).

Al-Degs, Y.; Khraisheh, M. A. M.; Allen, J. S.; Ahmad, M. N. "Effect of Carbon Surface Chemistry on the Removal of Reactive Dyes from Textile Effluent". *Water Res*., **34**, 927-935, (2000).

Banat, I. M.; Nigam, P.; Singh, D.; Marchant, R. "Microbial Decolorization of Textile-Dye-Containing Effluents: a Review. Biores". *Technol*. **58**, 217-227, (1996).

Barrett, E. P.; Joyner, L. G.; Halenda, P. P. "The Determination of Pore Volume and Area Distributions in Porous Substances. I. Computations from Nitrogen Isotherms". *J. Am. Chem. Soc*., **73,** 373-380 **(**1951).

Baughman, G. L.; Weber, E. J. "Transformation of Dyes and Related Compounds in Anoxic Sediment: Kinetics and Products". *Environ. Sci. Technol*., **28**, 267-276 (1994).

Bhattacharyya, K. G.; Gupta, S. S. "Adsorption of a Few Heavy Metals on Natural and Modified Kaolinite and Montmorillonite: A Review". *Advances in Colloid and Interface Sci*., **140**, 114-131 (2008).

Branauer, S.; Emmett, P.H.; Teller, E. "Adsorption of Gases in Multimolecular Layers". *J. Am. Chem. Soc.,* **60**, 309-319 (1938).

Bulut, E.; Özacar, M.; Şengil, İ. A. "Equilibrium and Kinetic Data and Process Design for Adsorption of Congo Red onto Bentonite". *J. Hazard. Mater*., **154**, 613-622 (2008).

Carliell, C. M.; Barclay, S. J.; Naidoo, N.; Buckley, C.A.; Mulholland, D.A .; Senior, E. "Microbial Depolarization of a reactive azo dye under anaerobic conditions". *Water S.A*., **21** (1), 61-69 (1995).

Chan, L. S.; Cheung, W. H.; Allen, S. J.; McKay, G. "Separation of acid-Dyes Mixture by Bamboo Derived Active Carbon". *Sep. Purify. Technol*, **67**, 166-172, (2009).

Cheung, C. W.; Porter; J. F.; McKay, G. "Sorption Kinetic Analysis for the Removal of Cadmium Ions from Effluents Using Bone Char". *Water Res.*, **35** (3), 605-612, (2001).

Cheung, W. H.; Szeto, Y. S.; McKay, G. "Enhancing the Adsorption Capacities of Acid Dyes by Chitosan Nano Particles". *Bioresour. Technol*., **100**, 1143-1148, (2009).

Crini, G.; Badot, P. "Application of Chitosan, a Natural Aminopolysaccharide, for Dye Removal from Aqueous Solutions by Adsorption Processes Using Batch Studies: A Review of Recent Literature". *Prog. Polym. Sci*., **33**, 399-447 (2008).

Crini, G.; Gimbert, F.; Robert, C.; Martel, B.; Adam, O.; Morin-Crini, N.; Giorgi, F.D.; Badot, P. "The Removal of Basic Blue 3 from Aqueous Solutions by Chitosan-Based Adsorbent: Batch Studies". *J. Hazar. Mater*., **153**, 96–106 (2008).

Dögan, M.; Hamdi, M.; Karaoğlu, K.; Alkan, M. "Adsorption Kinetics of Maxilon Yellow 4GL and Maxilon Red GRL Dyes on Kaolinite". *J. Hazard Mater*, **165**, 1142-1152, (2009).

El Nemr, A.; Abdelwahab, O.; El-Sikaily, A.; Khaled, A. "Removal of Direct Blue-86 from Aqueous Solution by New Activated Carbon Developed from Orange Peel". *J. Hazard. Mater*., **161**, 102-110, (2009).

El Qada, E. N.; Allen, J. S.; Walker, G. M. "Kinetic Modeling of the Adsorption of Basic Dyes onto Steam-Activated Bituminous Coal". *Ind. Eng. Chem. Res*., **46**, 4764-4771, (2007).

El-Geundi, M. S. "Adsorption Equilibria of Basic Dyestuffs onto Maize Cob", *Adsorption Sci. & Technol*., **7**, 114-123, (1990).

El-Geundi, M. S.; Farrag, T. E.; Abed El-Ghany, H. M. (2005). "Adsorption Equilibrium of Herbicide (Pendimethalin) onto Natural Clay", *Adsorpt. Sci. Technol.*, **23**, 437-453(2005)

El-Nahhal, Y. Z.; Safi, J. M. "Adsorption of Phenanthrene on Organoclays from Distilled and Saline Water",. *J. Colloid Interface Sci*., **269**, 265-269 (2004).

Freundlich, H. M. F. "Over the Adsorption in Solution". *J. Phys. Chem*., **57**, 385-471 (1906).

Gad, H. M. H.; El-Sayed, A. A. "Activated Carbon from Agricultural By-Products for the Removal of Rhodamine-B from Aqueous Solution". *J. Hazard. Mater.*, **168**, 1070-1081, (2009).

Gilles, C. H.; Macewan, T. H.; Nakhwa, S. N.; Smith, D. A "System of Classification of Solution Adsorption Isotherms, and its Use in Diagnosis of Adsorption Mechanisms". *J. Chem. Soc*., **4**, 3973-3993, (1960).

Gömez, V.; Larrechi, M. S.; Callao. M. P. "Kinetic and Adsorption Study of Acid Dye Removal Using Activated Carbon", *Chemosphere*, **69**, 1151-1158(2007).

Grant, P. G.; Lemke, S. L.; Dwyer, M. R.; Timothy D. Phillips, T. D. "Modified Langmuir Equation for S-Shaped and Multisite Isotherm Plots", *Langmuir*, **14**, 4292-4299(1998).

Gregg, S. J.; Sing, K. S. W. "Adsorption Surface Area and Porosity", 2nd ed.; *Academic Press*, London, U.K. 1982.

Günay, A.; Arslankaya, E.; Tosun, E. "Lead Removal from Aqueous Solution by Natural and Pretreated Clinoptilolite: Adsorption Equilibrium and Kinetics". *J. Hazard. Mater*, **146**, 362-371, (2007).

Ho, Y. S. "Second-Order Kinetic Model for the Sorption of Cadmium onto Tree Fern: A Comparison of Linear and Non-Linear Methods". *Water Research*, **40**, 119-125,((2006).

Ho, Y. S.; Porter, J. F.; McKay, G. "Equilibrium Isotherm Studies for the Sorption of Divalent Metal Ions onto Peat: Copper, Nickel and Lead Single Component Systems". *Water, Air, and Soil Pollution*, **141**, 1-4, (2002).

Langmuir, I. "The Constitution and Fundamental Properties of Solids and Liquids", *J. Am. Chem. Soc*., 38, 2221-2295,(1916).

Mane, V. S.; Mall, I. D.; Srivastava, V. C. "Kinetic and Equilibrium Isotherm Studies for the Adsorptive Removal of Brilliant Green Dye from Aqueous Solution by Rice Husk Ash". *J. Environ. Manage.* **84**, 390-400, (2007).

Nassar, M. M.; Daifullah, A. A.; Magdy, Y. H.; Ebrahiem, E. E. "Uptake of Cationic Dyes by Cement Kilen Dust: Sorption Mechanism and Equilibrium Isotherm". *Adsorpt. Sci. Technol.,* **20** , 657.668,(2002).

Özcan, A.; Öncü, E. M.; Özcan, A. S. "Adsorption of Acid Blue 193 from Aqueous Solutions onto DEDMA-sepiolite". *J. Hazard. Mater*, 244.263, (2006)

Panday, K .K.; Parasad, G.; Singh, V. N. "Removal of Cr (VI) from Aqueous Solutions by Adsorption on Fly Ash-Wollastonite". *J. Chem. Technol. Biotechnol.,* **34**A, 367-374, (1984).

Ponnusami, V.; Vikram, S.; Srivastava, S. N. "Guava (Psidium guajava) Leaf Powder: Novel Adsorbent for Removal of Methylene Blue from Aqueous Solutions". *J. Hazard. Mater*, **152**, 276-286 , (2008).

Ramakrishna, K. R.; Viraraghavan, T.; Andreadakis, A. "Dye Removal Using Low Cost Adsorbents". *Water Sci. Technol.*, **36**, 189-196, (1997).

Rao, P. H.; He, M. "Adsorption of Anionic and Nonionic Surfactant Mixtures from Synthetic Detergents on Soils". *Chemosphere*, **63**, 1214-1221, (2006).

Redlich, O.; Peterson, D. L. "A Useful Adsorption Isotherm". *J. Phys. Chem*., **63**, 1024-1024, (1959).

Robinson, T.; Chandran, B.; Nigam, P. "Removal of Dyes from a Synthetic Textile Dye Effluent by Biosorption on Apple Pomace and Wheat Straw". *Water Res*., **36**, 2824-2830, (2002).

Robinson, T.; McMullan, G.; Marchant, R.; Nigam, P. "Remediation of Dyes in Textile Effluent: A Critical Review on Current Treatment Technologies with a Proposed Alternative". *Biores. Technol*., **77**, 247-255, (2001).

Sips, R. "Combined form of Langmuir and Freundlich Equations", *J. Chem. Phys*., **16**, 490-495, (1948).

Temkin, M. I. "Adsorption Equilibrium and the Kinetics of Processes on Nonhomogeneous Surfaces and in the Interaction between Adsorbed Molecules", *Zh. Fiz. Chim*., **15**, 296-332, (1941).

Treybal, R. E. "Mass Transfer Operation". 3rd ed.; *McGraw-Hill Book Company*, New York, U.S., 1985.

Vandevivere, P. C.; Bianchi R.; Verstraete, W. "Treatment and Reuse of Wastewater from the Textile Wet-Processing Industry: Review of Emerging Technologies". *J. Chem. Technol. Biotechnol*., **72**, 289-302, (1998).

Weber, T. W.; Chakravorti, R. K. "Pore and solid Diffusion Models for Fixed Bed Adsorbers". *Inst. of Chem. Eng. J.*, **20**, 228-, (1974).

Wong, Y. C.; Szeto, Y. S.; Cheung, W. H.; McKay, G. "Effect of Temperature, Particle Size and Percentage Deacetylation on the Adsorption of Acid Dyes on Chitosan:. *Adsorption*, **14**, 11-, (2008).

Wong, Y. C.; Szeto, Y. S.; Cheung, W. H.; McKay, G. "Equilibrium Studies for Acid Dye Adsorption onto Chitosan", *Langmuir*, **19**, 7888-7902, (2003).

Yener, J.; Kopac, T.; Dogu, G.; Dogu, T. "Dynamic Analysis of Sorption of Methylene Blue Dye on Granular and Powdered Activated Carbon", *Chem. Eng. J*., **144**, 400-406, (2008).

Yurdakoç, M.; Yolda¸s Seki, Y. S.; Senem Karahan, S.; Yurdakoç, K. "Kinetic and Thermodynamic Studies of Boron Removal by Siral 5, Siral 40, and Siral 80", *J. of Colloid and Interface Sci.*, **286**, 440-446, (2005).

Zollinger, H. "Colour Chemistry: Synthesis Properties and Application of Organic Dyes and Pigments", *VCH Publishers*, New York, 1991.

Smith predictor-based PI control of a wet granulation process

Tamir Shaqarin*

Mechanical Engineering Department, Tafila Technical University, Tafila 66110, Jordan

The need for prediction and reference updating in feedback control of a wet granulation process is addressed. The granulation process is often modeled as a multi-input multi-output (MIMO) linear model with dead-time. Industrial implementation of granulation process poses strict constraints on the process inputs & outputs. The presence of dead-time and the physical necessity of the input-output constraints are the key challenges of the wet granulation control. These challenges motivated the use of model predictive control (MPC) for such processes.
In this work, a Smith predictor-based proportional-integral (PI) controller is designed for the dead-time compensation. Accompanied with the reference updating method to handle the physical constraints. The regulation and reference tracking control problems are assessed via closed-loop simulations of the wet granulation model. The ability of the proposed control approach of dead-time compensation and coping with input/output constraints is rigorously proved. The current approach is compared to MPC of a similar granulation process and found superior in terms of output stability, performance and reference tracking.

Keywords: Granulation control, Dead-time compensation, Smith predictor, Reference updating, Constrained MIMO control

Introduction

In the last decade, the control of granulation is an active research field for the major benefits associated with pharmaceutical, agricultural, and chemical industries. Granulation is a process of making granules of fine particles with controlled properties such as attrition resistance, size uniformity, porosity, break-up rates, etc. Granulation process can be classified based on binder nature as dry or wet. In dry granulation, solid particles binders are added to the agitated powder then the adherence is stimulated by compaction and milling. On the other hand, wet granulation consisting of adding a liquid binder to the agitated powder blend, subsequently, the granules are processed and dried. The liquid binder is provided to the powder mixture by spraying, pouring, or dripping. Many reviews were reported on wet granulation in terms of granulator technologies, granule attributes, modeling and simulation, characterization tools, process control, and kinetics (Suresh *et al*., 2017; Iveson *et al*., 2001; Reynolds *et al*., 2005; Cameron *et al*., 2005; Burggraeve *et al*., 2013; Hansuld & Briens, 2014). The attributes measures of granules are interconnected, mainly, to bulk density and particle size distribution (Pottmann *et al*., 2000). The oversized and undersized granules are crushed and recycled to the granulation process again. The oversized granules are those greater than an upper limit and undersized granules are those smaller than a lower limit. These limits are typically considered in order to attain a desired product quality (Pottmann *et al*., 2000). The mechanism of moisture and binder addition plays a significant role in average granule size. The spray nozzle locations and the moisture and binder ow rates through nozzles influence the particle growth rate and the granulation mechanism (Pottmann *et al*., 2000). Rankell *et al*. (1964) showed that the average granule size relates directly to the spray rate and inversely to the powder bed velocity. Tardos *et al*, (1997) reported that increasing the spray surface area will effectively narrow down the particle size distribution.

Granulation improves the flow properties, reduces explosion risks, as well as gives other specific performance aspects of the granules. The complexity and the difficulties encountered in inline/online measurement of product parameters make control of the processes a key difficulty because a small change to one variable affects several process responses. According to Merkus & Meesters (2016), model based control overcomes this problem.

Efficient process control plays an essential role in realizing the preferred attributes of granules. However, it requires complex feedback control approaches and in-line or on-line monitoring of the process. One important challenge in granulation process control is finding accurate mathematical models to simulate the entire process due to infinite dimensional character of the process (Buck *et al*., 2015). Thus, in general, a process control needs to be achieved through unified use of characterization methods. These methods track the changes in granule attributes with time and modifying process parameters accordingly (Suresh *et al*., 2017). There are different control schemes for controlling granulation process. Pottmann et al., (2000) suggested using the model predictive control (MPC) for a drum granulation process. They fitted experimental data to linear discrete-time model for the process. Their control objectives are tracking the bulk density to a reference value and keeping the particle diameters within limits. Gatzke & Doyle III (2001) controlled the same model of (Pottmann *et al*., 2000) using MPC with relaxed output constraints and prioritized control objectives. Sanders *et al*. (2009) presented a linear MPC valid for a nonlinear granulation process. The linearized state-space model was derived from a nonlinear discretized population balance model. They showed that MPC provides more stability than generic PID controller. Burggraeve et al. (2012) designed a feed-forward control strategy for a top-spray fluid bed granulation process. They also presented a partial least squares (PLS) model to predict the end product density. Closed-loop feedback control for continuous wet granulation in silico was tested by Singh *et al*. (2014).

Received on June 11, 2018; accepted on 20 August, 2018
Correspondence concerning this article should be addressed to Tamir Shaqarin (E-mail address: tshagareen@ttu.edu.jo).
ORCiD ID of T. Shaqarin https://orcid.org/ 0000-0003-3327-3147

They coupled controller parameter tuning strategy with an optimization strategy. The tuning strategy includes an integral of time absolute error method. The disturbance rejection capabilities were investigated. Model free control approaches such as fuzzy logic and artificial neural network were implemented to model and control granulation process (Petrovic *et al*., 2011).

In present work, the control problem of a wet granulation process is addressed. A linear MIMO model with dead-time presented by Pottmann *et al*. (2000) is considered. A Smith (1957) predictor-based PI controller is used for dead-time compensation. In addition, the reference updating method is used to cope with the input/output constraints.

1.Material and Methods

1.1 Problem formulation

Generally, enlargement of the particle size of the granules is mainly targeted by a granulation process among other physical properties of granular material. **Figure 1** shows schematic of the wet granulation process studied herein. The spray nozzles flow rates of the liquid mixture ((u_1, u_2 and u_3) are the manipulated variables of the process. The liquid mixture that contains binding agent is introduced into particulate feed. The controlled variables of the process (y_1, y_2 and y_3) are the bulk density of the product slurry, the product particle size of particles in the 5th percentile, and the product particle size of particles in the 90th percentile. Such process set-up was previously investigated and modelled by a linear MIMO system with dead-time. For example, a black-box MIMO model introduced by Pottmann *et al*. (2000) is considered here. This model was used as a benchmark by Gatzke & Doyle III (2001) on which they implemented MPC to control the granulation. The model is represented by:

$$G(s) = \left[\frac{k_{i,j}}{\tau_{i,j}s+1} e^{-\theta_j s}\right] \qquad (1)$$

$$G(s) = \begin{bmatrix} \frac{0.20}{2s+1}e^{-3s} & \frac{0.58}{2s+1}e^{-3s} & \frac{0.35}{2s+1}e^{-3s} \\ \frac{0.25}{3s+1}e^{-3s} & \frac{1.10}{3s+1}e^{-3s} & \frac{1.30}{3s+1}e^{-3s} \\ \frac{0.30}{4s+1}e^{-3s} & \frac{0.70}{4s+1}e^{-3s} & \frac{1.20}{4s+1}e^{-3s} \end{bmatrix} \qquad (2)$$

where k is the steady state gain, τ time constant, θ dead-time, i number of outputs and j number of inputs. The steady state values for y_1, y_2 and y_3 are 40, 400, and 1620, and for u_1, u_2 and u_3 are 175, 175, and 245, respectively. The model input and output values were normalized in non-dimensional units. More details on the aforementioned model can be found in (Pottmann *et al.* 2000; Gatzke & Doyle III, 2001).

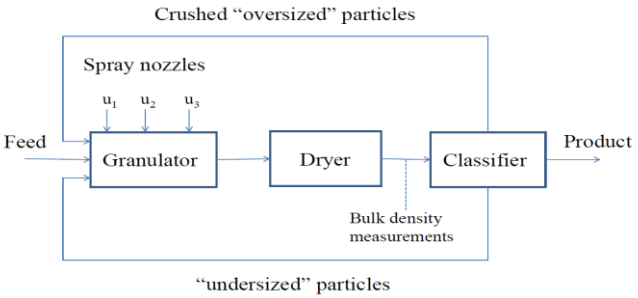

Fig.1 Continuous wet granulation process (Pottmann *et al.*, 2000)

1.2. Controller design

The control of granulation process requires the regulation of the bulk density to a certain set-point while keeping the product 9th percentile below 1650 and the product 5th percentile above 350. Meanwhile, all the nozzles flow rates must be maintained between 100 to 340. The control of granulation process suffers from the dead-time problem and the input-output constraints. In the following a Smith predictor-based PI controller is used for dead-time compensation. Furthermore, a reference updating technique is exploited to cope with the input/output constraints.

Processes with large dead-time are key challenges in the classical control feedback loop as seen in Figure 2(a), this can be

attributed to several reasons. Primarily, the control effort (u) takes some time to have an effect in the controlled variable (y). Moreover, the control effort that is generated based on real-time measurements attempts to correct past events. Furthermore, the effect of the disturbances is not detected by the controller until a significant time has passed. In general, large time-delay decreases the phase margins of classical controller that urges the closed-loop system toward instability (Normey-Rico, 2007).

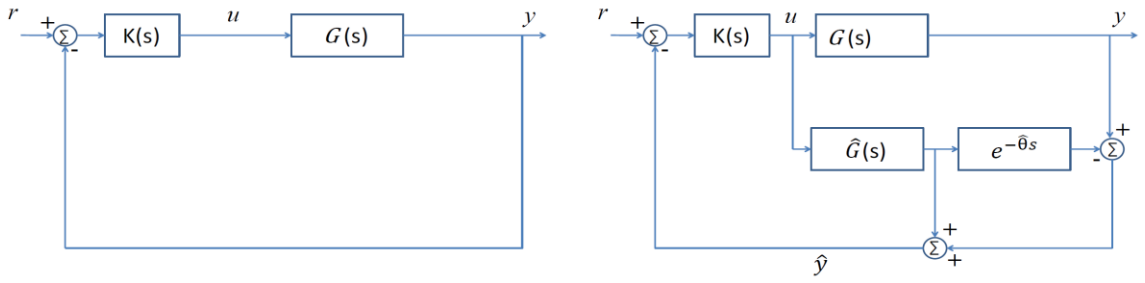

(a) Without Smith predictor (b) With Smith predictor

Fig. 2 Closed-loop control structure.

The Smith (1957) predictor is the most common technique for dead-time compensation. The structure of this predictor is depicted in **Figure 2**. The controller output u is fed through a model of the process and through the same model without dead-time. This way, the controller acts on a simulated process which behaves as if there was no dead-time in the process (in the ideal case of a perfect modeling). The MIMO granulation model in Eq. (1) & (2) can be substantially simplified as a MIMO system with single dead-time, such as

$$G(s) = \left[\frac{k_{i,j}}{\tau_{i,j}s+1} e^{-\theta_j s}\right] := \left[\frac{k_{i,j}}{\tau_{i,j}s+1}\right] e^{-\hat{\theta}s} = \hat{G}(s)e^{-\hat{\theta}s} \qquad (3)$$

Then, the model is decomposed into rational part ($\hat{G}(s)$) and irrational part ($e^{-\hat{\theta}s}$). Such decomposition benefits from the fact that the time-delays θ_j in the aforementioned nominal model are all equal. From Figure 2(b), the predicted output $\hat{y}$ in the Laplace domain can be written as:

$$\hat{Y} = GU - \hat{G}Ue^{-\hat{\theta}s} + \hat{G}U$$

In the nominal case ($G(s) = \hat{G}(s)e^{-\hat{\theta}s}$), then:

$$\hat{Y} = \hat{G}U = \hat{G}K(R - \hat{Y})$$

$$\hat{Y} = (I + \hat{G}\,K)^{-1}\ \hat{G}KR$$

That is used to compute the output y, such as:

$$Y = GU = GK\left(R - \hat{Y}\right) = GK\left(R - (I + \hat{G}\,K)^{-1}\ \hat{G}KR\right)$$

$$Y = GK\left(I + \hat{G}\,K\right)^{-1}R$$

where the closed-loop transfer function from r to y is $\left(I + \hat{G}\,K\right)^{-1}$. This extension of Smith predictor to MIMO system with single dead-time ensures all the SP benefits for the SISO systems (Normey-Rico, 2007); the delay free characteristic equation ($det\left(I + \hat{G}\,K\right) = 0$), output prediction ($\hat{Y} = \hat{G}U$) and ideal decoupled dynamic compensation ($G = \hat{G}e^{-\hat{\theta}s}$).

The controller K is a chosen as a diagonal matrix of PI controllers, such that:

$$K(s) = \begin{bmatrix} \frac{g_1(T_1s+1)}{T_1s} & 0 & 0 \\ 0 & \frac{g_2(T_2s+1)}{T_2s} & 0 \\ 0 & 0 & \frac{g_3(T_3s+1)}{T_3s} \end{bmatrix} \qquad (4)$$

The design of the PI controllers is based on the method presented in Normey-Rico (2007). The controller gain g_i is selected to be proportional to the inverse of the diagonal model gain k_{ii}. Then it is tuned to have the desired performance characteristics. The

integral time T_i is selected to be equal to the diagonal model time constant τ_{ii}. Then,

$$g_i \propto \frac{1}{k_{ii}}, \qquad T_i = \tau_{ii}$$

The control of MIMO system is more difficult when imposing input/output constrains. Generally, controlling constrained MIMO systems motivates the use of MPC (Goodwin *et al.*, 2005) or adaptive MPC (Landau *et al.*, 2011). The control of the granulation process is a constrained MIMO control problem. Fortunately, only one output (y_1) should be regulated to a set point while the other outputs (y_2 & y_3) are constrained within certain limits. This fact makes the granulation process an excellent candidate for reference updating method. **Figure 3** depicts the fundamental concept of the reference updating method. Basically, simultaneous change of the reference of the unregulated output as a function of u, can limit the control action within certain bounds, such that

$$r = K_r f(u) \qquad (5)$$

The design of the proportional gain K_r is dictated by the steady state input-output relationship in Eq. (6). Basically, K_r is designed in such a way that when the control action u is approaching towards one of the bounds, the reference is adjusted accordingly to drive the control action in the opposite direction.

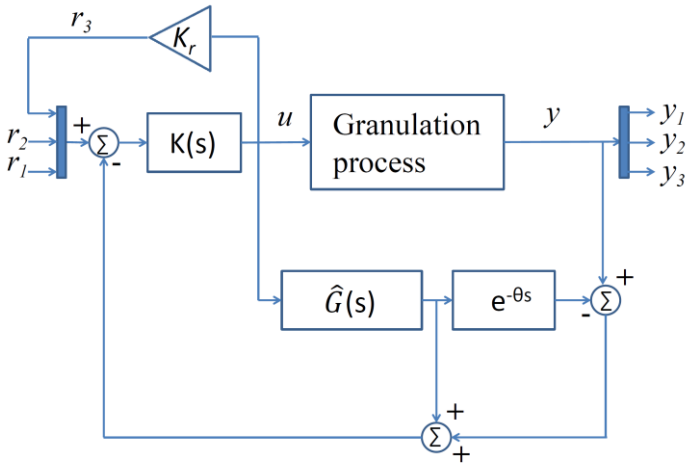

Fig. 3 Closed-loop control structure with Smith predictor and reference updating.

$$\begin{bmatrix} y_1 \\ y_2 \\ y_3 \end{bmatrix}_{ss} = \begin{bmatrix} 0.20 & 0.58 & 0.35 \\ 0.25 & 1.10 & 1.30 \\ 0.30 & 0.70 & 1.20 \end{bmatrix} \begin{bmatrix} u_1 \\ u_2 \\ u_3 \end{bmatrix}_{ss} \qquad (6)$$

Assuming zero steady state error ($r = y_{ss}$).

$$\begin{bmatrix} u_1 \\ u_2 \\ u_3 \end{bmatrix}_{ss} = \begin{bmatrix} 5.1282 & -5.6410 & 4.6154 \\ 1.1257 & 1.6886 & -2.1576 \\ -1.9387 & 0.4253 & 0.9381 \end{bmatrix} \begin{bmatrix} r_1 \\ r_2 \\ r_3 \end{bmatrix} \qquad (7)$$

For example, if the goal is to minimize u_1 in the case of positive r_1, one possibility is the following: r_2 and r_3 should be chosen to be positive and negative, respectively, as shown from the first raw of Eq. (7).

2. Results and Discussion

Assessment of the performance of the proposed control approach requires classic closed-loop simulations of the granulation process. The MIMO PI controller parameters were designed as was discussed here. The PI controller parameters are as follows:

$$K(s) = \begin{bmatrix} \frac{2(2s+1)}{2s} & 0 & 0 \\ 0 & \frac{2.27(3s+1)}{3s} & 0 \\ 0 & 0 & \frac{2.083(4s+1)}{4s} \end{bmatrix}$$

The closed-loop simulations of the wet granulation process with the Smith predictor-based PI controller and the PI controller are shown in **Figure 4**. The figure depicts the closed-loop response of the controlled variables (y_1, y_2 and y_3) and the control effort (u_1, u_2 and u_3) against step reference for the bulk density (y_1). As shown in Figure 4, the response from the PI controller without prediction is on the verge of instability, which proves the need for prediction in the granulation process. Although the Smith predictor-based PI controller produces an improved performance stable closed-loop response with zero steady-state error, it significantly violates the quality constraint on the first nozzle flow rate u_1.

Apart from the stability improvements due to prediction, the control constraints problem needs further improvements. Since the control objective is to regulate the bulk density (y_1) while keeping the other controlled variables y_2 and y_3 bounded. This gives rise to the reference updating method, which is a good candidate to limit the controller effort in the control of MIMO process as discussed in section 3.2. Assume that $r_2 = 0.6r_1$ and$r_3 = K_r u_1$, where $K_r = -0.1$, so that u_1 have a negative action on r_3 and consequently u_1 is decreased. **Figure 5** depicts the closed-loop response of the granulation process with the Smith predictor-based PI controller and reference updating. Obviously, it can be seen from the figure that this approach is successful to limit the control action u_1 within its bounds. The figure also compares the result from the Smith predictor-based PI controller with closed-loop results for the granulation system using prioritized objective MPC control (Gatzke & Doyle III, 2001). It is evident that the results from the current method are more superior in many aspects: stabilizations, regulation, respecting quality constraints, etc.

The proposed control approach is examined against reference tracking problem as seen in **Figure 6**. The controlled variables (y_1, y_2 and y_3) were able to track references efficiently, even though the reference r_3 is a function of the control effort u_1. Meanwhile, all the control efforts (u_1, u_2 and u_3) were maintained within the quality constraints.

In order to test the controller robustness and the ability of the predictor to cope with the mismatched time-delays. A mismatched model is introduced via perturbing the time-delays (θ_j) by 33% of its nominal values, and the process parameters (k_{ij}, τ_{ij}) are increased by 10% of its nominal values. Figure 6 also compares the closed-loop response based on the nominal model (see Eq. (2)) with closed-loop response based on aforementioned mismatch model using the same control technique. In one hand, the figure shows that the proposed controller is robust against the specified model mismatch. But, on the other hand the control effort u_1 is trying to violate its lower bound due to model uncertainty. Hence, the robustness of such approach still needs further investigations.

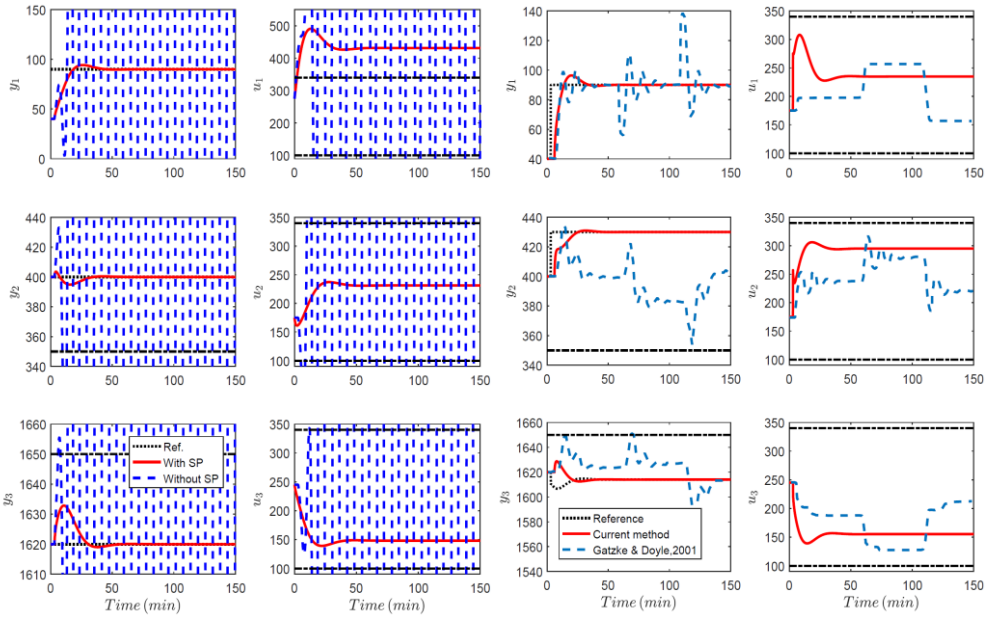

Fig.4 Closed-loop response of the granulation system with/without Smith predictor.

Fig. 5 Closed-loop response of the granulation system with SP and reference updating compared to MPC (Gatzke & Doyle, 2001).

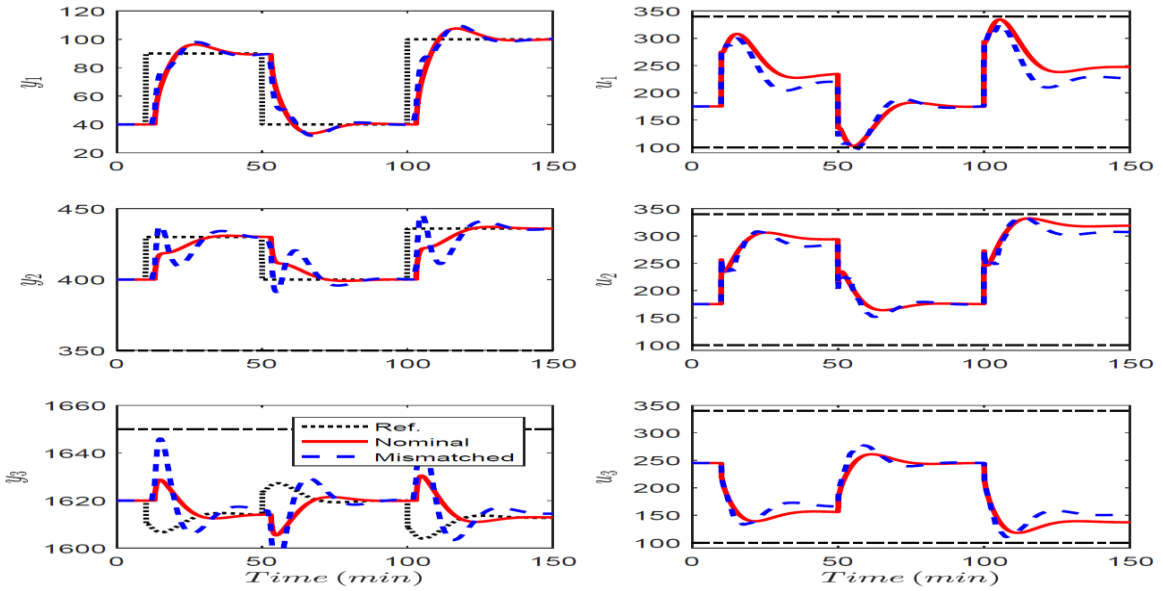

Fig. 6 Aspect ratio closed-loop response of the granulation system with SP and reference updating for the nominal and mismatched case.

Conclusions

A successful MIMO controller design of a wet granulation process is achieved. The MIMO control approach involves the design of Smith predictor-based PI controller for dead-time compensation. Along with the reference updating method that is introduced to cope with the input/output physically imposed constraints. The performance of the suggested control approach is examined and verified through closed-loop simulations. The proposed control approach was found more efficient than other widely used control techniques for the granulation process such as model predictive control. Although promising model uncertainty robustness of the controller is achieved, a complete robustness analysis still needs further investigations in the future work.

Nomenclature

g	= controller gain	[—]
$G(s)$	= granulation model transfer function	[—]
$\hat{G}(s)$	= rational part of G(s)	[—]
k	= steady state gain	[—]
K	= controller transfer function	[—]
K_r	= reference updating gain	[—]
r	= reference	[—]
s	= Laplace operator	[—]
T	= integral time	[min]
$u_{1,2,3}$	= dimensionless nozzles flow rate	[—]
y	= dimensionless model output	[—]
$\hat{y}$	= dimensionless predicted output	[—]
y_1	= dimensionless bulk density of the product slurry	[—]
y_2	= product particle size in the 5th percentile	[—]
y_3	= product particle size in the 90th percentile	[—]
y_{ss}	= steady state output	[—]
τ	= time constant	[min]
θ	= dead time	[min]
$\hat{\theta}$	= nominal dead time	[min]

References

Buck, A., Palis, S. & Tsotsas, E." Model-based control of particle properties in fluidized bed spray granulation", *Powder Technology*, **270**, 575-583 (2015)

Burggraeve, A., Monteyne, T., Vervaet, C., Remon, J. & De Beer, T. "Process analytical tools for monitoring, understanding, and con-trol of pharmaceutical fliuidized bed granulation: a review", *European Journal of Pharmaceutics and Biopharmaceutics*, **83**, 2-15 (2013)

Burggraeve, A., Silva, A., Van Den Kerkhof, T., Hellings, M., Vervaet, C., Remon, J., Vander Heyden, Y. & De Beer, T. "Development of a uid bed granulation process control strategy based on real-time process and product measurements". *Talanta*,**100**, 293-302 (2012)

Cameron, I. T., Wang, F. Y., Immanuel, C. D. & Stepanek, F."Process systems modelling and applications in granulation: A review", *Chem. Eng. Sci*., **60**, 3723-3750 (2005)

Gatzke, E. P. & Doyle III, F. J. "Model predictive control of a granulation system using soft output constraints and prioritized control objectives", *Powder Tech.*, **121**, 149-158 (2001)

Goodwin G. C., Seron M. M. & De Don J. A.,"Constrained Control and Estimation: An Optimization Approach", *Springer*, London, (2005).

Hansuld, E. M. & Briens, L. "A review of monitoring methods for pharmaceutical wet granulation", *Inter. Jour. of pharmaceutics*, **472**, 192-201 (2014)

Iveson, S. M., Litster, J. D., Hapgood, K. & Ennis, B. J. "Nucleation, growth and breakage phenomena in agitated wet granulation processes: A review", *Powder Tech.*, **117**, 3-39 (2001)

Landau I. D., Lozano R., M'Saad M. & Karim A. "Adaptive Control: Algorithms, Analysis and Applications", *Springer*, New York, (2011)

Merkus, H. G. & Meesters, G. M. :"Production, Handling and Characterization of Particulate Materials", *Springer*, (2016)

Normey-Rico, J. E.;"Control of Dead-Time Processes", *Springer Science & Business Media*, (2007)

Petrovic, J., Chansanroj, K., Meier, B., Ibric, S. & Betz, G. "Analysis of fluidized bed granulation process using conventional and novel modeling techniques", *Euro. Jour. of Pharmaceutical Sci.*, **44**, 227-234 (2011)

Pottmann, M., Ogunnaike, B. A., Adetayo, A. A. & Ennis, B. J. "Model-based control of a granulation system", *Powder Tech.*, **108**, 192-201 (2000)

Rankell, A. S., Scott, M. W., Lieberman, H. A., Chow, F. S. & Battista, J. V. "Continuous production of tablet granulations in a fluidized bed II. operation and performance of equipment", *Jour.of Pharmaceutical Sci.*, **53**, 320-324 (1964)

Reynolds, G. K., Fu, J. S., Cheong, Y. S., Hounslow, M. J. & Salman, A. D. "Breakage in granulation: a review", *Chem. Eng. Sci.*, **60**, 3969-3992 (2005)

Sanders, C. F., Hounslow, M. J. & Doyle III, F. J. "Identification of models for control of wet granulation", *Powder Tech.*, **188**, 255-263 (2009)

Singh, R., Barrasso, D., Chaudhury, A., Sen, M., Ierapetri-tou, M. & Ramachandran, R. "Closed-loop feedback control of a continuous pharmaceutical tablet manufacturing process via wet granulation", *Jour. of Pharmaceutical Innov.*, **9**, 16-37 (2014)

Smith, O. J. M. "Posicast control of damped oscillatory systems", *Proceedings of the IRE*, **45**, 1249-1255 (1957)

Suresh, P., Sreedhar, I., Vaidhiswaran, R. & Venugopal, A. "A comprehensive review on process and engineering aspects of pharmaceutical wet granulation", *Chem. Eng. Jour.*, **328**, 785-815 (2017)

Tardos, G. I., Khan, M. I. & Mort, P. R. "Critical parameters and limiting conditions in binder granulation of ne powders", *Powder Tech.*, **94**, 245-258 (1997)

Improved Configurations For Liquefied Natural Gas Cycles

Said Al Rabadi[1]*, Rainer Sapper[2], Sadeq Emeish[3], , Falah Fahed Banihani[4]

1) Al-Balqa Applied University , Department of Chemical Engineering, , 19117 Salt, Jordan,

2) Technical Manager, The Linde Group, Dr.-Carl-von-Linde-Strase 6-14, 82049 Pullach im Isartal/ Germany

3) Department of Chemical Engineering, Al-Balqa Applied University, 19117 Salt, Jordan

4) *Department of Chemical Engineering, Al-Balqa Applied University, 19117 Salt, Jordan*

Keywords: Liquefaction, natural gas, mixed refrigerant cycle, power-efficient, design criteria

The most important challenge in a natural gas liquefaction plants is to improve the plant energy efficiency. A process topology should be implemented, which results in a considerable reduction of energy consumption as the natural gas liquefaction process consumes a large amount of energy. In particular, system design focusing on configuring cold part cycle is an attractive option. In this study, various energy recovery-oriented process configurations and the potential improvements of energy savings for small- & mid-scale liquefied natural gas plants were proposed and compared with almost exclusively commercial trademarks processes. These improved simulation based investigations were validated under the variation in feed gas pressure, mixed refrigerant cooling reference temperature and the pinch temperature of cryogenic plate fin heat exchanger. The simulation results exhibited considerable reduction of specific total energy consumption. Therefore, the proposed liquefaction cycles have a simple topology, hence lower capital cost and compacter plant layout, which is compatible for power-efficient, offshore, floating liquefied natural gas liquefaction plants**.**

Introduction

Liquefaction process of natural gas includes the physical conversion of NG from gas to liquid phase. Liquefied natural gas takes up a factor of about 1/600th the volume of natural gas in the gaseous state. The natural gas is then condensed into a liquid phase at close to atmospheric pressure by cooling it to approximately −160 °C (−260 °F) (Smith *et al* . (1996), Cengel and Boles (2002), Jacobson (2009)). Cryogenic LNG carriers or cryogenic road/trail tankers are used for its transport. LNG is principally used for transporting natural gas, where it is then re-gasified and distributed to the markets.

The natural gas fed into the LNG plant will be treated to remove condensate, Mercury, H_2S, COx and NOx that will freeze under the cryogenic temperature ranges (Devold (2013), Metz and Davidson (2005)). A typical LNG process is shown in Fig. 1. NG is first extracted and transported to a processing plant, where the feed gas pressure is presumed at a certain value. After that NG is treated against any heavy hydrocarbons and mud/ slug, it is then purified by removing acid gases such as CO_2, NOx and H_2S by utilizing an Amine washing solvent. This solvent is regenerated by introducing it to stripper column (by products like sour gas and waste water are obtained and disregarded to a battery limit). At this stage the sweet NG stream is wet and still might contain traces of Mercury, LNG process train is designed to remove any Hg content to prevent mercury amalgamizing with aluminium in the cryogenic heat exchangers, while the water content is adsorbed in a special dehydration unit. The drier is regenerated by the boil off gas obtained from downstream LNG storage unit. The gas is then cooled down in stages until it is liquefied. LNG is finally stored in storage tanks to be loaded and shipped.

The heart of a LNG plant, as highlighted in **Figure 1**, is NG liquefaction and refrigeration cycle, where these stages are the highest energy density units of a LNG plant. Hence then designing these units will have the major impact on the capital and operating costs of the plant. In order to reach the cryogenic temperature ranges for liquefying NG, a mixture of Nitrogen and light hydrocarbons mainly Methane, Ethane and Propane is implemented as refrigerant.

As shown in PT curve for different gases, presented in **Figure 2**, where the vapour pressure is plotted as a function of gas temperature. Such a refrigerant mixture can reduce the process temperature to a cryogenic range lower than -190°C at 1 bar, which is quite enough for liquefying NG. The composition of MRC is subject to alternation depending on the NG composition as well to the feed gas operating pressure (shown in the variation of NG condensation curves at pressure of 1 bar and 25 bar) and the reference cooling refrigeration temperature

Received on June 4, 2018; accepted on 20 August, 2018

Correspondence concerning this article should be addressed to Said Al Rabadi (E-mail address: said.alrabadi@bau.edu.jo).

ORCiD ID of Said Al Rabadi https https://orcid.org/0000-0002-6007-2853

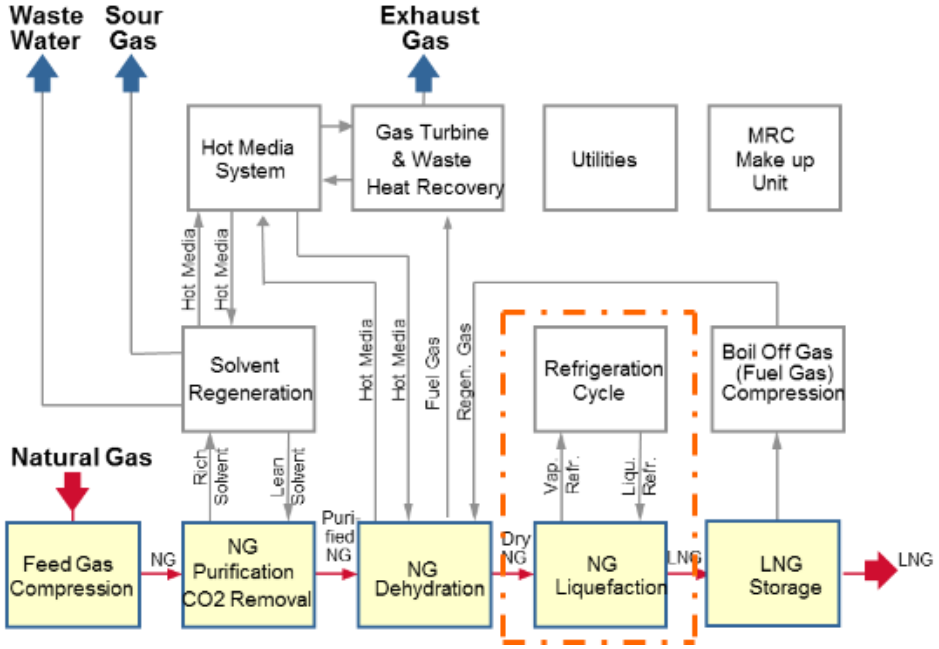

Fig. 1 Block diagram of a LNG process, (Devold (2013)**)**

.

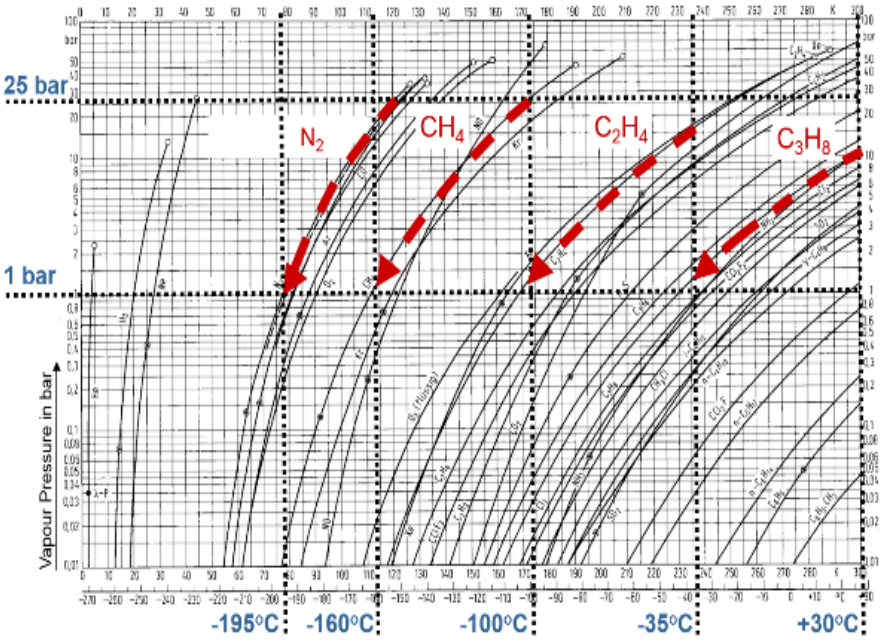

Fig. 2 PT diagram from different gases (Smith *et al.* (1996))

LNG processes are licensed by large oil and gas companies, but are generally based on a one- or multi-stage cooling process with pure or mixed refrigerants (Long *et al*. (2016)). The main types of LNG process are listed in **Table 1**, including mainly cascade, MR and expander/ booster processes. Each process has different characteristics in scalability, investment cost and energy efficiency. For floating LNG, e.g., possibly lower weight is desired due to its low CAPEX, even its energy efficiency is significantly lower than the best cascade or MR processes. The reason is that the gas has a heat load to temperature (Q/T) curve that will improve stability, throughput and efficiency. The curve tends to show three distinct regions; pre-cooling, liquefaction and sub-cooling. All of these regions are characterized by having different curve behaviours, or specific heats, along the process. Keep in mind that the (Q/T) curve shape is different for different gas compositions.

Table 1 List of commercial LNG refrigeration processes

Process		Licenser	Features
SMR	PRI CO [Andress (1996)]	Black & Veatch	SMR, Limited capacity ≤ 1.3 MTPA, low CAPEX
	DMR [Agrawal (1998)]	Shell	Two refrigerant cycles, large scale, high CAPEX
	MFCP [Foss (2005), Coll (2008), Wonsub and Kwangho (2013)]	Statoil/ Linde	Mixed refrigerant cycles, large capacity, need for external refrigerants storage, high CAPEX
	LIMUM [Stockman *et al*. (2002)]	Linde	SMR, large scale, need for external refrigerants storage
Cascade	Cascade cycle [Pereira and Lequisiga (2014), Andress (1996)]	Conoco Phillips	Separate refrigerant cycles with C1, Ethylene and C3, large capacity, high CAPEX
	C3MR [Pereira and Lequisiga (2014)]	APCI	Utilizes two C3 and MR cycles, widely spread, large capacity ≥ 5 MTPA, low energy density
	Self-refrigerated LNG [Fischer-Calderon (2003)]	BP	No compressor, low production rate (high energy density), capacities ≥ 1.3 MTPA
Expander/ booster	Expander cycle [Perez and Dietz (2009), Wonsub and Kwangho (2013)]]	Kryopak	Expander/ booster, no liquid refrigerant, high energy density

1.Material and Methods

In this study, simulation based investigations on the NG liquefaction and refrigeration cycle with different topologies were performed, utilizing the so called OPTISIM® as the process simulator, which is still under development and is thus no fully adopting actual mainstream strategies in process industry. Nevertheless, OPTISIM proves its strength in process design and rating as well as in process dynamic simulations. An outline of the simulator's key features is presented in (Kroner (2006)).

Also these investigations are valid for small- & mid-scale plants from the plant capacity point of view. The purpose of these theoretical investigations is to identify the improvements of process configurations of natural gas liquefaction cycles, and to be compared with trademarks of refrigeration processes. The comparing criteria include the specific energy consumption with respect to the variation in feed gas pressure, MR cooling reference temperature and the pinch temperature of PFHE. impacts on the design criteria of PFHE, named as NG stream to PFHE, LNG product stream from PFHE routed to LNG storage tank and Fuel stream obtained as boil off gas stream from storage tank. The Fuel stream is principally a cold temperature stream that should be warmed to near room temperature conditions for better combustion conditions as well to get benefit of its cooling duty in PFHE, hence to decrease cooling duty of MRC compressor.

The pre-defined process parameters are listed in **Table 2**. Three main streams are foreseen that have the major impacts on the design criteria of PFHE, named as NG stream to PFHE, LNG product stream from PFHE routed to LNG storage tank and Fuel stream obtained as boil off gas stream from storage tank. The Fuel stream is principally a cold temperature stream that should be warmed to near room temperature conditions for better combustion conditions as well to get benefit of its cooling duty in PFHE, hence to decrease cooling duty of MRC compressor. A typical lean natural gas feed stream is considered for the theoretical investigations, where its Methane content concentrates to more than 90 mol % due to upstream processing units (namely Slug Catcher for capturing solid particulates in NG feed, Amine washing and dehydration (Jacobson (2009), Devold (2013), Metz and Davidson (2005), Laursen and Karavanov (2006)) of other associated components in NG. Ethane and Propane contents in LNG stream are presumed around the typical figures in order to meet the foreseen heating value of LNG; typical LNG heating values in the range of 41,000 – 50,000 kJ/kg (Foss (2005)). Nitrogen due to its lower boiling temperature than that of Methane basically concentrates in the fuel gas stream, which can be operated by conventional gas turbine without further obstacles (Coll *et al*. (2008))

Table 2 Process parameters of natural gas streams

Stream		NG	LNG	Fuel
Temp.	[K]	303.2	112.0	299.0
P	[bar]	65	1.2	1
Mass flow	[t/h]	339.7	300	39.7
CH4	[mol %]	91.7	92.9	81.98
C2H6	[mol %]	5.25	5.9	0.01
C3H8	[mol %]	0.35	0.4	trace
N2	[mol %]	2.7	0.8	18.01

Table 3 Overview of MRC boundary conditions for all investigated processes valid for a MR cooling reference temperature of 30 ºC and an outlet pressure of 65 bar from MRC 2nd stage cycle compressor

	MRC process conditions (These figures are deduced from reference operating plant)						
Process	1	2	3	4	5	6	7
PFHE							
dT_{min} [K]	2.0	3.7	3.7	3.8	3.6	3.6	3.6
d_{pFuel} [bar]	0.2	0.2	0.2	0.2	0.2	0.2	0.2
d_p [bar]	0.4	0.4	0.4	0.4	0.4	0.4	0.4
Q_{iso} [kWh/tLNG]	3.33	3.33	3.33	3.33	3.33	3.33	3.33
MRC 1st Stage Compressor							
η_{isen} [%]	80	80	80	80	80	80	80
T_{inlet} [K]	299.9	298.2	298.6	300.5	299.5	300.6	298.9
T_{outlet} [K]	376.9	409.6	383.5	389.6	376.3	373.4	385.2
Poutlet [bar]	26.2	39.0	25.9	17.3	24.8	25.8	26.1
d_p [bar]	0.3	0.3	0.3	0.3	0.3	0.3	0.3
MRC 2nd Stage Compressor							
η_{isen} [%]	80	80	80	80	80	80	80
T_{outlet} [K]	423.1	339.4	369.0	393.7	380.6	370.5	395.6
P_{outlet} [bar]	65	65	65	65	65	65	65
MRC_{pump}							
P_{inlet} [bar]	-	-	25.4	16.8	24.3	25.3	-
Cooling Water Heat Exchangers							
dp_{MR} [bar]	0.5	0.5	0.5	0.5	0.5	0.5	0.5

Table 3 shows the boundary conditions for all MRC processes. These boundary conditions are valid for a MR cooling reference temperature of 30°C and an outlet pressure of 65 bar from 2nd stage cycle compressor. Based on practice of the MRC processes for small- & mid-scale plants with different configurations, seven topologies are presented below for the purpose of these investigations. They utilize SMR liquefaction process with two stages MRC compressors. In the first stage the pressure is increased from suction pressure of about 2 bar to MP figures, and in the second stage the MP values are increased to HP of 65 bar. This value is kept identical and is set as simulation constraint for all investigated processes. Process 1 and 7 represent the so called PRICO and the enhanced PRICO processes respectively (Andress (1996)), while 2 till 5 actual topologies collected from built small- & mid-scale LNG plants (Foss (2005), Coll (2008), Wonsub and Kwangho (2013)), which were constructed and taken in operation under different metrological regions. Process 6 is enriched with potential modifications with the aim to increase the refrigeration process efficiency as well as plant stability (Al Rabadi (2017)). Followingly, a brief description of each process is presented.

In principle, process 1 (Andress (1996)), is a MRC process without MRC pump nun MP separator, Fig. 3. The cooling is provided by a closed MRC, which consists of a components mixture like Nitrogen, Methane, Ethane and Propane, its composition depends on the process operating conditions. The refrigerant is withdrawn from PFHE at a temperature of approx. 299.9K and a pressure of about 2 bar. It is compressed in the 1st stage refrigerant cycle compressor, and cooled against cooling water in Cycle Compressor After cooler to a MR cooling reference temperature of 30°C.

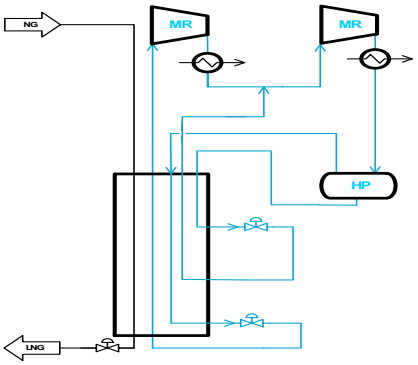

Fig. 3 Descriptive sketch of process 1 (Andress (1996))

The gaseous refrigerant is further compressed in the 2nd stage cycle compressor and afterwards cooled against cooling water to a MR cooling reference temperature of 30°C. The gas will be partially condensed. Liquid and gas are separated in HP Separator. The liquid from the HP separator is rooted to PFHE where it is sub-cooled and then is used for the pre-cooling of the natural gas after expansion in a Joule-Thomson expansion valve. The gas MR from HP separator is cooled in PFHE and provides the final cold for the natural gas sub-cooling after expansion in Joule-Thomson expansion valve. After expansion to a pressure of approx. 2.6 bar, the gas MR stream is warmed up in PFHE and returns to the suction side of the 1st stage Cycle Compressor. The composition of the MRC stream to the 2nd stage cycle compressor is changed due to mixing the liquid MR stream routed from HP separator to PFHE with the outlet stream from 1st stage after cooler. The cycle liquid refrigerant stream routed from HP separator to PFHE is overheated above dew point temperature with a temperature safety margin of 5 K for protecting the downstream MRC compressor from two-phase flow. Make up for the refrigerant system is required mainly due to MR losses via the gas seals of the MRC Compressor.

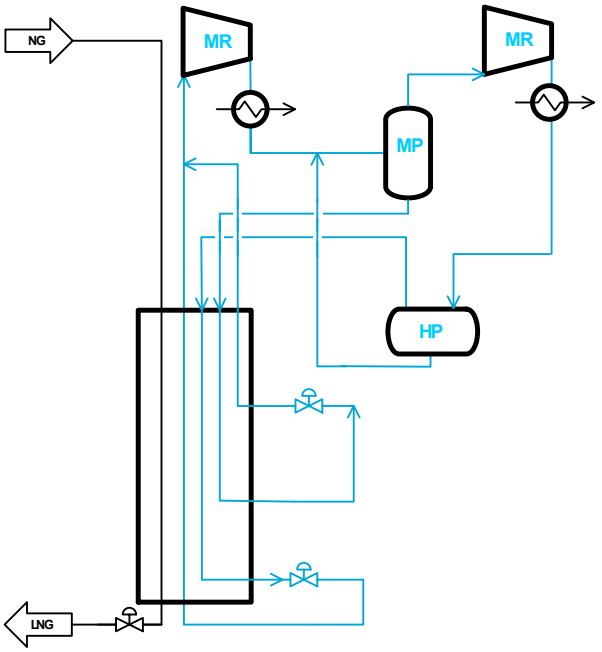

Fig. 4 Descriptive sketch of Process 2 (Foss (2005))

Process 2: MRC Process (Foss (2005)) is without MRC pump identical to process 1, nevertheless with inclusion of MP separator, refer to **Figure 4**, other process flow conditions are almost similar. MP separator is foreseen to have an impact on the behaviour of (Q/T) diagram in the pre-cooling region, through the inclusion of liquid MP MR to PFHE and hence changing the NG pre-cooling duty. HP MR liquid stream provides the pre-cooling duty of NG after expansion in JT valve at provides the sub-cooling duty of NG at the warm end of PFHE. While HP MR gas stream provides the sub-cooling at the cold end of PFHE after

expansion in JT valve.

Process 3: Coll (2008) presents this MRC process with MP separator like in process 2, with the difference the liquid MR from MP separator is pumped and combined with the partially condensed outlet MR stream from MRC 2nd stage compressor after cooler, then it is routed to HP separator. Although of the expected higher energy consumption due to MRC pump as well the increased CAPEX, Process 3 is modified to meet certain cooling process demands, refer to **Figure 5.**

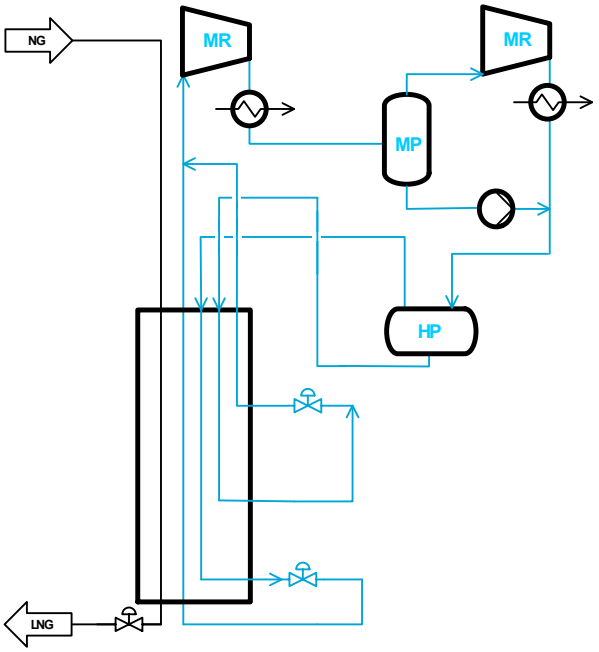

Fig. 5 Descriptive sketch of Process 3 (Coll (2008))

Process 4: is given in (Wonsub and Kwangho (2013)) as a MRC Process with mixing liquid and gaseous MR streams from both warm & cold ends of PFHE, refer to **Figure 6**, other MRC process conditions are identical to process 3. The MR gas stream from HP separator is combined with the MR liquid stream (mixing cold and warm parts of PFHE), then both streams are joined and warmed up in PFHE and return to the suction side of the 1st stage Cycle Compressor. Although keeping this stream at a safety margin from dew point to protect the downstream 1st stage MRC compressor, the combination of both streams have to a great extent an impact on liquefaction duty of PFHE.

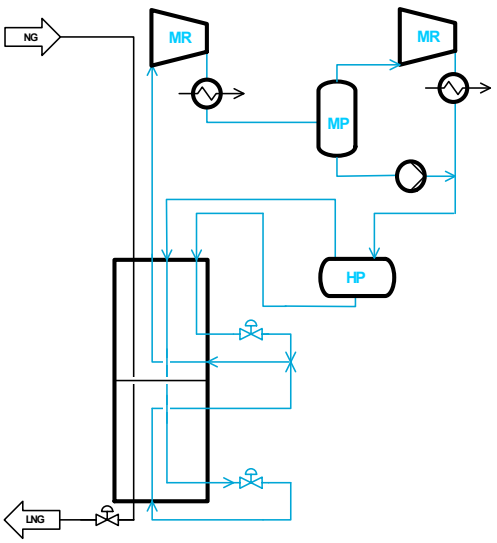

Fig. 6 Descriptive sketch of Process 4 (Wonsub and Kwangho (2013))

Process 5: Refrigeration Process with mixing liquid and gas HP MR streams from both warm & cold ends of PFHE, and using a cold MRC separator at the cold end of PFHE (Wonsub and Kwangho (2013)), other MRC process conditions are identical to process 4, refer to **Figure 7**. The liquid from the cold MRC separator is sub-cooled in PFHE and is used as refrigerant for PFHE after expansion in a Joule Thomson expansion valve. The gas stream from the cold MRC separator is cooled, hence is partially condensed in PFHE to provide the final cold for NG sub-cooling after expansion in a JT val.ve. Then the HP MR gas stream is warmed up in PFHE and mixed with the cycle MR liquid stream from the cold MRC separator after expansion at the cold part of PFHE, then the resulting two phase stream is warmed up in PFHE. The two phase stream is mixed again with the cycle liquid MR stream after expansion at the warm part of PFHE then returns to the suction side of the 1st stage Cycle Compressor. In spite of the increased CAPEX of this process, it is believed that the combined two phase MR stream would provide more significant pre-cooling duty of PFHE, as well achieve a considerable safety margin from dew point of this stream to protect 1st Stage MRC compressor.

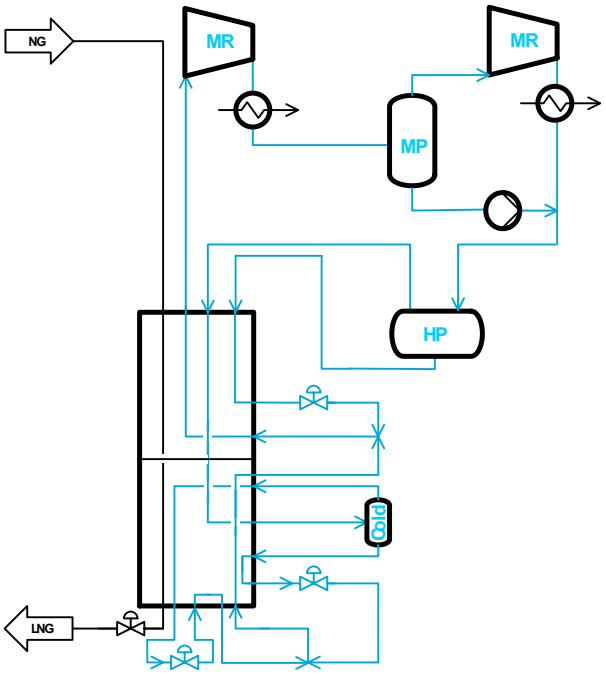

Fig. 7 Descriptive sketch of Process 5 (Wonsub and Kwangho (2013))

Process 6: MRC Process with PFHE, is considered for the comparison in these investigations and is briefly presented in (Al Rabadi (2017)). New process improvements are introduced to its topology with respect to what was given in (Stockman *et al.* (2002)); two MRC pumps are implemented in this process. First to pump liquid MR stream from MP separator to HP separator, the second pump is used to transport liquid MR from HP separator to be combined with the gaseous MR from HP separator. Combined stream, after expansion in JT valve, it provides the liquefaction and pre-cooling duties of PFHE, refer to Figure 8. It is believed, even of the increased number of pumps, that the PFHE is compacter compared to process 5. Hence then a significant lower layout of the cold box is achieved.

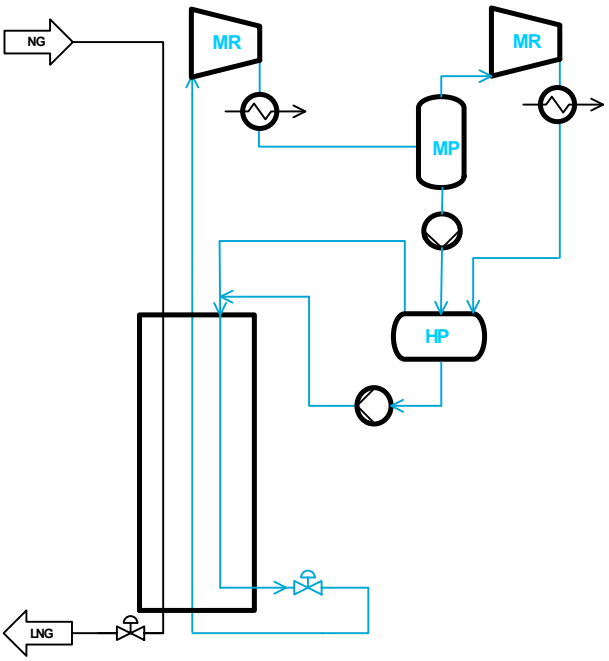

Fig. 8 Descriptive sketch of Process 6 (Model Refrigeration concept)

Process 7: so called Enhanced PRICO process is presented in (Andress (1996)) and is illustrated in **Figure** 9. Briefly, this MRC process topology is almost similar to that of process 5, with the difference that liquid MR from HP separator is routed back after expansion in JT valve to a traditional shell and tube heat exchanger, where it is warmed against the liquid MR from MP separator to essentially provide the pre-cooling duty of PFHE through the liquid MR from MP separator after its JT expansion at the warm end of PFHE. As mentioned above, the presence of cold MR separator promotes the sub-cooling duty of PFHE.

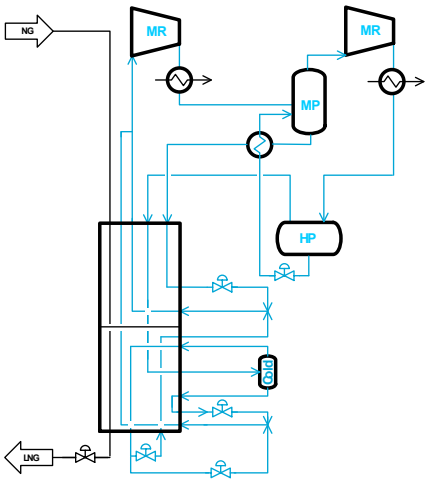

Fig. 9 Descriptive sketch of Process 7 (Andress (1996))

2. Results and Discussion

The findings of the theoretical investigations of above mentioned processes are outlined through the behavior of (Q/T) diagram of PFHE for each process, and the specific total energy consumption (energy consumed per produced ton of LNG) under the variation of the MR cooling reference temperature as well the feed gas pressure.

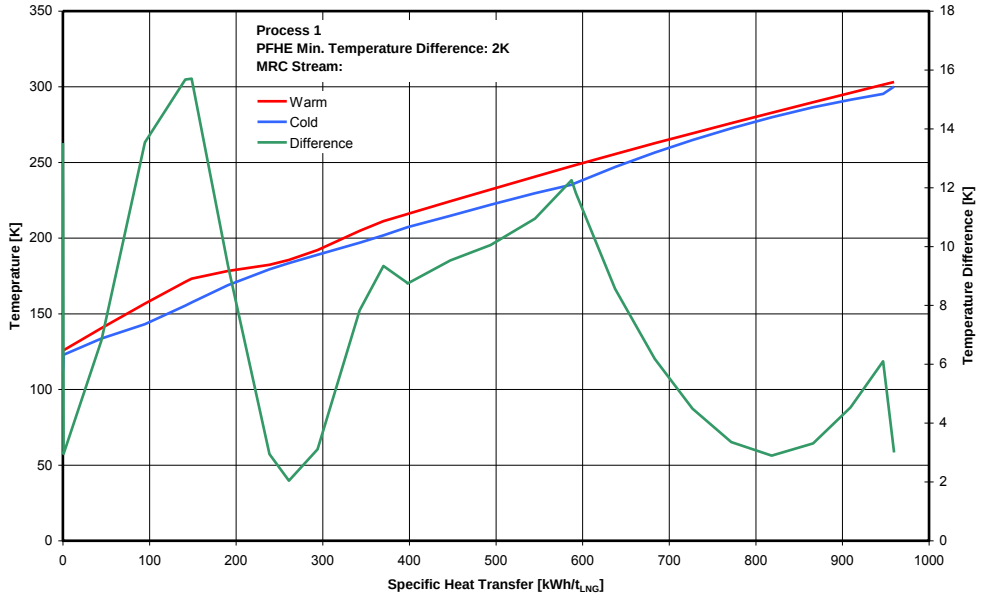

Fig. 10 (Q/T) diagram of PFHE in Process 1

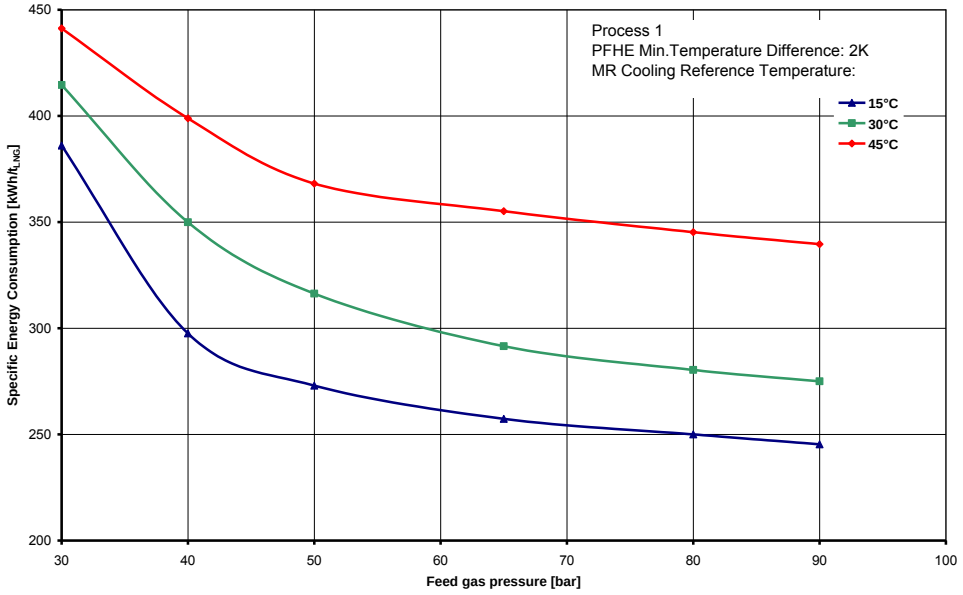

Fig. 11 Specific energy consumption's behaviour in Process 1 for a minimal temperature difference of 2K and MR cooling reference temperature of 15, 30 & 45°C

Figure 10 shows (Q/T) diagram of the cold and warm streams of PFHE (left abscissa) as well the temperature difference (right abscissa) as a function of specific heat transfer within the PFHE for process 1. As both warm and cold streams of PFHE lay close to each other without intersection; it can be indicated that the work done by MRC compressor is minimum. Here the maximal temperature difference of about 16 K is found on the warm part of PFHE, providing a phase change in MR, while a temperature difference of about 6K is obtained on the cold part of the PFHE referring to the exergy losses on the cold part of the process. This adaptability in (Q/T) diagram is, in general, taken as an indication to the effectiveness of the MRC process.

As **Figure 11** shows the specific energy consumption as a function of MR cooling reference temperature and feed gas pressure. In general, the MRC process is more effective (less specific energy consumption) when feed gas is operated under high pressures and lower MR cooling reference temperatures (low to moderate climate conditions), since lower cooling duty on MRC Compressor is required. By optimized process conditions achieving a pinch temperature (minimum temperature difference between cold and warm

streams) for PFHE of 2K, the specific energy consumption for this process1 is reading the value of 285 kWh/tLNG at 65 bar feed gas pressure and MR cooling reference temperature of 30C, which is within the range of conventional single MRC process (typically 250 – 350 kWh/tLNG ([Jacobson (2009), Devold (2013) and Long *et al*. (2016)).

Figure 12 shows (Q/T) diagram of the cold and warm streams of PFHE (left abscissa) as well the temperature difference (right abscissa) as a function of specific heat transfer within the PFHE for process 2. As expected the inclusion of MP separator enhances the pre-cooling duty of PFHE. An improvement on total energy consumption is achieved for process 2 with respect to process 1, enhancement of pre-cooling duty means a significant reduction on the isentropic work done by 1st MRC stage compressor. The maximal temperature difference is reduced to 13K, obtained at the warm part of PFHE, that is synchronized with a temperature difference of 18K, this is due to the phase change in the light and heavy MR streams in PFHE. On the other hand, the cold and warm streams are laying closer, which is in turn an indication for the further improvement of the effectiveness of process 2.

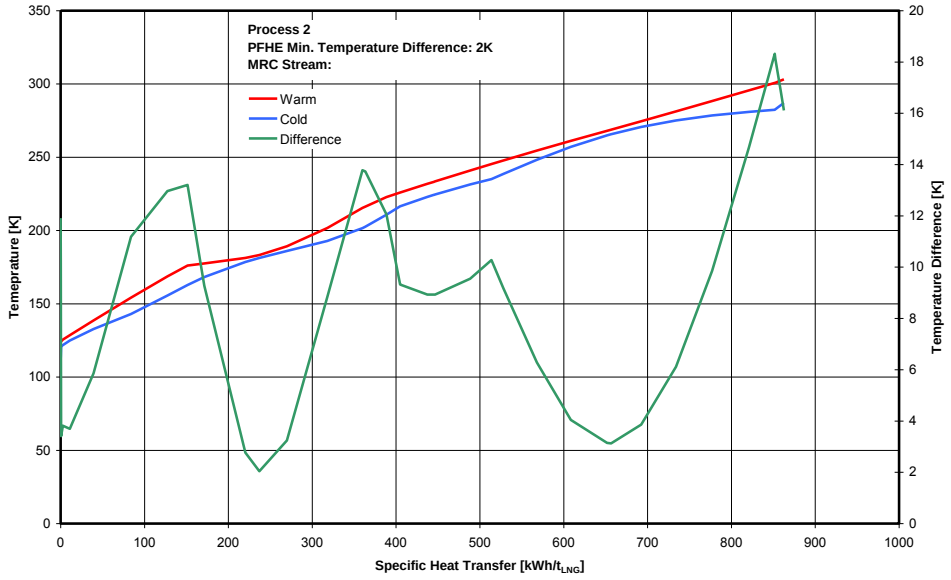

Fig. 12 (Q/T) diagram of PFHE in Process 2

Figure 13 shows the specific energy consumption as a function of MR cooling reference temperature and feed gas pressure. In comparison to **Figure 11** lower specific energy consumption is obtained with respect to that of process 1 by a factor of 3%.

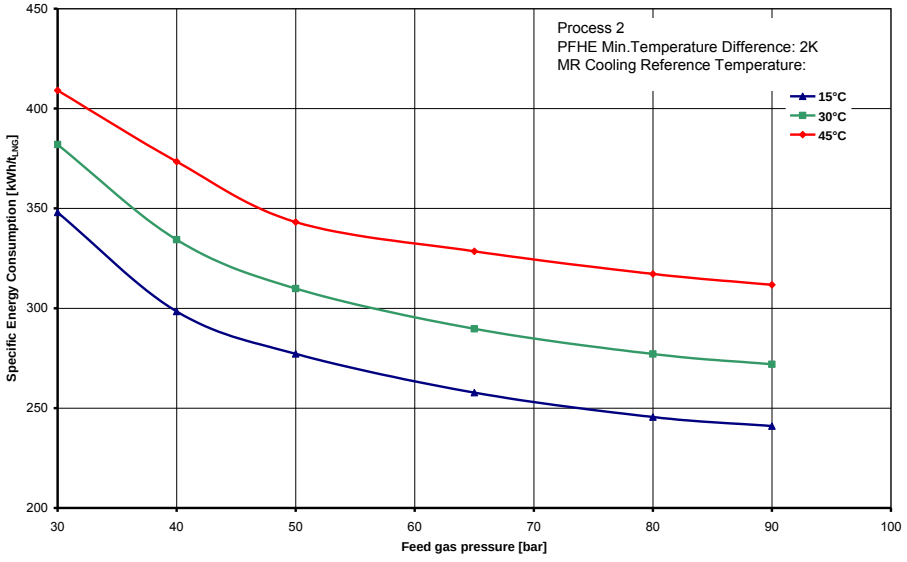

Fig. 13 Specific energy consumption's behaviour in Process 2 for a minimal temperature difference of 2K and MR cooling reference temperature of 15, 30 & 45°C

Figure 14 shows (Q/T) diagram of the cold and warm streams of PFHE (left abscissa) as well the temperature difference (right abscissa) as a function of specific heat transfer within the PFHE for process 3. The maximal temperature difference is reduced to 12K on the warm part of PFHE in comparison to that of process 1, a temperature difference of about 14K obtained on the cold part of PFHE.

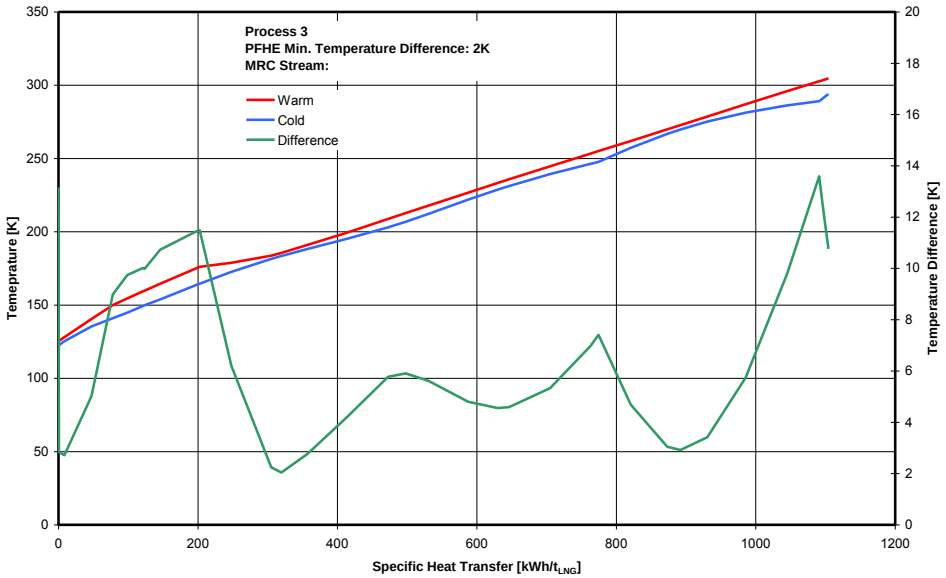

Fig. 14 (Q/T) diagram of PFHE in Process 3

Similar findings in **Figure 15** are obtained compared to those of above Figures 11 & 13.

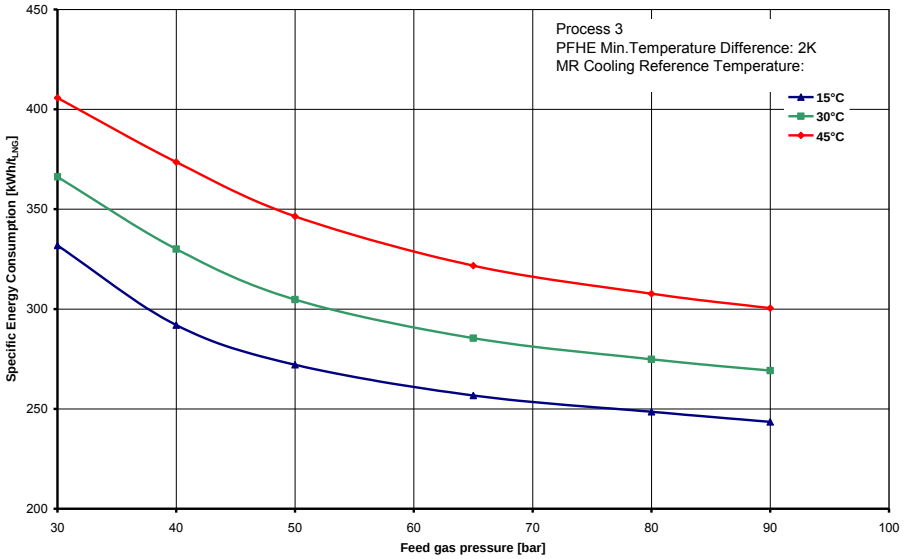

Fig. 15 Specific energy consumption's behaviour in Process 3 for a minimal temperature difference of 2K and MR cooling reference temperature of 15, 30 & 45°C

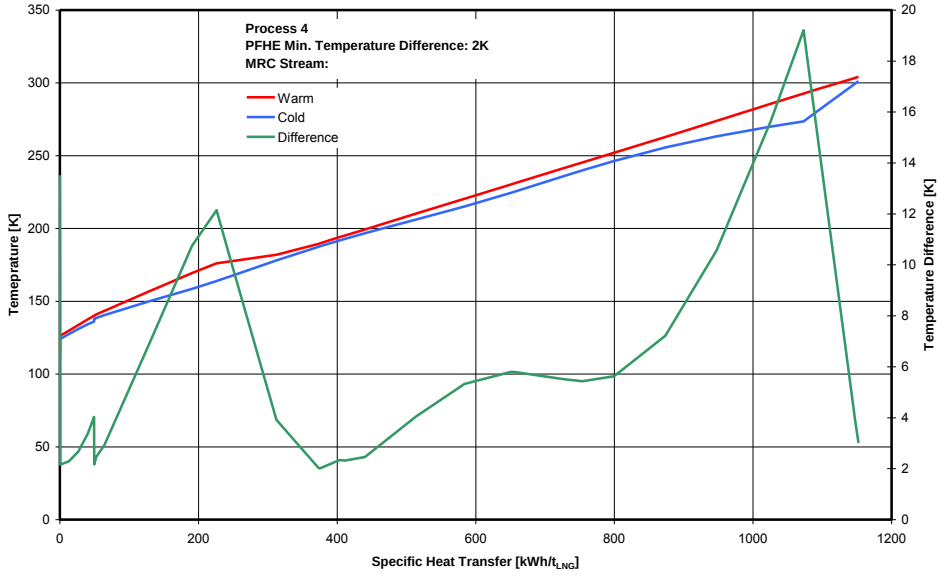

Fig. 16 (Q/T) diagram of PFHE in Process 4

Figure 16 presents (Q/T) diagram of the cold and warm streams of PFHE (left abscissa) as well the temperature difference (right abscissa) as a function of specific heat transfer within the PFHE for process 4. A reduce of about 7% in total specific heat transfer. Here the effect of the further improvements (MRC pump and mixing the cold and warm parts of PFHE) on MRC process performance highlights that a maximal temperature difference of about 12 K on the warm part of PFHE and 18K on the cold part of PFHE are obtained. This process reads a further reduction in the specific energy consumption of about 12 % in comparison to that of process 1. Figure 17 presents that the findings are in good agreement with previous relevant schemes. Energy consumption in comparing to that of process 1 at 65 bar inlet feed pressure and MR cooling reference temperature of 30 ºC. It is observed that the behaviour of temperature difference in the liquefaction region of PFHE has two jumps, due to enhanced in the condensation curve for NG. This is achieved because of the MRC pump.

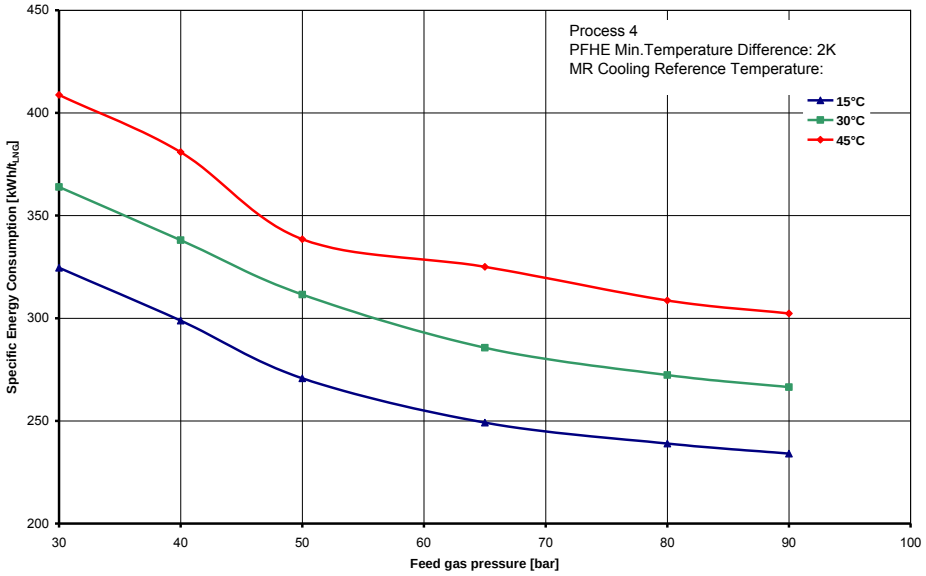

Fig. 17 Specific energy consumption's behavior in Process 4 for a minimal temperature difference of 2K and MR cooling reference temperature of 15, 30 & 45°C

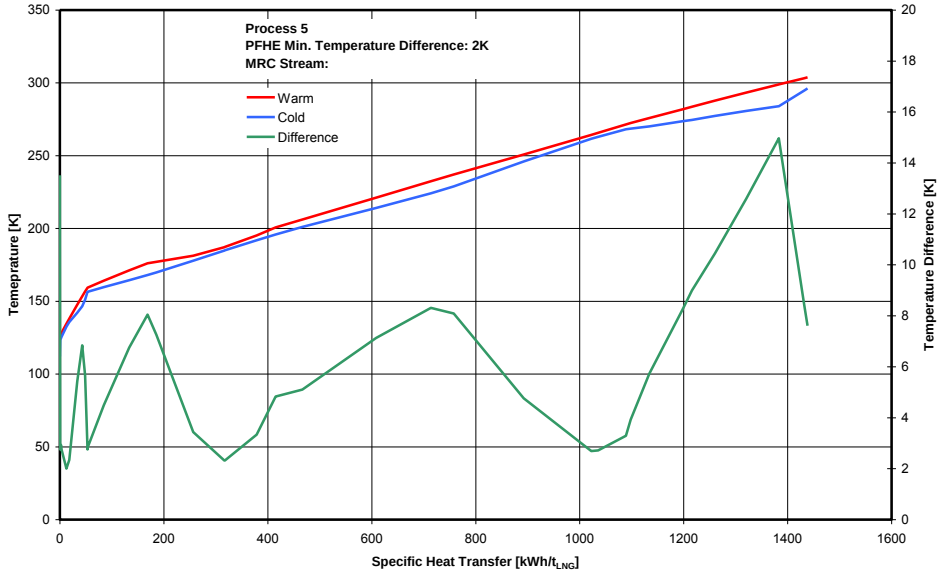

Fig. 18 (Q/T) diagram of PFHE in Process 5

Figure 18 presents (Q/T) diagram of the cold and warm streams of PFHE (left abscissa) as well the temperature difference (right abscissa) as a function of specific heat transfer within the PFHE for process 5. The relevant improvements include MRC pump, mixing of cold and warm streams as well MR cold separator. These improvements indicate significant enhancements on pre-cooling and liquefaction duties compared to those obtained in process 4, further enhancement is gained for sub-cooling duty of PFHE because of MR cold separator. This finding is proven in the behavior of temperature difference curve with respect to that of process 4, where a maximal temperature difference of about 8K is obtained on the warm part of PFHE, 8K around the mixing point and 14K at cold part of PFHE. Also, findings in **Figure 19** are in good agreement with above mentioned facts. The MRC process is more effective (less specific energy consumption) with a factor about 14% with respect to that of process 1.

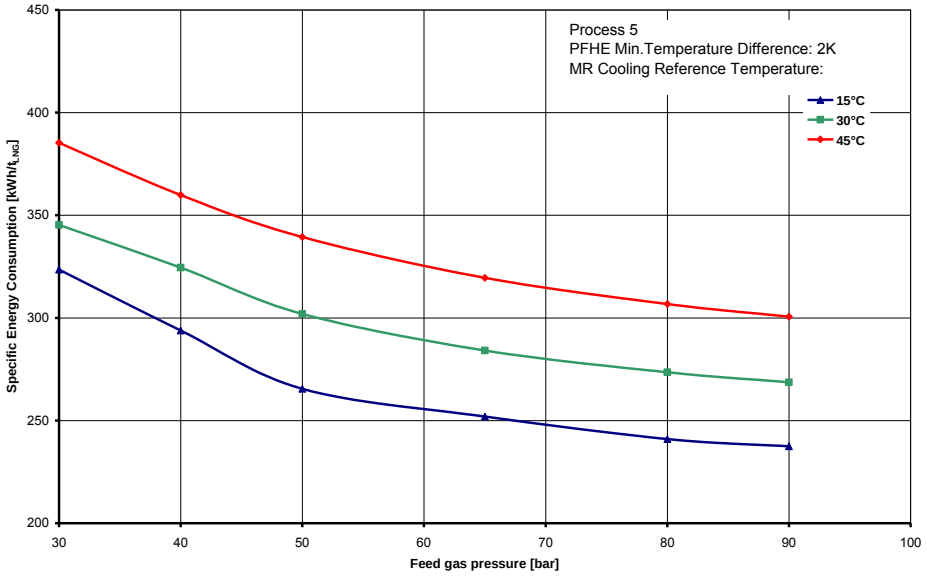

Fig. 19 Specific energy consumption's behaviour in Process 5 for a minimal temperature difference of 2K and MR cooling reference temperature of 15, 30 & 45°C

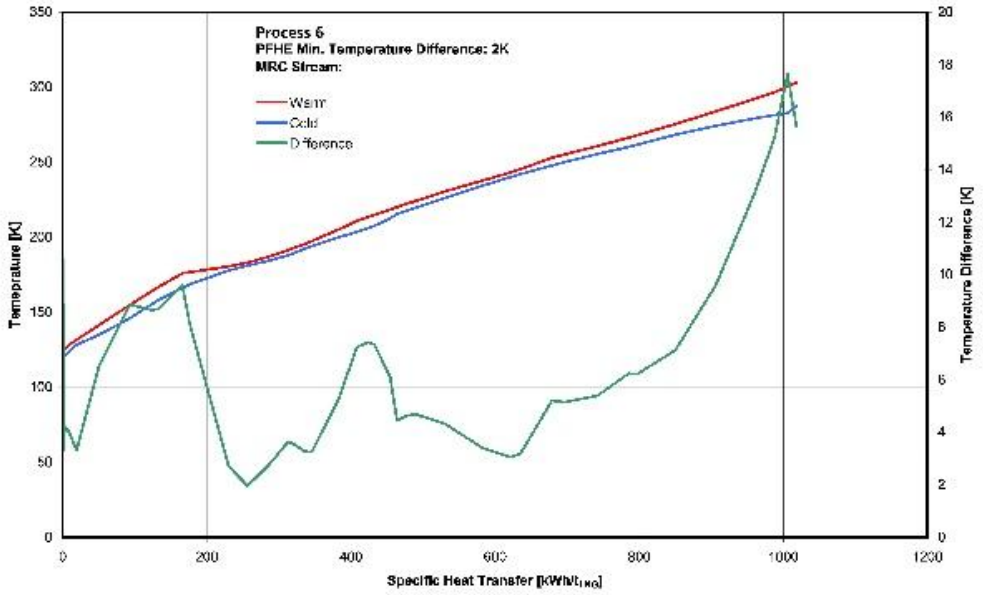

Fig. 20 (Q/T) diagram of PFHE in Process 6

Figure 20 presents (Q/T) diagram of the cold and warm streams of PFHE (left abscissa) as well the temperature difference (right abscissa) as a function of specific heat transfer within the PFHE for process 6. Obtaining a maximal temperature difference of about 8K on the warm end and 18K on the cold end of PFHE respectively, due to the warming of two phase stream fed from the position of mixing gas and liquid MR from HP separator prior to be routed to PFHE and finally expanded in JT valve to provide the essential sub-cooling duty of PFHE. Both warm and cold streams in PFHE are closely laying, which implies, in turn, an indication of relatively higher process effectiveness.

Figure 21 shows the simulation outputs of specific energy consumption as a function of a MR cooling reference cooling temperature and feed gas pressure. Effectiveness of process 6 reads an enhancement factor of about 16% of total energy consumption compared to process 1.

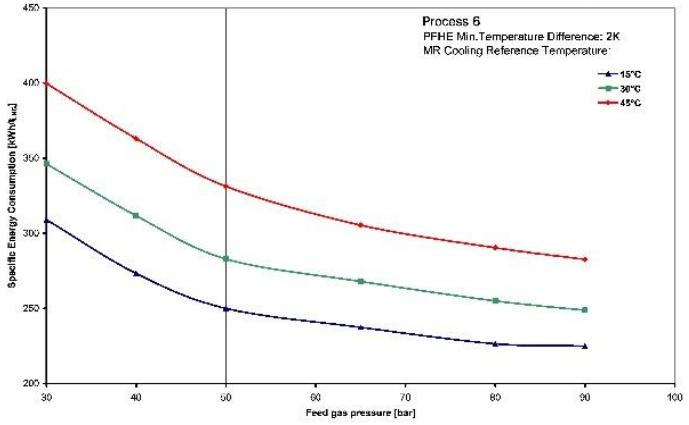

Fig. 21 Specific energy consumption's behaviour in Process 6 for a minimal temperature difference of 2K and MR cooling reference temperature of 15, 30 & 45°C

The results of process 7 regarding (Q/T) diagram of the cold and warm streams of PFHE (left abscissa) as well the temperature difference (right abscissa) as a function of specific heat transfer within the PFHE is presented in **Figure 22**. Obtaining a maximal temperature difference of about 12K on the warm end and 17K on cold end of PFHE, due to the cooling of MP MR with expanding HP MR prior to be routed to PFHE, the other process configurations are identical to those of process 5.

Achievements on specific energy consumption of process 7 is shown in **Figure 23**. This process records a further improvement in the energy consumption of a factor of about 14%, which is near to that of process 5 under identical MRC configurations.

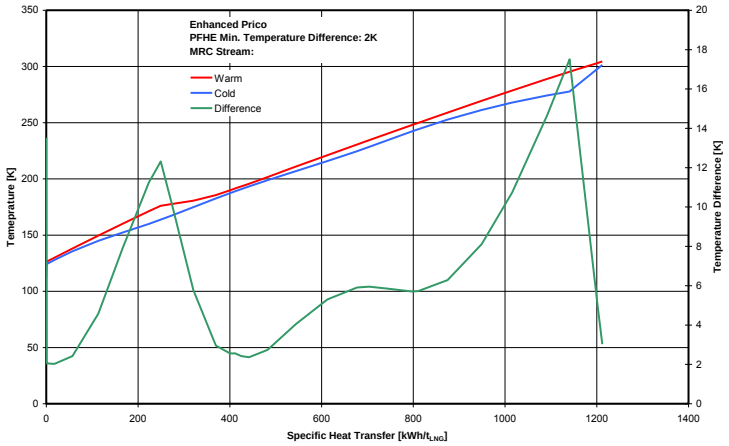

Fig. 22 (Q/T) diagram of PFHE in Process 7

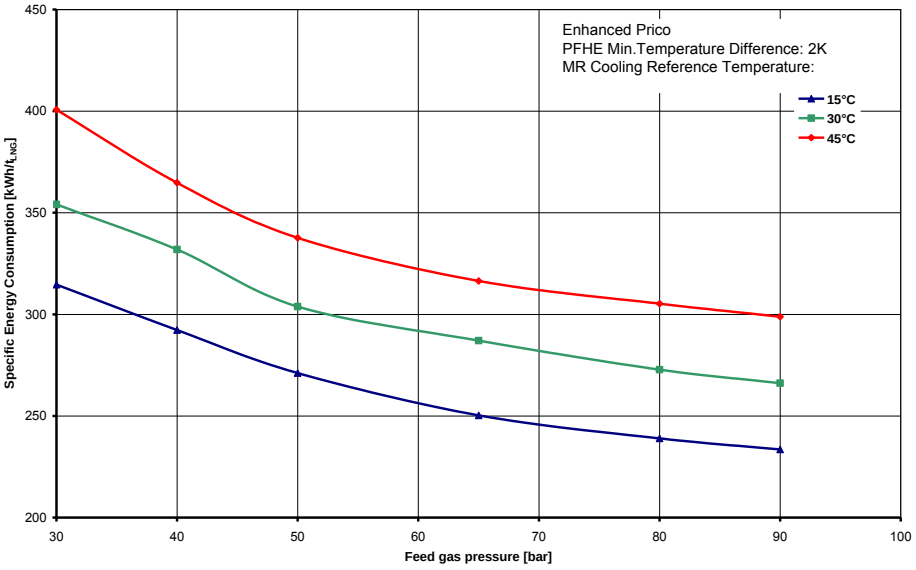

Fig. 23 Specific energy consumption's behaviour in Process 7 for a minimal temperature difference of 2K and MR cooling reference temperature of 15, 30 & 45°C

Table 4 dedicates the comparison design criteria for the investigated process concepts, run for MRC process boundary conditions listed in Table 3. All investigated concepts are performed under cryogenic temperature ranges, the operating conditions for considering the relevant topology are classified either simple or sophisticated according to the account of Joule Thomson valves implemented in the concept. Process 6 involves 2 Joule Thomson valves, so is considered as simple concept: Because it is run under basically the easiest controlled operating conditions, hence then has the lowest process complexity as well the relatively simplest automation scenario.

Table 4 Comparison criteria for LNG processes (Based on MRC process conditions listed in Table 3)

Process	1	2	3	4	5	6	7
Expected energy consumption [%]	115	110	115	115	115	100	105
Expected total installation costs [%]	90	90	100	110	120	100	150
Equipment count [-]	1 Comp. 1 Vessel	1 Comp. 2 Vessel	1 Comp. 2 Vessel	1 Comp. 2 Vessel	1 Comp. 3 Vessel	1 Comp. 2 Vessel	1 Comp. 3 Vessel

	3 HEX, 3 Valve	3 HEX 3 Valve	1 Pump 3 HEX 3 valve	1 Pump 4 HEX 3 valve	1 Pump 4 HEX 4 Valve	2 Pump 3 HEX 2 Valve	5 HEX 6 Valve
Plant availability [%]	High	High	Fair	Fair	Fair	Fair	High
Operating conditions [-]	Sophisticated cryogenic temperature	Sophisticated cryogenic temperature	Sophisticated cryogenic temperature	Sophisticated cryogenic temperature	Sophisticated cryogenic temperature	Simple cryogenic temperature	Sophisticated cryogenic temperature

Plant availability is justified by the presence of rotating equipments (cryogenic pumps) in the process as fair. While the absence of cryogenic pumps indicates a high plant availability, in this context processes 1, 2 and 7 prevail. The design criteria including OPEX and CAPEX indicate that processes 2 & 7 are comparable with respect to process 6. From the above findings, the improvements, performed for all above processes, are achieving the best readings for process 6. These finding will be further examined under different feed gas pressures and MR cooling reference temperatures, moreover will be compared with process 7, where enormous effects of process topology variation cause the process to be significantly effective. Designing of PFHE with minimal temperature difference less than 2K is not preferable due to economic reasons, hence then a PFHE with a relatively large heat transfer area is required. By comparing between the MRC processes 1 to 5, generally process 2 is recording the best results for the investigated range of minimal temperature difference of 2K. So that process 2 will also be considered for further investigations.

The Fig. 24 – 26 summarize the difference in specific total consumption energy as a function of the investigated range of feed gas pressures, for processes 2 (Foss (2005)) and 7 (Andress (1996)) with respect to process 6 (Stockman *et al*. (2002), Al Rabadi (2017)), considering similar conditions of PFHE minimum temperature of 2K and various reference temperature refrigerant of 15, 30 and 45 ºC, for simulating the diverse of metrological conditions for different LNG plants' locations around the world. The process calculations are done for PEHE minimal temperature difference with 2K. It is obvious that the process is showing a better performance with lower minimal temperature difference on PFHE, and higher inlet feed gas pressure. More over lower specific energy consumption is obtained with the low MR cooling reference temperature, since then lower duty on the MRC compressor is required.

Process 2 and 7 are recording higher figures for difference in total energy consumption with respect to those of process 6. As observed from Figure 24 the findings for process 2 decreases with feed gas pressure. The major influencing factor on the specific energy consumption in the refrigerant condensation process is the attainable enthalpy difference, hence the more refrigerant, condensed with using the cooling water, the more energy efficient is the condensation process. Considering the situation in process 7, it is reading of a relatively better performance due to inclusion of cold MR separator on the cold end of PFHE. The difference for process 7 reaches a maximum around the feed gas pressure of 50 bar due to thermodynamic equilibrium between liquid and gas phases of MR.

The findings in Figure 25 take a different trend that seems to be almost identical difference for each process starting from a feed gas pressure of 40 bar. Meaning that the process configurations, of MR cooling reference temperature refrigerant of 30 ºC, are recording almost the same level of specific energy consumption. Whereas in warm metrological regions the trend of difference in total energy consumption is increased for both processes 2 and 7, hence then higher energy consumption figures are expected on the MRC compressors, refer also to Figure 26.

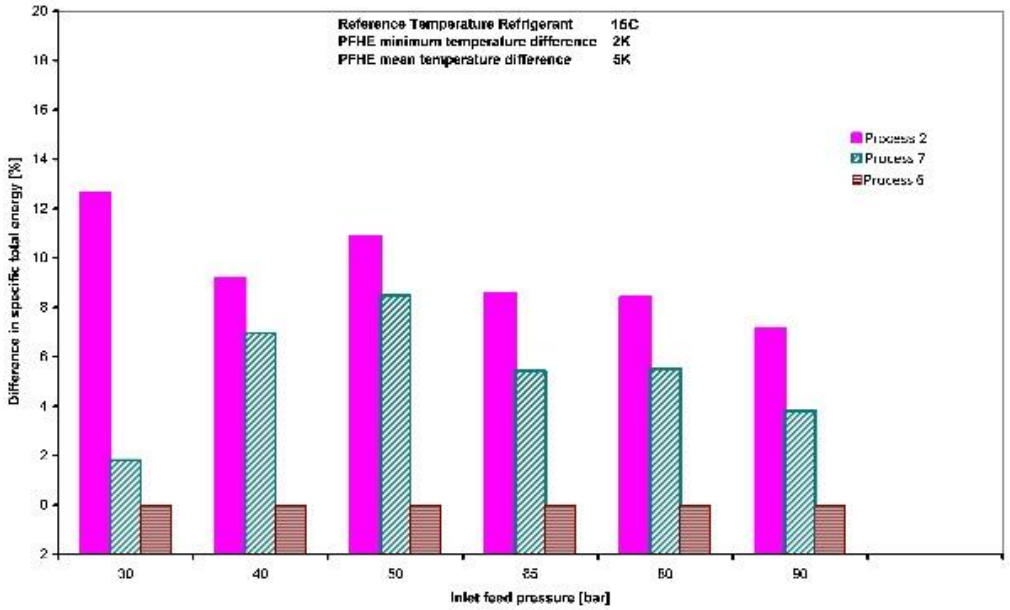

Fig. 24 Difference in total consumption energy for 15 ºC as MR cooling reference temperature

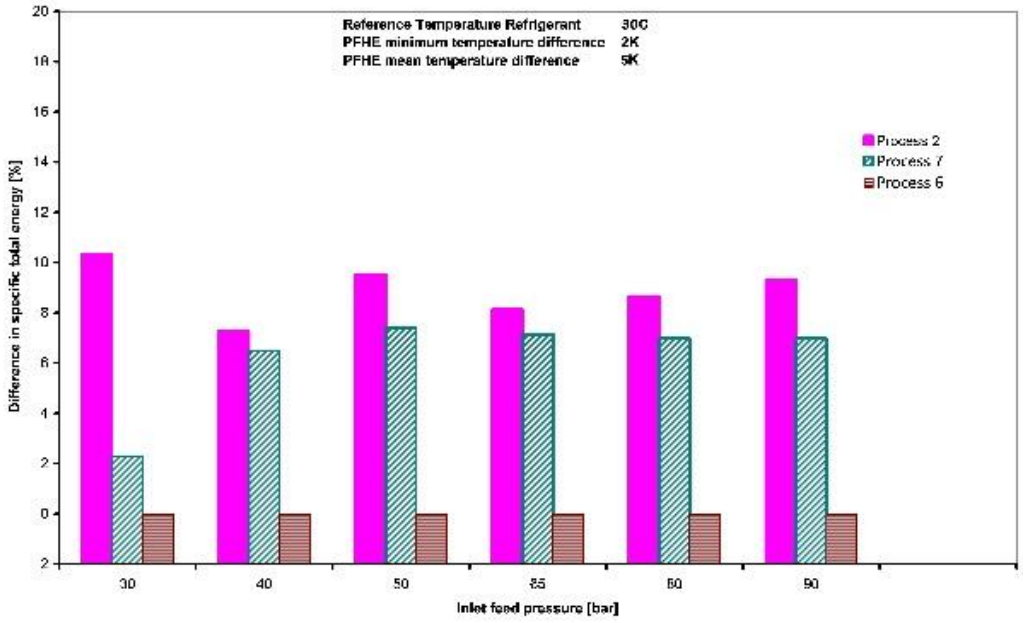

Fig. 25 Difference in total consumption energy for 30 ºC as MR cooling reference temperature

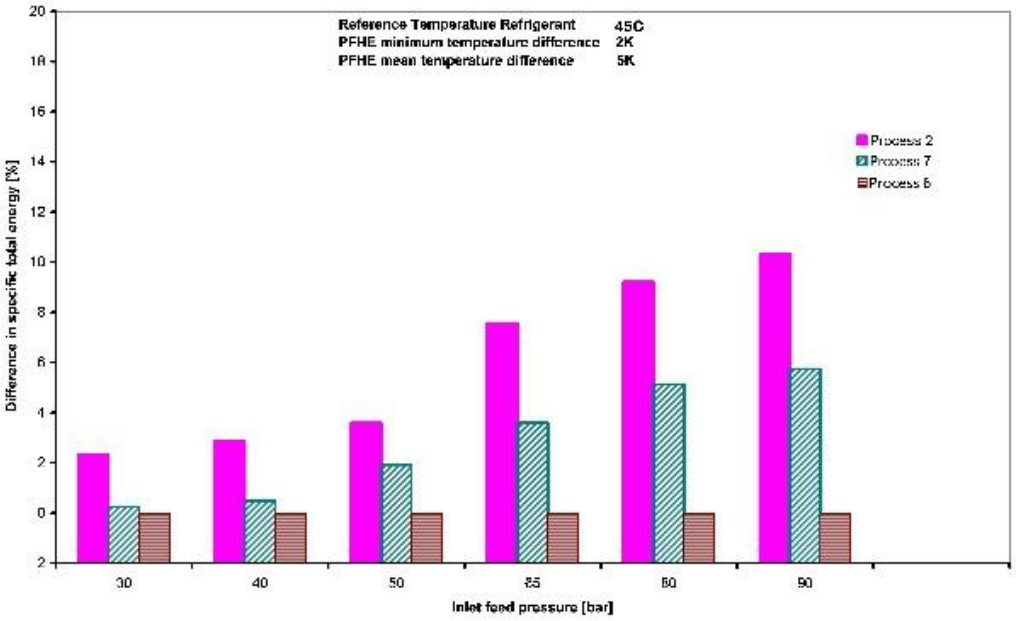

Fig. 26 Difference in total consumption energy for MR cooling 45 ºC as reference temperature

Conclusions

From the above findings, it can be concluded that the new improvements, proposed and compared with almost exclusively commercial trademarks processes in NG plant design, which mainly include the design of NG liquefaction and refrigeration cycle, are achieving considerable energy savings as well potentially are reducing the capital and operating costs of the plants, through reducing its footprint. These improvements are compatible for power-efficient, off- & onshore liquefaction plants, decreasing plant complexity scenarios from automation engineering point of view, as well for ecological reasons. So can assembly simulations parameters, be concerning energy density and equipment design, have the major impact on cost, or the so called benefit ratio, this is defined as the ratio between the price of the product and the plant efficiency. These parameters are indication on the potential energy savings by means of integration the traditional liquefaction processes with the proposed improvements on the plant layout, as well with optimization of the process conditions of MRC. More investigations are required to account for a moderate scalability of the modeled process improvements with respect to large scale plants. Furthermore, considerations for plant design with other commercial types of cryogenic heat exchangers are meriting further theortical and industry related investigations.

Acknowledgments

Grateful thanks for the support awarded by The Linde Group Firm, a special addressing to Mr. Rainer Sapper for the high-valued supervision in the execution of this research work. This work substantially overlaps research interests and corporation between The Linde Group and the academia.

Nomenclature

Acronym	Description
APCI	Air Products & Chemicals, Inc.
BP	British Pertoleum Corp. North America
C3MR	Propane mixed refrigerant
dT_{min}	Minimal Temperature difference
dp_{Fuel}	Pressure drop on Fuel gas stream
dp	Pressure drop on MRC steams
DMR	Dual mixed refrigerant
η_{isen}	Isenstropic efficiency
JT	Joule-Thomson

Q_{iso}	Insulation heat loss
η_{isen}	Isentropic compressor efficiency
T_{inlet}	Inlet temperature
T_{outlet}	Outlet temperature
p_{outlet}	Outlet Pressure
P_{inlet}	Inlet pressure
CAPEX	Capital costs
dp_{MR}	Mixed refrigerant stream pressure drop
HP	High pressure
LNG	Liquefied natural gas
MP	Medium Pressure
MR	Mixed refrigerant
MTPA	Million tonne per annum
NG	Natural gas
MFCP	Mixed fluid cascade process
MRC	Mixed refrigerant cycle
PFHE	Plate Fin Heat Exchanger
PRICO	Poly Refrigerant Integrated Cycle Operations
SMR	Single mixed refrigerant

References

Agrawal, M. R., "Dual mixed refrigerant cycle for gas liquefaction", **Patent No.09/208,562** (1998).

Al Rabadi, S., "Improvements to configurations of natural gas liquefaction cycles", *The 8th Jordan International Chemical Engineering Conference*, Amman – Jordan, 7 – 9 November (2017).

Andress, D. L., "The Phillips optimized cascade lng process a quarter century of improvement", *The Permission of the Institute of Gas Technology* (1996).

Cengel, Y. A. and M. A. Boles, "Thermodynamics an engineering approach". *McGraw-Hill*, New York (2002).

Coll, R., E. Carbon, and J. Delgado, "Technology evaluation Methodology for Stranded Gas Monetization Options", *19th WPC*, 2008 29th June - 3rd July, Madrid, Spain.

Devold, H., "Oil and gas production handbook An introduction to oil and gas production, transport, refining and petrochemical industry", Edition 3.0 Oslo, ISBN 978-82-997886-3-2 (2013).

Fischer-Calderon, E., "Self-refrigerated LNG process", **US Patent 6564578 B1**(2003).

Foss, M, "Global Natural Gas Issues and Challenges", *The Energy Journal*, **26**, 111-128 (2005).

Jacobson, M. Z., "Review of solutions to global warming, air pollution, and energy security", *Energy Environ. Sci*. 2, 148–173 (2009).

Kroener, A., "An engineering Company's approach to filling "CAPE gaps" in process simulation", *Computer Aided Chemical Engineering*, **21**, 781-786, (2006).

Laursen, J. K. and A. N. Karavanov, "Processes for sulfur recovery, regeneration of spent acid, and reduction of NOx emissions", *Chem. Petrol. Eng.* **42**, 229–234 (2006).

Long, N. V. D., L.Q. Minh, T.N. Pham, A. Bahadori, M. Lee, "Novel retrofit designs using a modified coordinate descent methodology for improving energy efficiency of natural gas liquid fractionation process", *Jour. Nat. Gas Sci. Eng*., **33**, 458–468 (2016).

Metz, B. and O. Davidson, "IPCC special report on carbon dioxide capture and storage. Working Group III. Intergovernmental Panel on Climate Change", *Cambridge University Press*, Cambridge (2005).

Pereira, C. and D. Lequisiga, "Technical Evaluation of C3-MR and Cascade Cycle on Natural Gas Liquefaction Process", *Inter. Jour. of Chem. Eng. and Appl.*, **5**, 451 – 456 (2014).

Perez, S. and R. Dietz, Opportunities of monetising natural gas reserves using small to medium scale LNG technologies". *REPSOL* (2009).

Smith, J. M., M. Van Ness and M. Abbott, "Introduction to Chemical Engineering Thermodynamics", 5th edition, *Mc Graw Hill* International Editions, (1996).

Stockmann, R., M. Bolt, M. Steinbauer, C. Pfeiffer, P. Paurola, W. Forg, A. O. Fredheim and O. Sorensen, "Process for liquefying a hydrocarbon-rich stream", **US Patent 6334334 B1** (2002).

Wonsub, L., C. Kwangho and M. I, "Current Status and Perspectives of Liquefied Natural Gas (LNG) Plant Design", *Ind. Eng. Chem. Res*., **52** , 3065–3088 (2013).

Study the effect of Substituents X on Methylenecyclopentane and 1-Methylcyclopentene System

Ghassab Al-Mazaideh [1]*, Ashraf Al-Msiedeen[1], Fadi Alakhras[2], Hammad Aldal'in[3], Haya Salman[1], Zeinab Al-Itiwi[1], Khaled Al Khalyfeh[4], Salim Khalil[1]

1) Department of Chemistry and Chemical Technology, Faculty of Science, Tafila Technical University, P.O.Box 179, Tafila 66110, Jordan
2) Department of Chemistry, College of Science, Imam Abdulrahman Bin Faisal University, P.O. Box 1982, Dammam 31441, Saudi Arabia
3) Department of Medical Support, Al-Balqa Applied University, Al-Karak University College, Al-Karak, Jordan
4) Department of Chemistry, College of Sciences, Al-Hussein Bin Talal University, Ma'an, Jordan

In this study, geometry optimizations, orbital energies (HOMO-LUMO) and relative stabilities of methylene cyclopentane and 1-methylcyclopentene were investigated by DFT calculations. 1-methylcyclopentene was found to be more stable than methylene cyclopentane isomer with enthalpy value H = 18.518 kJ/mol. Also, the effect of substituents X (F, OH, CH3, NH2, CN, NO2, CHO and CF3) was also studied on the relative stabilities of these two tautomers. The results showed that the stability of both isomers is increased by all substitutes. Gibbs free energy calculations have been used to find the effect of substituents X on the system**.**

Keywords: methylene cyclopentane, 1-methylcyclopentene, substituent, tautomer, DFT

Introduction

Tautomerism is a constitutional isomer, where one or a group of atoms can be moved to provide a new form that differs from initial instability (Moradi *et al.*, 2012). Currently, the system with a transfer proton between the two-tautomer is important in mechanistic chemistry and industrial synthesis (Sway *et al.*, 2004). Methylenecyclopropane/1-methylcyclopropene system (**Scheme 1**) has been studied by DFT/B3LYP; and it was found that methylenecyclopropane is more stable than 1-methylcyclopropene by 11.535 kcal/mol (Khalil, 2008). This agreed with a calculated Gibbs free energy, ΔG for the system (ΔG = 11.615 kcal/mol), which indicates that this system is non-spontaneous; and methylenecyclopropane is more stable than 1-methylcyclopropene. Also, it was found that an increase in the number of substituting fluorine atoms causes a destabilization of methylenecyclopropane.

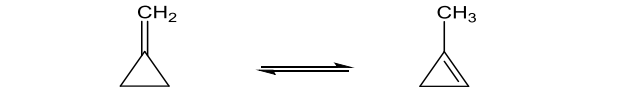

Scheme 1

This system was compared to fluorinated Cyclopropenone Keto-Enol and Fluorinated Methylene cyclopentane/1-Methylcyclopentene system. It was found that an increase in the number of fluorine atoms causes a destabilization of cyclopropenone and methylene cyclopentane (El-Alali *et al.*, 2003). Both experimental data and quantum mechanical calculations indicate that fluorination is strongly destabilize the acyclic alkenes and the forward reaction is less favorable. Theoretical calculations data show that multiple fluorination is strongly destabilizes a double bond, but a single fluorine atom stabilizes a double bond by an amount near to methyl group (2-3 kcal/mol) (Lindner *et al.*, 1997; Smart, 1986).

Received on July 11, 2018; accepted on 23 August, 2018
Correspondence concerning this article should be addressed to Ghassab Al-Mazaideh (E-mail address: gmazideh@ttu.edu.jo).

Parameterized Model number 3 PM3 and DFT (Density Functional Theory) calculations were performed on the methylene cyclobutane, 1-methylcyclobutene with different substituents X (F, CH_3, NH_2, CN, NO_2, CHO and CF_3) in the gas and aqueous phases. The results show that methylene cyclobutane is more stable than 1-methylcyclobutene in the gas and aqueous phases. Also, it is found that the stability of 1-methylcyclobutene increases by all substituents (Al-Mazaideh *et al.*, 2016). DFT is the most accurate method in chemical calculations, where DFT at the B3LYP/ 6-311G basis set level and semiempirical methods (PM3, AM1, and MINDO/3) are applied using G03 on six new substituted Schiff bases derivatives of INHC (N-(3-(phenylidene-allylidene) isonicotino-hydrazide). In addition, it is found that DFT calculations of vibration frequencies and IR absorption intensities for these new INHC Schiff bases derivative molecules give very good assignment values in comparison to the experimental values (Kubba and Abood, 2015). Optimized geometries of stepwise fluorinated methylenecyclopentane and 1-methylcyclopentene are determined by DFT; and it is found that 1-methylcyclopentene is more stable than methylenecyclopentane by 5.612 kcal/mol (**Scheme 2**). Perfluorination of 1-methylcyclopentene is found to be present in substantial concentration (Al-Mazaideh et al., 2016). Recently (Wedian and Al-Qudaha, 2016; Al-Msiedeen *et al.*, 2016; Al-Mazaideh *et al.*, 2017; Al-Mazaideh *et al.*, 2016; Al-Mazaideh *et al.*, 2016; Khalil *et al.*, 2016; Al-Mazaideh, 2017; Al-Mazaideh, Al-Quran, 2018), DFT has been applied on the corrosion inhibitors of metals; and very satisfactory results are reached.

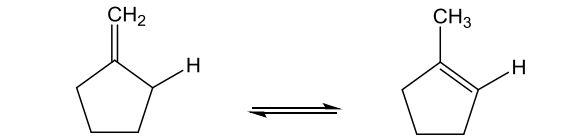

Methylenecyclopentane 1-methylcyclopentene

Scheme 2

The aim of this work is to give more theoretical insights to the problem of tautomerism of methylenecyclopentane and 1-methylcyclopentene by calculating the effects of substituents X (F, OH, CH_3, NH_2, CN, NO_2, CHO and CF_3) on the relative stabilities of these two tautomers. Gibbs free energy (ΔG) has been used to calculate and give indications about the spontaneity of the system. Dipole moments and the optimized geometries will be reported for the first time using DFT calculations.

1.Material and Methods

DFT calculations of methylenecyclopentaneand1-methylcyclopentene tautomerism and the effects of substituents X (F, OH, CH_3, NH_2, CN, NO_2, CHO and CF_3) on the relative stabilities of these two tautomers have been investigated by using the Gaussian 03 package program (Frisch *et al.*, 2003). The geometry and molecular energy of target compounds are completely minimized by DFT at the hybridity level of the three-parameter function of Becke (B3LYP)with 6-31G* (d, p) basis set in G03 program. In this work, the structures of the parent compounds have been designed by using Chem Office 2008 software. The final optimization of the methylenecyclopentane and its counterpart together with different substituents have been calculated and investigated by DFT method which is operated in theory of the levels B3LYP/6-31G*.

2. Results and Discussion

All DFT calculations of the structural geometry of Methylenecyclopentane and 1-methylcyclopentene and their derivatives (**Figure 1**) are carried out using the B3LYP /6-31G* basis set. Bond lengths and angles of all optimized compounds have been calculated in a gaseous state. These data are given in **Tables 1** and **2**.

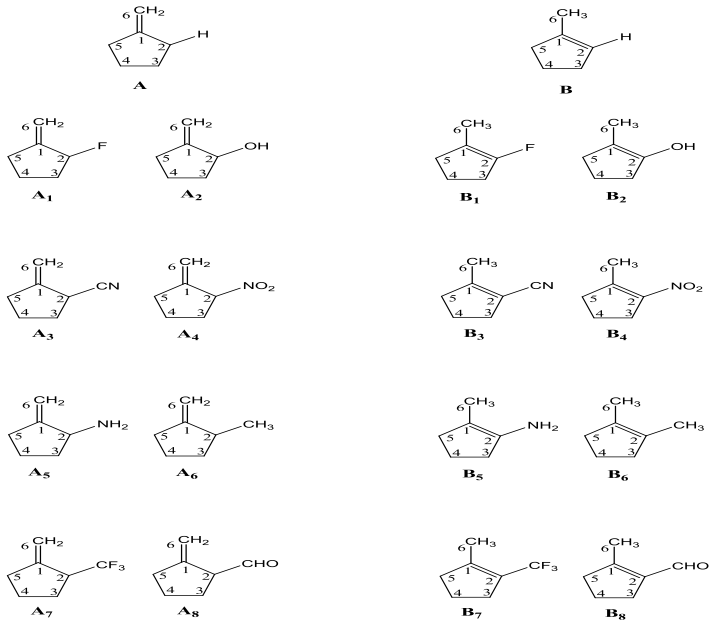

Fig. 1 Molecular structure of substituted methylene cyclopentane (A) and 1-methylcyclopentene (B)

The effect of substituents X on both parent structures shows that some C-C bonds have not been influenced. Methylenecyclopentane has been the most distinction bond length of C1-C2 on molecule A3 where the maximum difference value is at 0.017Å. 1-methylcyclopentene has the most distinction bond length of C1-C2 on molecule B8 where the maximum difference value is at 0.015 Å. Thus C-C bond length dissimilarity is not significant for all derivatives of parent compounds. It is clear from Table 1 that there is no variation between bonds length in methylene cyclopentane and its substituted derivatives and their counterparts in the 1-methylcyclopentene compounds, except for the bonds C1- C6 and C1 - C2 in compound **A** and **B**, where the variation in these bond lengths in all derivatives results from the existence of conjugation.

2.1 Orbital Energies (HOMO and LUMO) of parent compounds and their derivatives:

Table 1 Calculated bond lengths for methylene cyclopentane / 1-methylcyclopentene and their derivatives

Molecule	Bond distance (Å)						
	C1–C6	C1–C2	C2–C3	C3–C4	C4–C5	C5–C1	C2–X
A	1.333 C1=C6	1.526 C1–C2	1.543	1.540	1.543	1.526	**3.336 C2-H**
A1	1.333 C1=C6	1.517 C1–C2	1.527	1.542	1.547	1.525	1.411 **C2-F**
A2	1.335 C1=C6	1.523 C1–C2	1.531	1.542	1.547	1.524	1.438 **C2-OH**
A3	1.331 C1=C6	1.543 C1–C2	1.555	1.537	1.541	1.522	1.471 **C2-CN**
A4	1.332 C1=C6	1.532 C1–C2	1.535	1.540	1.541	1.521	1.528 **C2-NO_2**
A5	1.333 C1=C6	1.532 C1–C2	1.549	1.540	1.541	1.515	1.474 **C2-NH_2**
A6	1.334 C1=C6	1.532 C1–C2	1.549	1.540	1.542	1.524	1.541 **C2-CH_3**
A7	1.333 C1=C6	1.534 C1–C2	1.551	1.540	1.539	1.521	1.522 **C2-CF_3**
A8	1.334 C1=C6	1.539 C1–C2	1.554	1.543	1.539	1.517	1.517 **C2-CHO**
B	1.499 C1-C6	1.339 C1=C2	1.511	1.552	1.549	1.518	**3.199 C2-H**
B1	1.496 C1-C6	1.334 C1=C2	1.500	1.551	1.557	1.515	1.351 **C2-F**
B2	1.497 C1-C6	1.341 C1=C2	1.509	1.548	1.553	1.514	1.372 **C2-OH**
B3	1.495 C1-C6	1.350 C1=C2	1.521	1.549	1.548	1.513	1.425 **C2-CN**
B4	1.495 C1-C6	1.348 C1=C2	1.507	1.548	1.549	1.516	1.445 **C2-NO_2**
B5	1.499 C1-C6	1.348 C1=C2	1.513	1.545	1.549	1.515	1.400 **C2-NH_2**
B6	1.500 C1-C6	1.345 C1=C2	1.518	1.547	1.547	1.518	1.500 **C2-CH_3**

B7	1.499 C1-C6	1.344 C1=C2	1.518	1.547	1.545	1.519	1.492	**C2-CF_3**
B8	1.498 C1-C6	1.354 C1=C2	1.515	1.548	1.548	1.515	1.463	**C2-CHO**

In Table 2, the effect of substituent X on bond angle has no significance. On the other hand, in all derivatives of both parent compounds, a fluctuation exists among many bond angles that go from 0.01 degrees to 1.79 degrees for methylenecyclopentane compounds; and from 0.03 degrees to 3.57 degrees for 1-methylcyclopentene. For the methylenecyclopentane compounds, the bond angle C6–C1-C5 on molecule **A4** has the maximum value of 127.55 degrees. For 1-methylcyclopentene compounds the bond angle C6–C1-C2 on molecule **B7** has the maximum value of 130.84 degrees. In addition, C3–C4–C5 and C2–C3–C4 bond angles on molecules A**5** and **B1** are found to have the minimum value at 102.92 and 101.29 degrees compared to other compounds.

Table 2 Calculated bond angle for methylenecyclopentane / 1-methylcyclopentene and their derivatives

Molecule	**Bond angle in degree (°)**						
	C6–C1-C2	C6–C1-C5	C2–C1-C5	C1–C2-C3	C2–C3-C4	C3–C4-C5	C4–C5-C1
A	**125.78**	**125.78**	**108.44**	**104.70**	**103.48**	**103.48**	**104.70**
A1	124.18	127.30	108.51	104.27	103.11	103.69	104.73
A2	124.15	127.19	108.65	103.73	103.37	103.87	104.90
A3	124.43	127.08	108.49	103.94	103.69	103.40	104.76
A4	124.14	127.55	108.30	105.38	104.89	103.47	104.56
A5	124.73	126.40	108.79	104.48	105.24	102.92	103.28
A6	125.27	125.60	109.13	103.67	104.31	103.23	104.66
A7	125.24	126.02	108.74	104.59	104.70	103.47	104.67
A8	124.39	126.82	108.73	104.61	105.27	103.52	103.83
B	**127.27**	**121.85**	**110.83**	**112.84**	**102.87**	**105.28**	**103.70**
B1	127.04	124.06	108.85	115.93	101.29	105.92	104.22
B2	126.72	123.29	109.90	113.80	102.28	105.34	103.95
B3	127.37	122.33	110.27	112.72	102.51	105.31	104.14
B4	130.58	120.81	108.57	114.62	101.79	105.20	104.77
B5	127.56	121.76	110.55	112.28	103.02	104.95	103.63
B6	128.43	120.15	111.38	111.38	103.82	104.80	103.82
B7	130.84	119.20	109.92	112.78	102.84	104.80	104.34
B8	129.10	120.34	110.52	112.10	103.16	104.94	104.02

The introduction of substituents into methylene cyclopentane and 1-methylcyclopentene slightly affects their orbital energies (HOMO and LUMO) compared to parent compounds. In the case of methylene cyclopentane derivatives (**Table 3**), substitution causes a decrease in the energy gaps (E_g), suggesting consequently a decrease in the stability of these compounds. An exception is for the substituent CF_3, which causes a little increase in E_g.

Similarly, different substituents of 1-methylcyclopentene cause a decrease in E_g except for the case of structure **B1.** The introduced F atom results in a slight increase in Eg. In general, the change in E_g for all investigated structures is not significant in energy gaps for all substituents. E_g value can be calculated by E_{HOMO} - E_{LUMO} for the investigated compounds. The E_g value for methylene cyclopentane was found to be 6.947 eV compared to 7.086eV for 1-methylcyclopentene. This indicates that methylene cyclopentane is more stable than 1-methylcyclopentene by 0.139 eV.

Table 3 Calculated orbital energies (HOMO and LUMO, in eV) of methylenecyclopentane / 1-methylcyclopentene and their derivatives

Compound	**HOMO**	**LUMO**	E_g	**μ (D)**
A	-6.3475	0.5999	6.9474	0.59
A1	-6.9251	-0.0243	6.9008	1.74
A2	-6.7656	0.1809	6.9465	1.29
A3	-7.1002	-0.2078	6.8924	4.13

A4	-7.1719	-1.7287	5.4432	3.73
A5	-6.1721	0.4716	6.6437	1.18
A6	-6.3775	0.5680	6.9455	0.51
A7	-6.8704	0.1026	6.9730	2.20
A8	-6.5462	-0.5762	5.9700	3.14
B	-6.0755	1.0108	7.0863	0.23
B1	-6.0041	1.0934	7.0975	1.38
B2	-5.3363	1.4465	6.7828	1.65
B3	-6.7566	-0.8872	5.8694	4.60
B4	-7.1802	-2.1280	5.0522	4.76
B5	-4.9526	1.5278	6.4804	1.33
B6	-5.8312	1.0793	6.9105	0.14
B7	-6.7961	-0.0037	6.7924	2.68
B8	-6.5829	-1.3549	5.2280	3.87

E_g values can be used to investigate and show the effect of substituents on the stability of parent compounds. E_g values are given in Table 3 for all compounds. According to these calculations, the substituents X increase the stability of 1-methylcyclopenteneby, where the differences in E_g are greater than in the derivatives of methylenecyclopentane except in the case of adding of fluorine (F). B1 has greater E_g (7.097 eV) than A1 (6.900 eV) by 0.197 eV. As a result, the effect of substituent X on the stability of methylenecyclopentane according to E_g values is arranged as follows:

$$\mathbf{OH < CH_3 < CF_3 < F < CN < NH_2 < CHO < NO_2}$$

Their effect on the stability of 1-methylcyclopentene is arranged as follows:

$$\mathbf{F < CH_3 < CF_3 < OH < NH_2 < CN < CHO < NO_2}$$

2.2 Dipole Moment of parent compounds and their derivatives:

The introduction of substituent X (F, OH, CH_3, NH_2, CN, NO_2, CHO and CF_3) into methylene cyclopentane and 1-methylcyclopentene counterpart has also affected their dipole moment as compared to the parent compounds. This change in dipole moment is attributed to the change in the structural parameters and electronic structure of these derivatives. Table 3 shows a change in dipole moments for these compounds, where the dipole moment slightly decreases in the case of CH_3 from 0.59 Debye for parent compound to 0.51 Debye for CH_3 compound. Increases also occur for the rest of substituents. All substituents for 1-methylcyclopentene show increases in the dipole moment values except in the case of CH_3 (0.14 Debye) compared to its parent compound (0.23 Debye).

2.3 Thermodynamic calculation of parent compounds and their derivatives:

2.3.1 Parent compound:

Based on **Table 4**, the enthalpy of 1-methylcyclopentene B is lower than methylenecyclopentane A (Scheme 2), suggesting that B is more stable than A by 0.007053 Hartrees (18.518 kJ/mol). Moreover, substituents X increased the stability of compound B as compared to A. This is confirmed by thermodynamic calculations (Table 5), that showed a negative Gibbs free energy ($\Delta G_r° = -22.401$kJ/mol). They further indicate that 1-methylcyclopentene (B) is more stable than methylenecyclopentane A. This value of $\Delta G_r°$ (-22.401kJ/mol) is less than that of methylenecyclopropane ($\Delta G_r° = 48.597$ kJ/mol) and methylenecyclopentane ($\Delta G_r° = 27.719$kJ/mol) (Al-Mazaideh *et al.*, 2016) tautomerism. This result has been found due to lowering in the ring strain of the 1-

methylcyclopentene (five-member ring) with respect to three and four-member rings. Stabilization of 1-methylcyclopentene agrees with the reported study on methylenecyclopentane / 1-methycyclopentene system (Al-Mazaideh *et al.*, 2016).

Table 4 Calculated entropy S, enthalpy H and Gibbs free energy of methylenecyclopentane /1-methylcyclopentene and their derivatives

Compound	H° (kJ/mol)	S° (J/mol.K)	G° (kJ/mol)
A	**-615650.88**	**304.00**	**-615741.52**
A1	-876200.13	326.66	-876297.53
A2	-813097.42	331.85	-813196.37
A3	-857820.32	341.18	-857922.04
A4	-1152555.24	353.43	-1152660.60
A5	-760899.01	333.41	-760998.41
A6	-718791.87	336.13	-718892.09
A7	-1500527.70	370.00	-1500638.01
A8	-913131.51	345.97	-913234.66
B	**-615669.40**	**317.03**	**-615763.92**
B1	-876226.56	335.41	-876327.35
B2	-813133.32	341.78	-813235.22
B3	-857869.89	349.73	-857974.16
B4	-1152581.90	362.10	-1152689.93
B5	-760952.99	340.95	-761054.65
B6	-718825.69	344.67	-718928.45
B7	-1500546.30	380.10	-1500659.66
B8	-913178.76	354.07	-913284.33

2.3.2 Effect of substituents

Introduction of the substituents on the methylenecyclopentane and 1-methylcyclopentene system shows that a negative value of $\Delta G_r°$ can be obtained for all reactions (**Table 5**). The resulted values are less than those of methylenecyclopentane and 1-methylcyclopentene system. They indicate a spontaneous reaction as substitution increases the stability of 1-methylcyclopentene as compared to methylenecyclopentane. This conclusion is supported with smaller enthalpy values of all 1-methylcyclopentene substituents compared to methylenecyclopentane substituents (Table 4).

Table 5 Gibbs free energy (ΔG) of substituted methylenecyclopentane and 1-methylcyclopentene and their derivatives

No.	Tautomerism	ΔG_r° (kJ/mol)
Parent	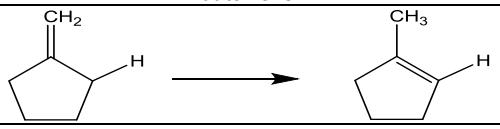	**-22.401**
1	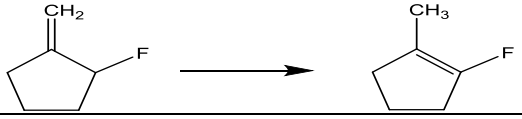	**-29.820**
2	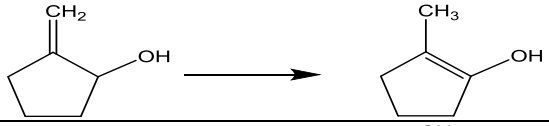	**-38.857**
3	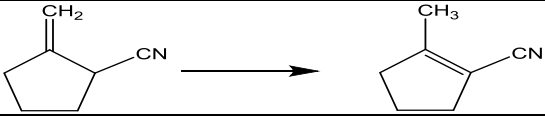	**-52.121**
4	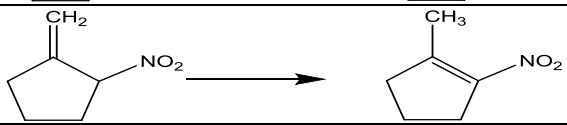	**-29.311**
5	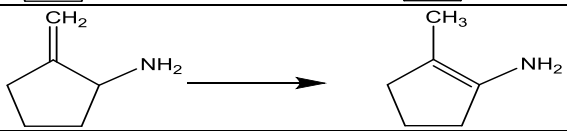	**-56.238**

6	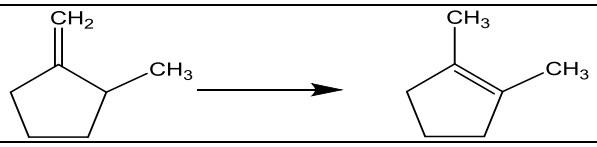	**-36.366**
7	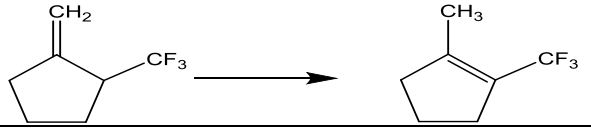	**-21.597**
8	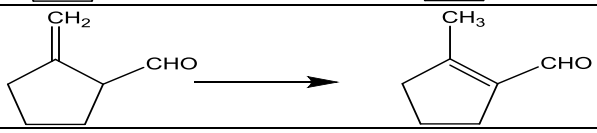	**-49.672**

Conclusion

The present study has investigated the effects of substituents X (F, OH, CH_3, NH_2, CN, NO_2, CHO and CF_3) on methylenecyclopentane and 1-methylcyclopentene system. The results of DFT method used in this study show that the 1-methylcyclopentene is more stable than methylenecyclopentane by18.518 kJ/mol. The variation between bonds length of methylenecyclopentane compounds and their counterparts in the 1-methylcyclopentene compounds is due to conjugation for both C1-C6 and C1- C2. Yet, the other bonds lengths have no variation. In all derivatives of both parent compounds, a fluctuation exists among many bond angles. All substituents have been found to influence on methylenecyclopentane and 1-methylcyclopentene by directing the reaction forward to products and stabilizing the 1-methylcyclopentene as explained by thermodynamic calculations.

Nomenclature

$\mathbf{E_{HOMO}}$	Energy of highest occupied molecule orbital [eV]
$\mathbf{E_{LUMO}}$	Energy of lowest un-occupied molecular orbital [eV]
ΔH	Enthalpy [kJ/mol]
DFT	Density Functional Theory
B3LYP	Becke, 3-parameter, Lee-Yang-Parr
ΔG	Gibbs free energy [kJ/mol]
PM3	Parameterized Model number 3
AM1	Austin Model 1
MINDO	Modified Intermediate Neglect of Differential Overlap
G03	Gaussian 2003
$\mathbf{E_g}$	Energy gap [eV]
μ	Dipole moment [Debye, D]
S	Entropy [J/mol.K]

References

Al-Mazaideh, G. M. "Carbohydrates as Green Corrosion Inhibitors of Copper Ab initio Study", *Jord. J. Chem*., **12**, 189-200 (2017)

Al-Mazaideh, G. M., K. A. Abu-Sbeih, S. M. Khalil,"Computational calculations of chitosan fragments as corrosion inhibitors of metals", *J. Chem., Biolo., Phy. Sci*.,**7**, 398-409 (2017)

Al-Mazaideh, G. M., R. A. Enwisry and S. M. Khalil "Effect of substituents on methylenecyclo-butane /1-methylcyclobutene system", *Inter. Res. J. Pure & Appl. Chem.*, **12**, 1-10 (2016)

Al-Mazaideh, G. M., S. A. Al-Quran "Inhibitive action of Chamomile extract on the corrosion of Iron: Density Functional Theory", *Mor. J. Chem.*, **6**, 195-202 (2018)

Al-Mazaideh, G. M., T. S. Ababneh, K. H. Abu-Shandi, R. M. A. Q. Jamhour, H. J. Ayaal Salman, A. M. Al-Msiedeen and S. M. Khalil "DFT calculations of Mesembryanthemum nodiflorum compounds as corrosion inhibitors of aluminum", *Phy. Sci. Inter. J*., **12**, 1-7 (2016)

Al-Mazaideh, G. M., W. B. Ejlidi and S. M. Khalil "A DFT study on stepwise fluorinated methylenecyclopentane and 1-methylcyclopentene system", *Inter. Res. J. Pure & Appl. Chem.*, **12**, 1-14 (2016)

Al-Mazaideh, G. M., W. A. Al-Zereini, A. H. Al-Mustafa and S. M. Khalil "The effect of nitro maleimides from a marine vibrio species compounds as a source of environment-tally friendly corrosion inhibitors for metals: A computational study", *Adv. Env. Biol.*, **10**, 159-168 (2016)

Al-Msiedeen, A. M., G. M. Al-Mazaideh and S. M. Khalil "A theoretical study of the enol contents of cyclohexanone, cyclopentanone and acetone", *Amer. Chem. Sci. J.*, **13**,1-8 (2016)

El-Alali, A., A. A. Marashdeh and S. M. Khalil "A theoretical study of substituted stepwise fluorinated cyclopropenone keto-enol system", *Z. Naturforsch*., **58a**,749-755 (2003)

Frisch, M.J., et al., Gaussian, Inc., Wallingford, CT, (2003).

Khalil, S. M. "A DFT study on the stepwise fluorinated methylenecyclopropane and 1-methylcyclo-propene system", *Z. Naturforsch*., **63a**, 42-48 (2008)

Khalil, S. M., G. M. Al-Mazaideh and N. M. Ali "DFT calculations on corrosion inhibition of Aluminum by some carbohydrates", *J. Biochem. Res. & Rev.*, **14**, 1-7 (2016)

Kubba, R. M., F. K. Abood "DFT, PM3, AM1, and MINDO/3 quantum mechanical calculations for some INHC Cs symmetry schiff bases as corrosion inhibitors for Mild steel", *Iraqi J. Sci.*, **56**, 602-126 (2015)

Lindner, P. E. and D. M. Lemal "Energetics of fluoroalkene double bond isomerizations", *J. Am. Chem. Soc*., **119,** 3267-3273 (1997)

Moradi, R., S. Jameh-Bozorghi, R. Kadivar, A. Mahdiani and H. Soleymanabadi "Study of mechanism keto-enol tautomerism (isomeric reaction) structure cyclohexanone by using Ab initio molecular orbital and density functional theory (DFT) method with NBO Analysis", *APCBEE Procedia*, **3**, 70-74 (2012)

Smart, B. E., J. F. Liebman and A. "Molecular structure and energetic", **3**, 141-191, Greenberg (eds.); VCH Publishers, Deerfield Beach, FL (1986)

Sway, M.I., I. D. M. Al-Shawabkeh and S. M. Khalil "A theoretical study of substituted cyclobuta-nones and their enols", *Z. Naturforsch*., **59**, 838-844 (2004)

Wedian, F., M. A. Al-Qudaha and A. N. Abu-Bakerb "The effect of capparis spinosa L.extract as a green inhibitor on the corrosion rate of copper in a strong alkaline solution", *Portugaliae Electro-chimica Acta.*, **34**, 39-51 (2016)

Hashemite Kingdom of Jordan

صندوق دعم البحث العلمي
Scientific Research Support Fund

Scientific Research Support Fund

جامعة البلقاء التطبيقية
AL-BALQA' APPLIED UNIVERSITY

AL-BALQA APPLIED UNIVERSITY

المجلة الأردنية للهندسة والصناعات الكيميائية

June 2018 | VOLUME 01 | NUMBER 01

ISSN 2616 - 9584 (Online)
ISSN 2616 - 9584 (Print)

JJECI

www.jjeci.com

info@jjeci.com

مجلة علمية عالمية متخصصة محكمة

تصدر بدعم من صندوق دعم البحث العلمي